

# **ANALYSIS OF THE ROLE OF THE E-(Epithelial) CADHERIN IN MURINE LUNG TUMORIGENESIS**

Dissertation

For completion of the Doctorate degree in Natural Sciences at the  
Bayerische Julius-Maximilians-Universität Würzburg



**Fatih Ceteci**

from Solingen, Germany

Würzburg 2008

The hereby submitted thesis was completed from Jun 2002 until Jun 2008 at the Institute for Medical Radiation and Cell Research (MSZ), Bayerische Julius-Maximilians University, Würzburg under the supervision of **Prof. Dr. Ulf R. Rapp** (Faculty of Medicine) and **PD Dr. R. Götz** (Faculty of Medicine).

Submitted on:

Members of the thesis committee:

**Chairman: Prof. Dr. Ulf R. Rapp**

**Examiner: PD Dr. R. Götz**

**Examiner: Prof. Dr. R. Benavente**

Date of oral exam:

Certificate issued on:

## ACKNOWLEDGMENTS

It is a pleasure to thank the many people who made this thesis possible.

I would like to express my deep and sincere gratitude to Prof. Dr. Ulf R. Rapp who allowed me to undertake my Ph.D. research in the MSZ Institute. It is difficult to overstate my gratitude to him not only for inviting me to the MSZ but also for his strong scientific guidance as well as for providing enthusiasm, inspiration, and strong motivation during my studies. His wide knowledge and his logical way of thinking have been of great value for me. His encouraging and personal guidance have provided a good basis for the present thesis.

I am deeply grateful to my supervisor, Dr. Rudolf Götz, for his continuous support, detailed constructive comments, and fruitful discussions and for his important support throughout this work.

I would like to thank Prof. Dr. Ricardo Benavente for his contribution to my research seminars and for his critical thesis evaluation.

I am indebted to thank all the members of mouse club for their important contribution and stimulating discussions. I would like to thank them for the many social and scientific events we have shared and for providing a stimulating and fun environment. I would not forget to thank our ex-members for the past in common. I am grateful to all technicians of our group for their perfect expertise in every aspect of mice.

I am grateful to many other co-workers in MSZ-Institute.

During this work I have collaborated with many colleagues for whom I have great regard, and I wish to extend my warmest thanks to all those who have helped me with my work.

I would like to thank all the members and organizers of the GK-639 for their excellent supervision, support and guidance for this work.

A penultimate thank-you goes to my wonderful parents. For always being there when I needed them most, and never once complaining about how infrequently I visit, they deserve far more credit than I can ever give them.

My final, and most heartfelt, acknowledgment must go to my wife and also my excellent-talented colleague Semra. Her support, encouragement, and companionship have turned my scientific journey into a pleasure. It is difficult to express in a few sentences the gratitude for my wife. The greatest acknowledgement I reserve for her to whom I dedicate this dissertation.

## TABLE OF CONTENTS

<b>ZUSAMMENFASSUNG</b> .....	1
<b>SUMMARY</b> .....	2
<b>1. INTRODUCTION</b>	
1.1. Lung Cancer .....	3
1.1.1. Definition and histopathology of lung cancer .....	3
1.1.2. Molecular biology of lung cancer .....	4
1.1.3. Factors play role in progression of NSCLC to metastasis .....	4
1.1.4. SP-C C-RAF BXB as a transgenic mouse NSCLC model .....	6
1.2. Cell adhesion molecules and cancer .....	7
1.2.1. Cadherin superfamily .....	9
1.2.2. E-cadherin as an adhesion molecule .....	12
1.2.3. E-cadherin as a tumor suppressor .....	17
1.2.4. Cross talk of E-cadherin with Wnt/ $\beta$ -catenin signalling .....	18
1.3. Experimental design and aim of the project .....	20
1.3.1. DOX inducible dn E-cadherin strategy .....	21
1.3.2. DOX inducible Cre recombinase-mediated <i>Cdh1</i> gene inactivation .....	22
<b>2. RESULTS</b>	
2.1. Construction of PBi5 dn E-cadherin plasmid .....	23
2.2. In vitro analysis of dn E-cadherin expression .....	24
2.3. Generation and characterisation of dn E-cadherin expressing transgenic mice .....	25
2.4. Loss of E-cadherin function in alveolar type II epithelial cells promotes hyperplasia, but is insufficient for tumorigenesis .....	29
2.5. dn E-cadherin expression in SP-C C-RAF BXB adenomas .....	33
2.6. Tumor progression in SP-C C-RAF BXB lung tumors after E-cadherin disruption .....	34
2.7. Expression of dn E-cadherin induces tumor vasculature .....	38
2.8. Restoration of E-cadherin expression reverses the angiogenic switch .....	39
2.9. Oncogenic C-RAF and E-cadherin ablation cooperate in progression to micro- metastasis .....	42
2.10. Lack of evidence for EMT in metastatic lung adenocarcinoma .....	44

---

2.11. Consequences of E-cadherin ablation in normal and oncogenic type II pneumocytes of mouse lung .....	46
2.12. Analysis of dn E-cadherin-mediated angiogenesis .....	53
2.13. Chronic expression of dn E-cadherin in SP-C RAF BXB expressing lung epithelial cells up-regulates $\beta$ -catenin-responsive genes that include endodermal and other lineage markers .....	60
<b>3. DISCUSSION</b>	
3.1. Is interference with E-cadherin function oncogenic? .....	62
3.2. Induction of angiogenic switch by disruption of E-cadherin .....	62
3.3. E-cadherin disruption promotes tumor progression to micrometastasis .....	63
3.4. Disruption of E-cadherin activates $\beta$ -catenin signalling .....	64
3.5. Up-regulation of $\beta$ -catenin target genes after E-cadherin ablation .....	66
<b>4. MATERIALS AND METHODS</b>	
4.1. Materials .....	68
4.1.1. Instruments .....	68
4.1.2. Chemical reagents and general materials .....	69
4.1.3. Cell culture materials .....	71
4.1.4. Antibodies .....	72
4.1.5. Enzymes .....	73
4.1.6. Kits .....	73
4.1.7. Plasmid DNA .....	74
4.1.8. Oligonucleotides .....	74
4.1.9. Cell lines, mouse lines and bacterial strains .....	77
4.2. Solutions and buffers .....	77
4.2.1. Bacterial medium and DNA isolation buffers .....	77
4.2.2. DNA buffers .....	78
4.2.3. Protein analysis buffers .....	79
4.2.4. Histological buffers .....	80
4.3. Methods .....	80
4.3.1. Bacterial manipulation .....	80
4.3.1.1. Preparation of competent cells (CaCl <sub>2</sub> method) .....	80
4.3.1.2. Transformation of competent bacteria .....	80

---

4.3.2. DNA methods .....	81
4.3.2.1. Electrophoresis of DNA on agarose gel .....	81
4.3.2.2. Isolation of plasmid DNA from agarose .....	81
4.3.2.3. Purification of plasmid DNA (QIAquick PCR purification kit) .....	81
4.3.2.4. Ligation of DNA fragments .....	81
4.3.2.5. Cohesive-end ligation .....	82
4.3.2.6. Mini-preparation of plasmid DNA .....	82
4.3.2.7. Maxi-preparation of plasmid DNA .....	82
4.3.2.8. Measurement of DNA concentration .....	82
4.3.2.9. Isolation of genomic DNA from cell and tissue .....	83
4.3.2.10. Southern blot .....	83
4.3.3. RNA methods .....	83
4.3.3.1. Isolation of RNA from cells and tissues using TRIzol reagent .....	83
4.3.3.2. Isolation of RNA from cells and tissues using BioRobot Technology ...	83
4.3.3.3. Quantification and determination of quality of RNA .....	84
4.3.3.4. RT-PCR .....	84
4.3.3.5. Isolation and RT-PCR analyses of RNAs obtained from microdissected tissues .....	85
4.3.3.6. Real Time RT-PCR analyses .....	85
4.3.4. Protein methodologies .....	85
4.3.4.1. Measurement of protein concentration (Bio-Rad protein assay) .....	85
4.3.4.2. Sodium dodecyl sulfate polyacrylamide gel electrophoresis .....	86
4.3.4.3. Immunoblotting .....	86
4.3.4.4. Immunoblot stripping .....	87
4.3.4.5. Immunoblotting of proteins isolated from type II pneumocytes .....	87
4.3.4.6. Luciferase reporter gene assay .....	88
4.3.5. Cell culture techniques .....	88
4.3.5.1. Transient transfection of cells using lipofectamine reagent .....	88
4.3.5.2. siRNA transfection of cells .....	88
4.3.5.3. Isolation of type II pneumocytes from mouse lung .....	88
4.3.6. Histological methods .....	90
4.3.6.1. Embedding in paraffin .....	90
4.3.6.2. Hematoxylin/eosin staining for paraffin embedded sections .....	90
4.3.6.3. Hematoxylin/eosin staining for LCM .....	90

4.3.6.4. Histopathology and immunofluorescence microscopy .....	91
4.3.6.5. TUNEL assay .....	92
4.3.7. Generation of dnE-cadherin transgenic mice .....	93
4.3.8. Statistical analysis .....	94

**REFERENCES**

**APPENDIX**

**CURRICULUM VITAE**

## **Zusammenfassung**

Beim humanen nichtkleinzelligen Bronchialkarzinom ist die schrittweise Progression vom gutartigen Tumor zur malignen Metastasierung weitestgehend ungeklärt. In einem transgenen Mausmodell für das humane nichtkleinzellige Bronchialkarzinom, in dem in Lungenepithelzellen eine onkogene Mutante der Proteinkinase C-RAF exprimiert wird, können einzelne Schritte im Prozess der malignen Progression entschlüsselt werden. Die durch C-RAF induzierten Adenome zeichnen sich durch eine hohe genomische Stabilität in den Tumorzellen, durch starke interzelluläre Adhäsionskontakte zwischen den Tumorzellen und das Fehlen einer malignen Progression aus. Hier wurde demzufolge untersucht, ob die Auflösung der E-Cadherin-vermittelten Zellkontakte zwischen den einzelnen Tumorzellen eine Metastasierung auslösen könnte. Es wurden zwei genetische Ansätze verfolgt, um die Rolle der Tumorzelladhäsion im C-RAF Modell zu bewerten, die konditionelle Eliminierung des E-Cadheringens *Cdh1* sowie die regulierbare transgene Expression von dominant-negativem E-Cadherin. Die Auflösung der E-Cadherin-vermittelten Zelladhäsion führte zur Neubildung von Tumorgefäßen, welche in der frühen Phase der Gefäßbildung durch Wiederherstellung des Zellkontakts reversibel war. Die vaskularisierten Tumore wuchsen schneller, bildeten invasive Fronten aus und führten zur Ausbildung von Mikrometastasen. Es konnte gezeigt werden, dass Beta-Catenin für die Induktion der Angiogenesefaktoren VEGF-A und VEGF-C in Lungentumorzelllinien des Menschen und der Maus essentiell war. Lungentumorzellen aus den in situ Tumoren mit aufgelösten E-Cadherin-vermittelten Zellkontakten exprimierten Gene endodermaler und anderer Zellabstammung, was epigenetische Reprogrammierung in Tumorzellen als den Mechanismus bei der malignen Progression vermuten lässt.



**SUMMARY**

Steps involved in the progression of non-small cell lung cancer (NSCLC) to metastasis are poorly understood. Expression of oncogenic *C-RAF* in lung epithelial cells has yielded a model for non-small cell lung cancer (NSCLC). The induced adenomas are characterised by high genomic stability, a lack of tumor progression and pronounced cell-cell contacts raising the question whether disruption of E-cadherin complexes would promote progression to metastasis. Two genetic approaches were used to evaluate the role of adherens junctions in a C-RAF driven mouse model for NSCLC: conditional ablation of the *Cdh1* gene and expression of dominant negative (dn) E-cadherin. Disruption of E-cadherin function caused massive formation of intratumoral vessels that was reversible in the early phase of induction. Vascularized tumors grew more rapidly, developed invasive fronts and gave rise to micrometastasis.  $\beta$ -catenin was identified as a critical effector of E-cadherin disruption leading to up-regulation of angiogenic inducers (VEGF-A and VEGF-C) in mouse and human lung tumor cell lines. In vivo, lung tumor cells with disrupted E-cadherin expressed  $\beta$ -catenin target genes of endodermal and other lineages suggesting that reprogramming may be involved in metastatic progression.

# **1. INTRODUCTION**

## **1.1. Lung cancer**

### **1.1.1. Definition and histopathology of lung cancer**

Lung cancer is a highly aggressive and challenging cancer that represents the leading cause of cancer death throughout the world. In comparison to other cancers, lung cancer is more frequently diagnosed at an advanced metastatic stage, which is generally not curable (Carny et al., 2002). More recently there has been modest success using novel agents, typically small molecules and monoclonal antibodies, to target signalling transduction pathways, growth factor receptors, oncogenes and tumor suppressor genes known to be aberrant in lung cancer (Smith et al., 2004). Despite major advances in cancer treatment in the past two decades, the prognosis of patients with lung cancer has improved only minimally. Further elucidation of the molecular mechanisms underlying lung cancer is essential for the development of new effective therapeutic agents.

There are two main types of lung cancer categorised by the size and appearance of the malignant cells: non-small cell lung cancer (NSCLC) and small-cell lung cancer (SCLC) (Sharma et al., 2007). SCLC (comprising 20% of lung cancers), always considered a systemic illness, is associated with poor prognosis and is usually treated with chemotherapy. NSCLC is the most frequent (comprising 80% of lung cancers) type of lung cancer with high metastatic potential and low cure rate (American Cancer Society, 2006). For advanced NSCLC, average survival is 6 months for untreated patients, and 9 months for patients treated with chemotherapy. NSCLC is thought to originate in lung epithelial cells and comprises diverse histological subtypes including squamous cell carcinoma, large cell carcinoma and adenocarcinomas. Adenocarcinoma is the most common subtype of NSCLC, accounting for 25-35 % of lung cancers ([www.merck.com/mmpe/sec05/ch062](http://www.merck.com/mmpe/sec05/ch062)).

### 1.1.2. Molecular biology of lung cancer

It has been demonstrated that multiple genetic and epigenetic changes are involved in the development and progression of lung cancer (Girard et al., 2000). These changes do not only occur at the chromosomal level as large deletions (LOH in chromosome 3p, 9p, 8p and 17p) or amplifications but also through nucleotide mutations (i.e. *KRAS* mutations) and epigenetic changes. An overview of prominent genetic aberrations found in NSCLC is summarized in Table 1 (Meuwissen and Berns, 2005).

**Table 1.** Major genetic aberrations in NSCLC

<i>Myc</i>	Amplifications	5%-20%
<i>K-RAS</i>	Mutations	15%-20%
<i>EGFR</i>	Mutations	20%
<i>INK4a</i>	LOH	70%
<i>p16 INK4a</i>	Mutations	20%-50%
<i>p14 ARF</i>	Mutations	20%
<i>TP53</i>	LOH	60%
<i>TP53</i>	Mutations	50%
<i>RB</i>	LOH	30%
<i>RB</i>	Mutations	15%-30%
<i>FHIT</i>	Mutations	40%
<i>DMBT1</i>	Mutations	40%-50%
<i>LOH</i>	3p, 4p, 4q, 8p	10%-100%
<i>INK4a</i>	Promoter hm	8%-40%
<i>RAR<math>\beta</math></i>	Promoter hm	40%
<b><i>CDH1 (E-cadherin)</i></b>	Promoter hm	55%
<i>TIMP-3</i>	Promoter hm	25%

### 1.1.3. Factors play role in progression of NSCLC to metastasis

The main characteristics of malignant tumors are invasive growth and the tendency to metastasise. Lung cancer is frequently highly invasive or metastatic at the time of initial diagnosis. Even without nodal metastasis, the 5-year survival is 50-70%, and death follows metastatic spread (Suzuki et al., 1999).

Increasing body of evidence indicated that excessive tumor cell proliferation alone is not sufficient to produce a malignant tumor. The generation of a lethal tumor mass requires tumor cell proliferation plus angiogenesis. Tumor cell proliferation alone, in the absence of

angiogenesis, can give rise to dormant (early benign neoplastic lesion characterised by the absence of angiogenic switch), harmless microscopic tumors of  $\sim 1 \text{ mm}^3$  or less (Folkman, J., 2002). Angiogenesis is required for invasive tumor growth and metastasis and constitutes an important point in the control of cancer progression. The formation of new blood vessels (angiogenesis) is crucial for the growth and persistence of primary solid tumors and their metastases. Furthermore, angiogenesis is also required for metastatic dissemination, since an increase in vascular density will allow easier access of tumor cells to the circulation (Folkman, J., 2006). Lung cancers engender angiogenesis. There is mounting evidence that angiogenesis plays a significant role in the survival of NSCLC patients (Herbst et al., 2005). High angiogenic activity in conjunction with high levels of vascular endothelial growth factors (VEGFs) has been noted in approximately 30-40 % of NSCLCs (O'Byrne et al., 2000). Specifically intratumoral VEGF-A and VEGF-C expression were shown to be major prognostic factors for patients with NSCLC (Nakashima et al., 2004). Vascularised NSCLC is well known for its ability to metastasize into regional lymph nodes even at early tumor stages and tumor lymphangiogenesis is directly correlated with lymph node metastasis (Renyi-Vamos et al., 2005).

Control of tumor metastasis is one of the most important problems in the design of therapies for cancer patients. Its initial step is the escape of the cells from the primary tumors, which is considered to be dependent on the status of various adhesion molecules, including cadherins, integrins, and the immunoglobulin superfamily (Bremnes et al., 2002). Among these adhesion molecules, cadherin family members were consistently shown to be involved in the progression of NSCLC. Functional disruptions of various cadherin members were shown to be correlated with tumor dedifferentiation and metastasis of NSCLC (Liu et al., 2001; Nakashima et al., 2003; Kim et al., 2005).

#### 1.1.4. SP-C C-RAF BXB as a transgenic mouse NSCLC model

In order to highlight mechanism(s) of lung tumor formation and progression, a range of mouse models for lung cancer have been described. Mouse models for lung cancer can serve as valuable tool not only for understanding the basic lung tumor biology but also for the development and validation of new tumor intervention strategies as well as for the identification markers for early diagnosis.

To gain insights into biology of NSCLC various transgenic mouse models have been developed in which oncogene expression is targeted to a specific subset of lung epithelial cells. One such model was previously described to generate benign lung adenomas after oncogenic C-RAF expression in alveolar epithelial type II pneumocytes (Kerkhoff et al., 2000) (Fig. 1.1 and Fig 1.2).

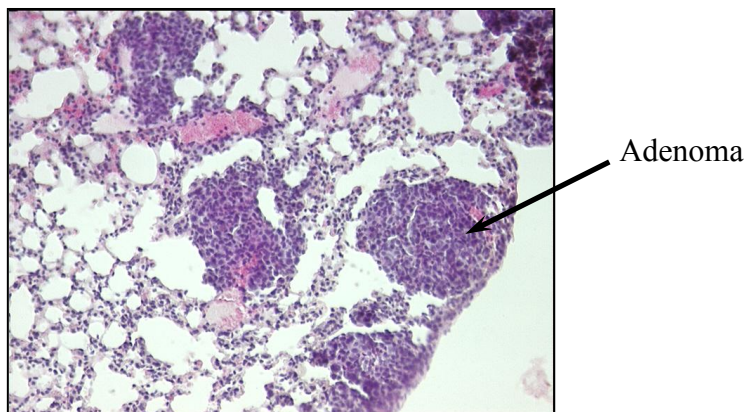


**Fig. 1.1.** H&E staining of a lung section from SP-C C-RAF BXB mouse shows benign lung adenomas.

SP-C C-RAF BXB mice reproducibly develop multiple lung adenomas early in postnatal life. Adenomas consist of cuboidal cells that grow continuously without signs of apoptosis (Fedorov et al., 2002; Götz et al., 2004) and eventually kill the host by elimination of gas exchange surface. Progression of the SP-C C-RAF BXB adenomas to metastasis was neither observed in aged animals (Kerkhoff et al., 2000) nor after removal of p53 (Fedorov et al., 2003) making this transgenic model an ideal system for identification of NSCLC progression factors (Rapp et al., 2003).

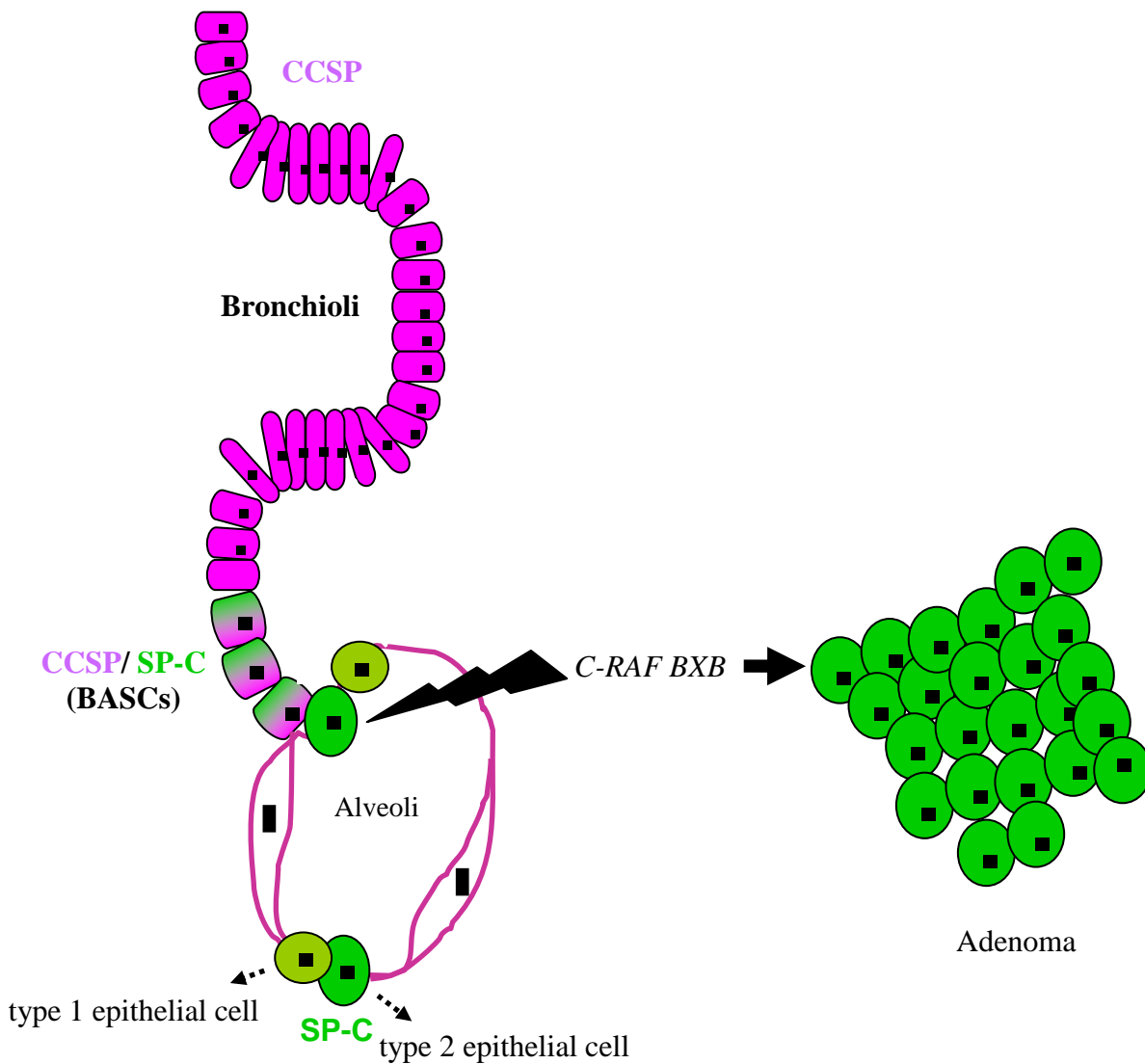


**Fig. 1.2.** Cartoon of a representative mouse distal lung demonstrates adenoma formation after oncogenic C-RAF expression in alveolar type II pneumocytes. Alveolar epithelial type II cells (**dark green**) were presented with surfactant protein C (SP-C) marker. Clara cells of the bronchioles (**purple**) were presented with clara cell secretory protein (CCSP) marker. BASC cells were highlighted by having both markers.

## 1.2. Cell Adhesion Molecules (CAMs) and Cancer

The observation that malignant tumor cells overcome intercellular adhesion to disseminate to distant organs has led to the notion that changes in cell-cell and cell-matrix adhesion coincide with tumor progression. Recent experimental results indicate that in addition to their adhesive functions, cell-adhesion molecules also modulate signal transduction pathways by interacting

with molecules such as receptor tyrosine kinases, components of WNT signalling pathway, and Rho-family GTPases.

Changes in the expression or function of cell-adhesion molecules can therefore contribute to tumor progression both by altering the adhesion status of the cell and by affecting cell signalling (Gupta and Massague, 2006; Kartenbeck et al., 2005; Cavallaro and Christofori, 2004). Most of the studies predominantly focused on the behaviour of four main CAMs including integrins, selectins, immunoglobulin family (IgSF) and cadherins (Fig. 1.3).

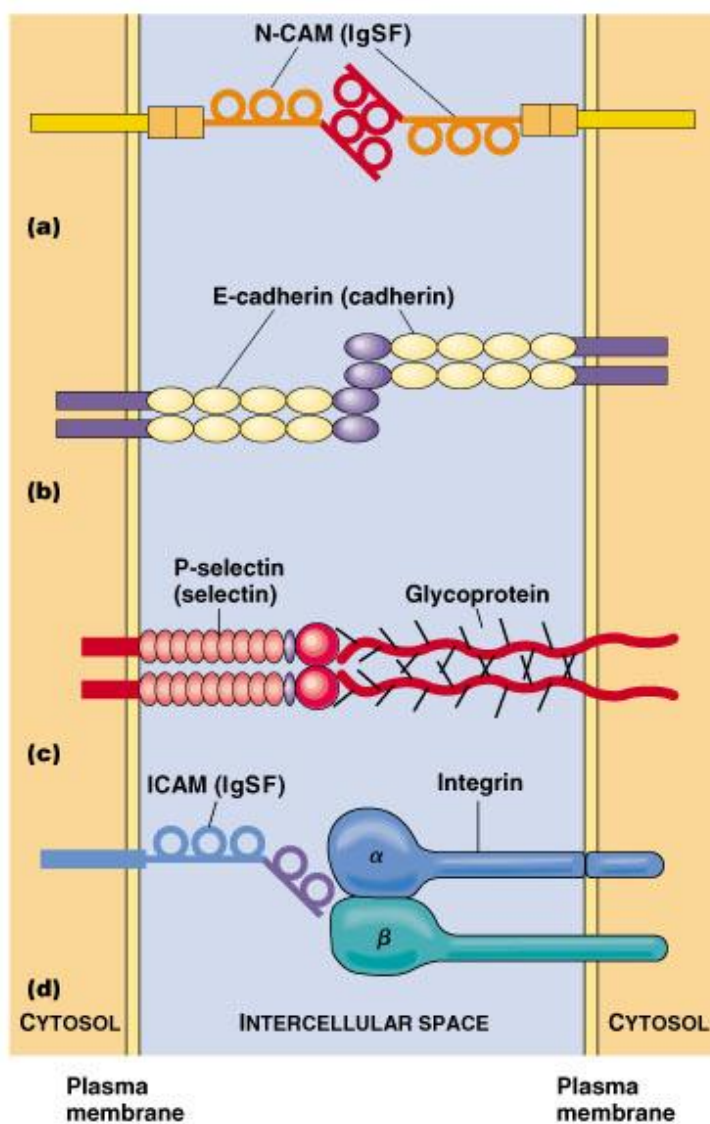
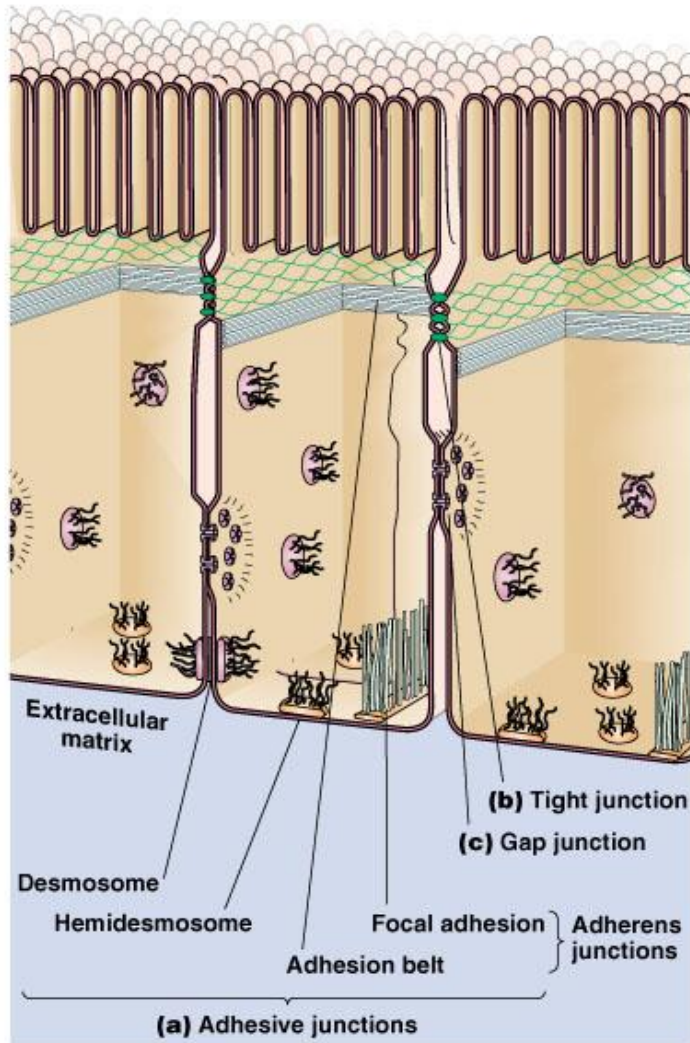


**Fig. 1.3.** Classes of cell adhesion molecules and some of their prototype members that are frequently involved in cancer progression.

### 1.2.1. Cadherin Superfamily

Adhesion between vertebrate cells is generally mediated by three types of junction: Tight junctions (TJ), adherence junctions (AJ) and desmosomes (Cavallaro and Christofori, 2004) (Fig. 1.4).



Copyright © 2003 Pearson Education, Inc., publishing as Benjamin Cummings.

**Fig. 1.4.** Three most common types of cell junctions.

Cadherins are transmembrane proteins that are organised in cell-cell attachment sites called zonula adherens or adherence junctions (Takeichi, M., 1995). Cadherins show an exquisite specificity in their homophilic interactions by almost exclusively binding the same type of cadherin on another cell. They play an important role in morphogenesis during embryonic development and in maintaining histoarchitectural integrity in adult tissues (Akimoto et al.,



1999). The cadherin superfamily is comprised of more than 100 members in vertebrates, grouped into subfamilies that are designated as classical cadherins, desmosomal cadherins, protocadherins, Flamingo/CELSRs and FAT (Takeichi, M., 2007) (Fig. 1.5).

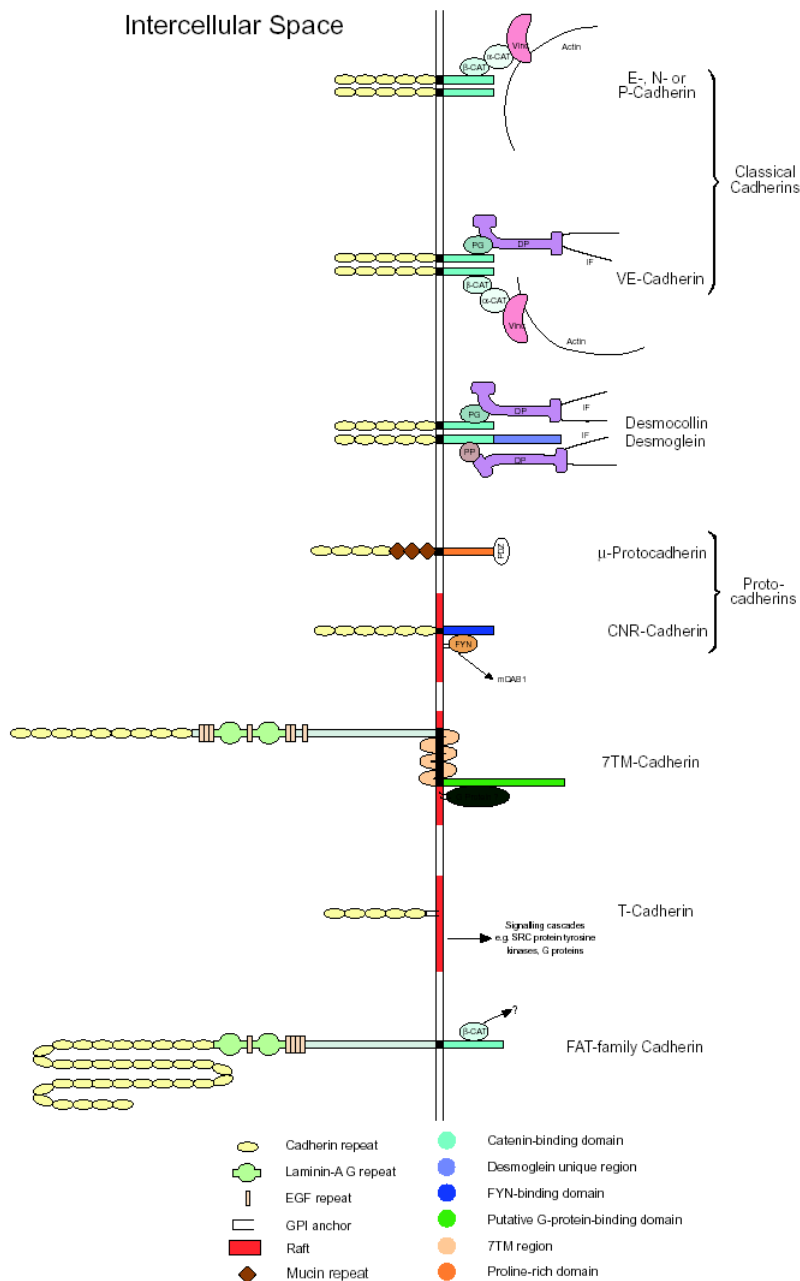


**Fig. 1.5.** Schematic overview of the cadherin superfamily depicting representative molecules for the respective subfamilies.  $\alpha$ -CAT,  $\alpha$ -catenin;  $\beta$ -CAT,  $\beta$ -catenin; PG, plakoglobin; PP, Plakophilin; Vinc, vinculin; IF, intermediate filament; DP, desmoplakin. Desmocollin and Desmoglein can each bind to DP via PG or PP, but, for simplicity, only one interaction is illustrated. Lateral dimmers are shown for classical and desmosomal cadherins. For the other

cadherins only monomers are shown for simplicity and because of lack of direct evidence for dimmers. VE-cadherin can interact with both the IF and actin systems; for illustrative purposes, both types of interaction are shown on the same lateral dimer (Angst et al., 2000).

The biological functions of the family members seem to have diverged: some of them, including classic cadherins and desmosomal cadherins, are well defined as adhesion molecules, but most of the other members do not necessarily show strong adhesion activities (Cavallaro and Christofori, 2004). The extracellular domain of cadherins contains repetitive subdomains called cadherin repeats, which contain sequences that are involved in calcium binding (Fig. 1.6).

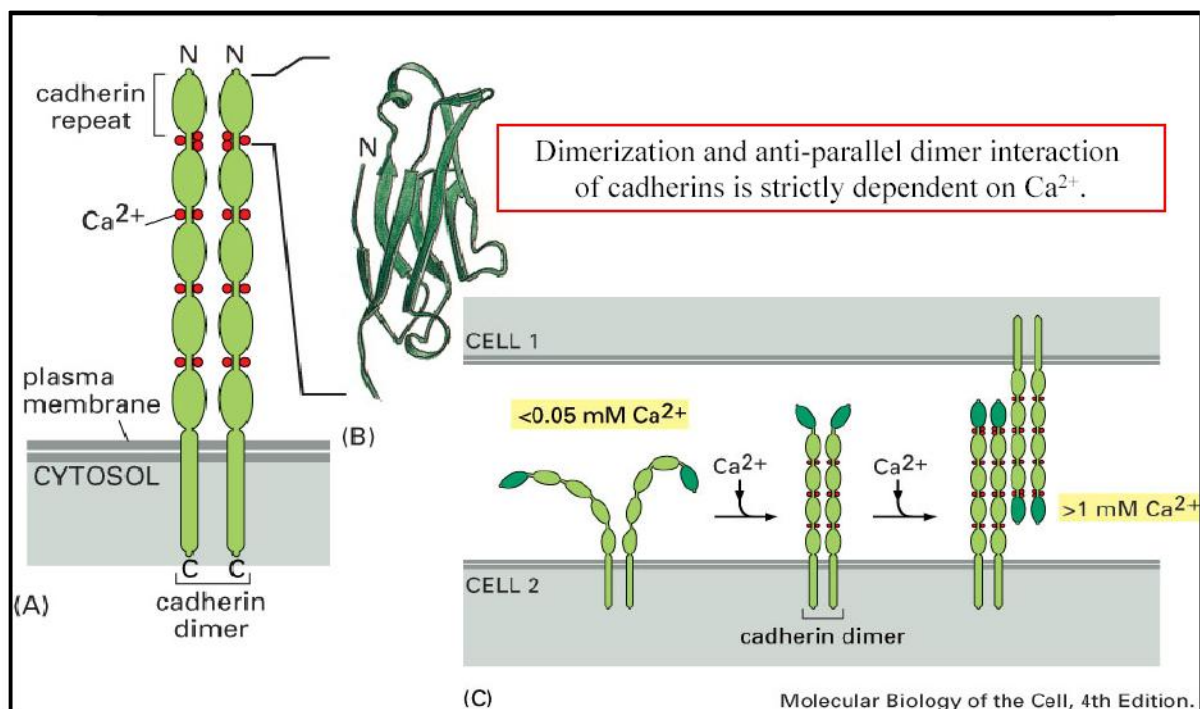


**Fig. 1.6.** Schematic overview of the cadherin regulation by  $\text{Ca}^{2+}$ .

The number of these repeats varies greatly among the members from 1-34 (Fig. 1.5). By contrast, the intracellular domain is not conserved among the subfamilies (Shapiro et al., 1995). The cytoplasmic tails of classical cadherins (which is lacking in non-classical cadherins and protocadherins) interacts with various catenin proteins (Fig. 1.5). The adhesive function of cadherins is dependent on their association with alpha, beta and gamma catenins. Catenins links cadherins with the actin cytoskeleton and mutations in catenin binding sites of

cadherins result in abolition of cadherin/catenin complex formation and a loss of adhesive properties of the cells (Stappert and Kemler, 1994).

Cadherins not only differ in their structures but also they display distinct localisation. Each subtype of classical cadherin tends to be expressed at the highest levels in distinct tissue types during development. For example, E-cadherin (*Cdh1*) is expressed in all epithelia, N-cadherin (*Cdh2*) is expressed in neural tissue and muscle, R-cadherin is expressed in fore-brain and bone, P-cadherin is present in the basal layer of epidermis and VE-cadherin (*Cdh5*) is expressed in endothelial cells (Angst et al., 2001). Other classical cadherins such as Cadherin-6 and Cadherin-11 are expressed preferentially in the kidney and mesoderm, respectively. T-cadherin is an atypical member of the cadherin superfamily (Angst et al., 2001). While processing the general extracellular structure of classical cadherins, T-cadherin lacks transmembrane and cytoplasmic domain and is anchored to the plasma membrane by a glycosylphosphatidylinositol (GPI) moiety. The up-regulation of T-cadherin expression in vascular cells of injured arteries, in vascular proliferative disorders such as atherosclerosis and restenosis, as well as in tumor associated neovascularisation, suggests the involvement of T-cadherin in pathological angiogenesis (Ivanov et al., 2001). In mammals, multiple protocadherins and seven transmembrane (7TM) are highly expressed in the nervous system. FAT family proteins are highly expressed in proliferating tissues during development and are usually less prevalent in adult tissues (Angst et al., 2001). The extraordinarily diverse structures of cadherin superfamily members have adopted to perform a vast array of functions involving intercellular recognition.

### **1.2.2. E-cadherin as an adhesion molecule**

The  $\text{Ca}^{2+}$ -dependent cell-cell adhesion molecule E-cadherin, the founder member of the classical cadherin family, is the major mediator of intercellular adhesion in epithelial tissues (Takeichi et al., 1995; Huber et al., 1996; Bracke et al., 1996). Physiologically, E-cadherin is crucial for the establishment and maintenance of a polarized cellular phenotype in addition to

role in variety of morphogenetic events, including cell migration, separation, and formation of boundaries between cell layers and differentiation of each cell layer into functionally distinct structures (Larue et al., 1994). E-cadherin (Uvomorulin) is the first adhesion molecule expressed in the mouse embryo (Peinado et al., 2004). Maternal and zygotic E-cadherin control the compaction process at the morula stage and the formation of the blastocyst (Ohsugi et al., 1997). Classical gene targeting has demonstrated that E-cadherin-deficient embryos die at the blastocyst stage and *E-cadherin* gene (*Cdh1*) inactivation affects the formation of the trophectoderm, the first epithelium generated during development (Larue et al., 1994). E-cadherin is a single-span transmembrane glycoprotein with an extracellular region, a transmembrane helix and a cytoplasmic domain (Gumbiner, B.M., 1996) (Fig. 1.7).

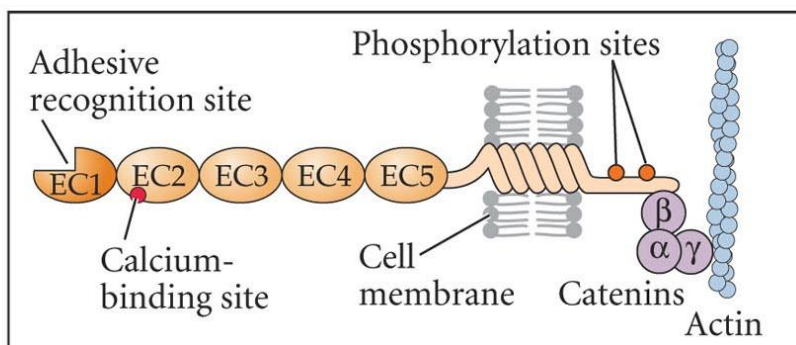


**Fig. 1.7.** Structure of E-cadherin.

Extracellular domain of E-cadherin composed of five cadherin-type repeats (EC 1-5 domains) that interact in a calcium dependent manner with cadherins molecules on neighboring cells and mediates intercellular adhesion through dimeric zipper-like homophilic interactions (Takeichi, M., 1991) (Fig. 1.7 and Fig. 1.8). The intracellular domain of E-cadherin interacts with multiple proteins that functionally link cadherins to the underlying cytoskeleton (Fig. 1.7). The cytoplasmic region of E-cadherin binds to  $\beta$ -catenin (or to its close relative plakoglobin) and to p120.  $\beta$ -Catenin in turn binds to  $\alpha$ -catenin (Fig. 1.8 and Fig. 1.7). The cadherin-catenin complex is connected through alpha catenin to the actin filaments, forming a stable adherens junction (Angst et al., 2001). Another catenin, p120<sup>ctn</sup>, which was originally

identified as a substrate of Src and several receptor tyrosine kinases, also interacts with cytoplasmic domain of E-cadherin and regulates the stability of the cadherin complex at the cell surface (Reynolds et al., 1994). The full adhesive function of E-cadherin depends on the integrity of the entire cadherin-catenin-actin network.

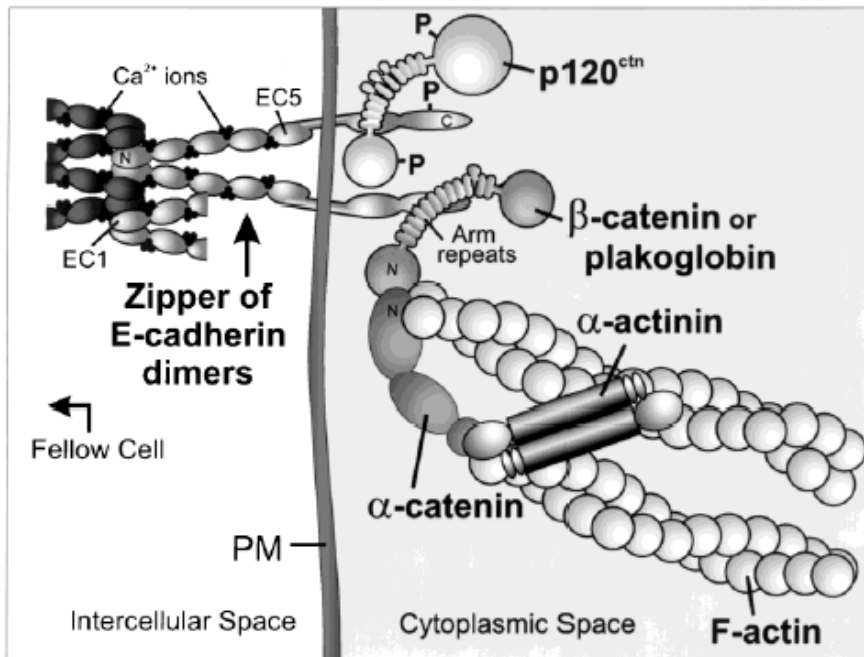


**Fig. 1.8.** Schematic overview of the E-cadherin-catenin-cytoskeleton complex at the plasma membrane (PM) of two neighbouring cells. The N-terminal ends of E-cadherin dimers extend into the intercellular space, where they interact in a homophilic zipper-like fashion with similar E-cadherin dimers (dark globules), extending from the opposing cell surface. The C-terminal ends of E-cadherin molecules extend into cytoplasm and associate with catenins (Takeichi, M., 1991).

E-cadherin expression is regulated at many levels including gene expression and transport to, and protein turnover at the cell surface. E-cadherin transcription is directly regulated by methylation and repression of promoter activity. During carcinogenesis, methylation of the E-cadherin promoter is associated with reduced E-cadherin expression, and with disease progression and metastasis (Strathdee, G., 2002). Several classical cadherin genes also possess an unusually large second intron (in humans, the size of intron 2 compared to total gene size for E-cadherin and N-cadherin are 63 kb to 98 kb and 134 kb to 245 kb, respectively), which has been shown for E-cadherin to contain regulatory elements that modulate overall cadherin levels and tissue-specific expression during development

(Stemmler et al., 2005). Zinc finger proteins of the Slug/Snail family and Smad-Interacting Protein (SIP1) are repressors of E-cadherin gene transcription (Cano et al., 1996; Batlle et al., 2000; Comijn et al., 2001 and Conacci-Sorrell et al., 2003) (Fig. 1.9). In addition to Slug/Snail family, other important transcriptional repressors of E-cadherin were also identified (Fig. 1.9).

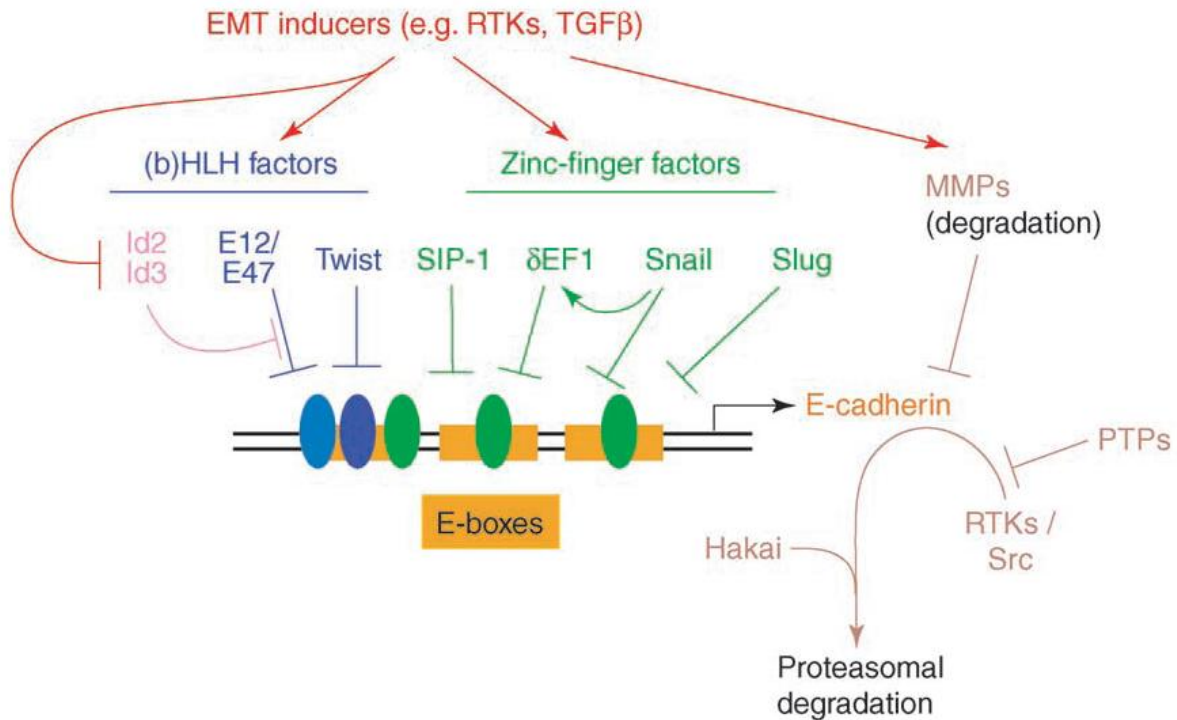


**Fig. 1.9.** E-cadherin expression is downregulated at the transcriptional level. The zinc-finger-containing proteins SIP-1, dEF-1, Snail and Slug (marked in green), and the helix–loop–helix transcription factors E12/E47 and Twist (blue) are important transcriptional repressors that bind to E-boxes in the promoter of the E-cadherin gene and actively repress its expression. Epithelial–mesenchymal transition (EMT) inducers such as RTKs or TGFb (red) stimulate expression of these E-cadherin repressors in tumor cells, while Id proteins (known to repress E12/E47 proteins) are inhibited (pink).

Decreased E-cadherin gene transcription results in a loss of cell–cell adhesion and increased cell migration (Thiery, J.P., 2002), as well as accumulation of cytoplasmic, signaling-competent  $\beta$ -catenin that may function independently of, or synergize with Wnt signaling (Ciruna and Rossant, 2001). Slug may be a target gene of the TCF/ $\beta$ -catenin complex (Conacci-Sorrell et al., 2003) that also binds to and represses the E-cadherin promoter (Jamora et al., 2003). Thus, repression of cadherin expression by Slug/Snail/SIP1 or TCF/ $\beta$ -catenin

complex may not only reduce cell–cell adhesion, but the concomitant increase in cytoplasmic  $\beta$ -catenin may lower the activation threshold of the Wnt pathway.

The cadherin-catenin adhesion complex is also regulated by post-translational mechanisms. The structural integrity of the cadherin/catenin complex is positively and negatively regulated by phosphorylation. Tyrosine phosphorylation of catenins has been shown to decrease cell-cell adhesiveness, whereas dephosphorylation appears to increase adhesion (Hirohashi, S., 1998).  $\beta$ -catenin, plakoglobin and p120<sup>ctn</sup> all demonstrate tyrosine phosphorylation by cytoplasmic protein kinases of the Src family and by transmembrane receptor tyrosine kinases (RTKs). RTKs may also disrupt cellular adhesion by phosphorylation of catenins. Both hepatocyte growth factor/scatter factor and epidermal growth factor (EGF) induce phosphorylation of  $\beta$ -catenin and plakoglobin in human carcinoma cell lines (Shibamoto et al., 1994). In addition to the potential role of kinases in post-transcriptional regulation of the cadherin-catenin complex, GTPases also appear to play a possible role in regulating cadherin-catenin function. Previous studies showed that Rho-family small GTPases, including proteins Rho, Rac, and Cdc42, function in cadherin-mediated cell-cell adhesion. Rho and Rac are required for the formation of cadherin-based cell-cell adhesion contacts (Braga et al., 1997; Takaishi et al., 1997). Specifically, p120<sup>ctn</sup> was shown to bind cadherins and RhoA in a mutually exclusive manner, binding to inactivate RhoA and retaining it in an inactive state (Anastasiadis et al., 2000), thus inhibiting downstream signaling believed to promote strong adhesion. Rho-family GTPases Cdc42 and Rac1 also directly regulate E-cadherin activity (Kaibuchi et al., 1999). When Cdc42 and Rac1 are in the inactive form, their effector protein, IQGAP1, binds both to the cytoplasmic domain of E-cadherin and to  $\beta$ -catenin, apparently causing disassociation of alpha-catenin from the cadherin-catenin complex and a decrease in cell adhesion (Kuroda et al., 1998; Fukuta et al., 1999). These findings suggest that any significant change in expression or structure of one of the involved components leads to

adherens junction disassembly and consequently nonadhesive invasive and metastatic cells (Pignatelli and Vessey, 1994; Birchmeier and Behrens, 1994).

### **1.2.3. E-cadherin as a tumor suppressor**

Changes in cell-cell and cell-matrix interactions or dysfunctions of the complex result in the loss of cell adhesion and cell polarity, thus accounting for the ability of cancer cells to cross normal tissue boundaries and metastasise (Takeichi, M., 1991). If not all, most human cancers originate from epithelial tissue. In addition to its well-established function in adhesion of epithelial cells, reduced expression or mutations in E-cadherin has been frequently implicated in tumorigenesis (Bex et al., 1998). Disruption of E-cadherin cell adhesion complex has been correlated with various pathologic and clinical features, such as tumor dedifferentiation, infiltrative growth, lymph node metastasis, and a poorer patient prognosis (Calvisi et al., 2004). Numerous in vitro studies have shown that E-cadherin overexpression inhibits cellular growth, transformation and invasiveness (Chen and Obrink, 1991; Vlamincx et al., 1991; Frixen et al., 1991). Furthermore, forced expression of E-cadherin blocked the transition from adenoma to carcinoma in a transgenic model of pancreatic  $\beta$ -cell carcinogenesis (Perl et al., 1998). These results indicated that restoring E-cadherin expression in tumor cells reduces or blocks progression to metastasis both in vitro and in vivo.

The loss of E-cadherin function during tumor progression can be caused by various genetic or epigenetic mechanisms (i.e. promoter methylation) (Matsumura et al., 2001). Perhaps, the strongest evidence in support of a causal role for cadherin alterations in cancer pathogenesis is the observation that germline mutations in the gene encoding *E-cadherin* (*Cdh1*) strongly predispose affected individuals to diffuse-type gastric cancer (Guilford et al., 1998). Somatic *Cdh1* gene mutations resulting in E-cadherin inactivation have also been demonstrated in carcinomas. The highest mutation frequencies were reported in diffuse-type gastric and infiltrative lobular breast carcinomas (Becker et al., 1994; Bex et al., 1995 and Bex et al., 1998). Somatic mutations in *Cdh1* have also been reported in subsets of other malignancies,



such as endometrial, thyroid, bladder and ovarian carcinomas (Risinger et al., 1994) and signet-ring cell carcinomas of the stomach (Muta et al., 1996). Although *Cdh1* mutations play a crucial role in different types of neoplasia, in most cases E-cadherin expression is either down-regulated or lost by different mechanisms during malignant conversion of tumors. Together, these data establish E-cadherin as an important metastasis and/or tumor suppressor, depending on the mechanism and timing of E-cadherin abrogation.

#### 1.2.4. Cross talk of E-cadherin with Wnt/ $\beta$ -catenin signaling

A connection between Wnt signaling and cadherin-mediated adhesion was early suggested because of the dual function of  $\beta$ -catenin in both systems. In addition to its important role in cell-cell adhesion, the multi-talented  $\beta$ -catenin protein also functions in the canonical Wnt/Lef pathway (Huelsenken and Behrens, 2000) (Fig. 1.10).

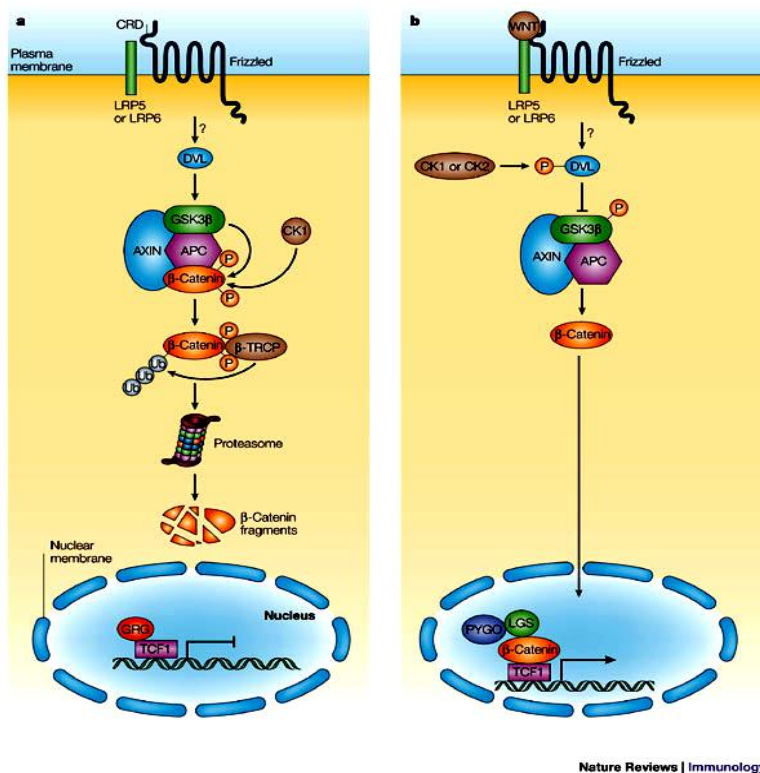


**Fig. 1.10.** Wnt signaling and regulation of  $\beta$ -catenin. Fate of  $\beta$ -catenin was shown in the absence (a) and presence (b) of Wnt signalling. Wnt binds to frizzled receptor (FZ) and LRP5 or LRP6 co-receptor, beginning cascade that frees  $\beta$ -catenin.  $\beta$ -catenin translocates to nucleus and helps activate the T-cell Factor (TCF) / Lymphocyte enhancer-binding factor (LEF) genes.

Under physiologic conditions most cellular  $\beta$ -catenin is bound to E-cadherin, a process regulated by tyrosine kinases and tyrosine phosphatases (Barth et al., 1997; Huber et al., 1996). Cellular levels of uncoupled (free)  $\beta$ -catenin are tightly regulated via its phosphorylation by the GSK3 $\beta$  kinase and binding to the tumor suppressor adenomatous polyposis coli (APC) and axin (Aberle et al., 1997) (Fig. 1.10).

In addition to the potential for Wnt-dependent up-regulation of  $\beta$ -catenin, it is well documented that  $\beta$ -catenin stability is regulated by numerous Wnt-independent mechanisms (Fig. 1.10).

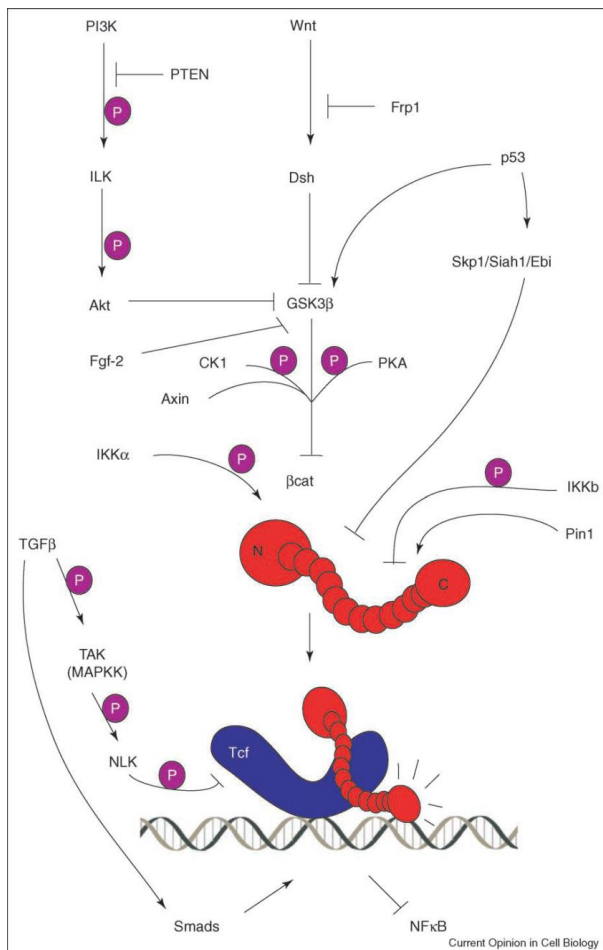


**Fig. 1.11.** A diagram of the signalling pathways acting on  $\beta$ -catenin (shown in red). The most studied of these is the Wnt pathway, which stabilizes  $\beta$ -catenin by inhibiting its N-terminal phosphorylations and ubiquitination. Other factors also stabilize  $\beta$ -catenin, such as Pin-1 and IKK $\alpha$ . P53, which is commonly mutated in cancer, promotes  $\beta$ -catenin degradation through activation of either GSK3 $\beta$  or the Skp/Siah/Ebi complex. PTEN decreases  $\beta$ -catenin signalling by inhibiting the PI3K pathway, which stabilize  $\beta$ -catenin by inactivating GSK3 $\beta$ . TGF $\beta$  has complex effects on  $\beta$ -catenin. It can reduce signalling by inhibiting Lef/Tcfs through NLK or co-activate target genes through Smads.

For example, inhibition of PI3K/Akt pathway was shown to decrease the content of cytoplasmic and nuclear  $\beta$ -catenin and the activity of canonical Wnt pathway through decreased GSK-3 $\beta$  phosphorylation (Persad et al., 2001) (Fig. 1.11). Other signalling pathways that control  $\beta$ -catenin fate were shown in Figure 10. Upon stabilization,  $\beta$ -catenin accumulates in the cytoplasm and subsequently translocates to nucleus in association with members of the T cell factor (TCF)/ lymphoid enhancer factor (LEF) DNA-binding transcription factor family (Miller and Moon, 1996) (Fig.1.10). The  $\beta$ -catenin/Tcf complex subsequently regulates the transcription of many genes involved in cell function, including survival, migration, differentiation and proliferation (current list of  $\beta$ -catenin target genes can be found at [www.stanford.edu/~rnusse/pathways/targets.html](http://www.stanford.edu/~rnusse/pathways/targets.html) homepage). Thus, dysregulation of  $\beta$ -catenin, resulting in its nuclear expression, has been shown to contribute to carcinogenesis in numerous tissues including lung cancer.

### **1.3. Experimental design and aim of the project**

Aberrant expression of E-cadherin was shown to be highly correlated with invasion and spread of NSCLC (Shibanuma et al., 1998). Moreover, reduced or absent expression of E-cadherin was reported to be a significant prognostic factor in patients with NSCLC (Liu et al., 2001; Huang et al., 2005). However, how disruption of E-cadherin complexes may cause lung tumor progression remains largely unresolved. In order to elucidate the role of E-cadherin in NSCLC, I took advantage of a transgenic mouse model of NSCLC, *SP-C C-RAF BXB*, that was generated in our institute and expresses oncogenic C-RAF in alveolar type II epithelial cells (Kerkhoff et al., 2000). It was hypothesized that oncogenic C-RAF might stabilize cell-cell interaction of the adenoma cells, that might in turn contribute to the stability of the tumor cells. I therefore investigated whether disruption of E-cadherin might cause progression of *SP-C C-RAF BXB* adenomas. I also aimed to address the consequences of E-cadherin loss in alveolar type II pneumocytes without oncogenic background to elucidate cellular function and

transformation capacity of E-cadherin. To disrupt E-cadherin function two different genetic approaches were planned as indicated below.

### **1.3.1. DOX inducible dn E-cadherin strategy**

Dominant negative cadherin mutants provide a powerful approach to study cadherin and catenin function both in cultured cells and in intact tissues and organisms (Takeichi, M., 1995). Two types of constructs have been used, one in which the cadherin cytoplasmic domain is deleted and one in which the extracellular domain is deleted. The extracellular domain deletion mutants appear to have a more powerful dominant negative effect than the cytoplasmic domain deletion mutants and they inhibit generally all endogenous cadherins, probably because of the high degree of sequence conservation of the cytoplasmic domain (Fujimori and Takeichi, 1993). The dominant negative mutant that we have used was an E-cadherin cDNA lacking most of its extracellular domain and was shown to efficiently inhibit E-cadherin and N-cadherin function in a pancreatic transgenic tumor model (Dahl et al., 1995). In order to express dn E-cadherin in a conditional manner, we first planned to clone this mutant into a tetracycline responsive element containing plasmid and thereby wanted to generate transgenic mice harbouring a conditional dn E-cadherin mutant (Fig 1.12). Expression of downstream genes driven by tetracycline response element (Tet-O) requires a responder activator, rtTA, and an rtTA-binding molecule, doxycycline, to accomplish inducible gene expression (Fig 1.12). In order to target dn E-cadherin expression into the cell where C-RAF BXB was expressed, I planned to cross SP-C C-RAF BXB mice with a SP-C driven rtTA mice (which were generated previously by the lab of J. Whitsett) so that expression of dn E-cadherin will be targeted to the same cell type (lung alveolar epithelial type II cells) in a way by generating triple transgenic mice (*SP-C C-RAF BXB/SP-C rtTA/Tet-O dn E-cadherin*) constellation (Fig 1.12). Evaluation of double transgenic mice (*SP-C rtTA/Tet-O dn E-cadherin*) in the absence a C-RAF BXB oncogenic background was also aimed to analyze tumorigenic potential of E-cadherin in lung epithelial cells.

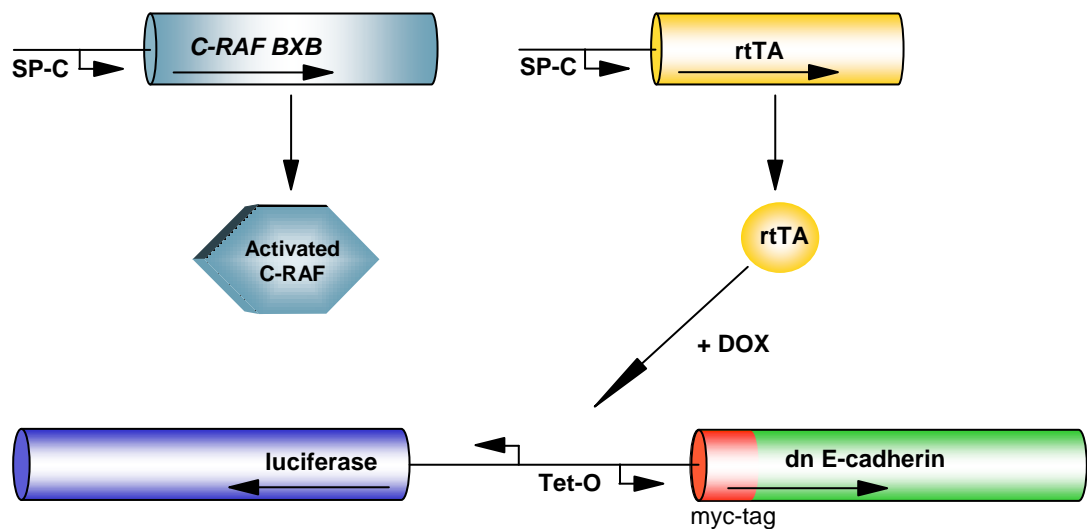


**Fig. 1.12.** Experimental strategy to investigate role of E-cadherin in normal and oncogenic lung epithelial type II pneumocytes. SP-C promoter was used to target type II pneumocytes of the lung. Using a bi-directional promoter of tetracycline operator (Tet-O) provides simultaneous expression of myc-tagged dn E-cadherin and a reporter gene, luciferase, to facilitate monitoring of gene expression upon induction.

### 1.3.2. DOX inducible Cre recombinase-mediated *Cdh1* gene inactivation

Conditional gene deletion is an important experimental approach for examining the functions of particular gene products in mouse models. Cre-mediated site-specific DNA recombination, Cre/*lox P* system, has become widely used in conditional gene targeting, conditional gene repair and activation, inducible chromosome translocation, and chromosome engineering (Florin et al., 2004). Having the availability of flox E-cadherin mice (Boussadia et al., 2002), I planned to inactivate E-cadherin function in type II pneumocytes using a Cre-mediated gene targeting strategy (Fig 1.13). For this purpose, mice expressing Cre recombinase under the tetracycline response element (Tet-O Cre) were planned to be obtained from H. Bujard lab to target E-cadherin deletion into the oncogenic type II epithelial cells of the lung by means of postnatal induction of quadruple mice (*SP-C C-RAF BXB/SP-C rtTA/Tet-O-cre/Cdh1<sup>flox/flox</sup>*) (Fig. 1.13).

Following the above strategies, generations of conditional triple and quadruple mice will be very important in order to obtain a tool for the detailed examination of E-cadherin function in NSCLC development and progression.

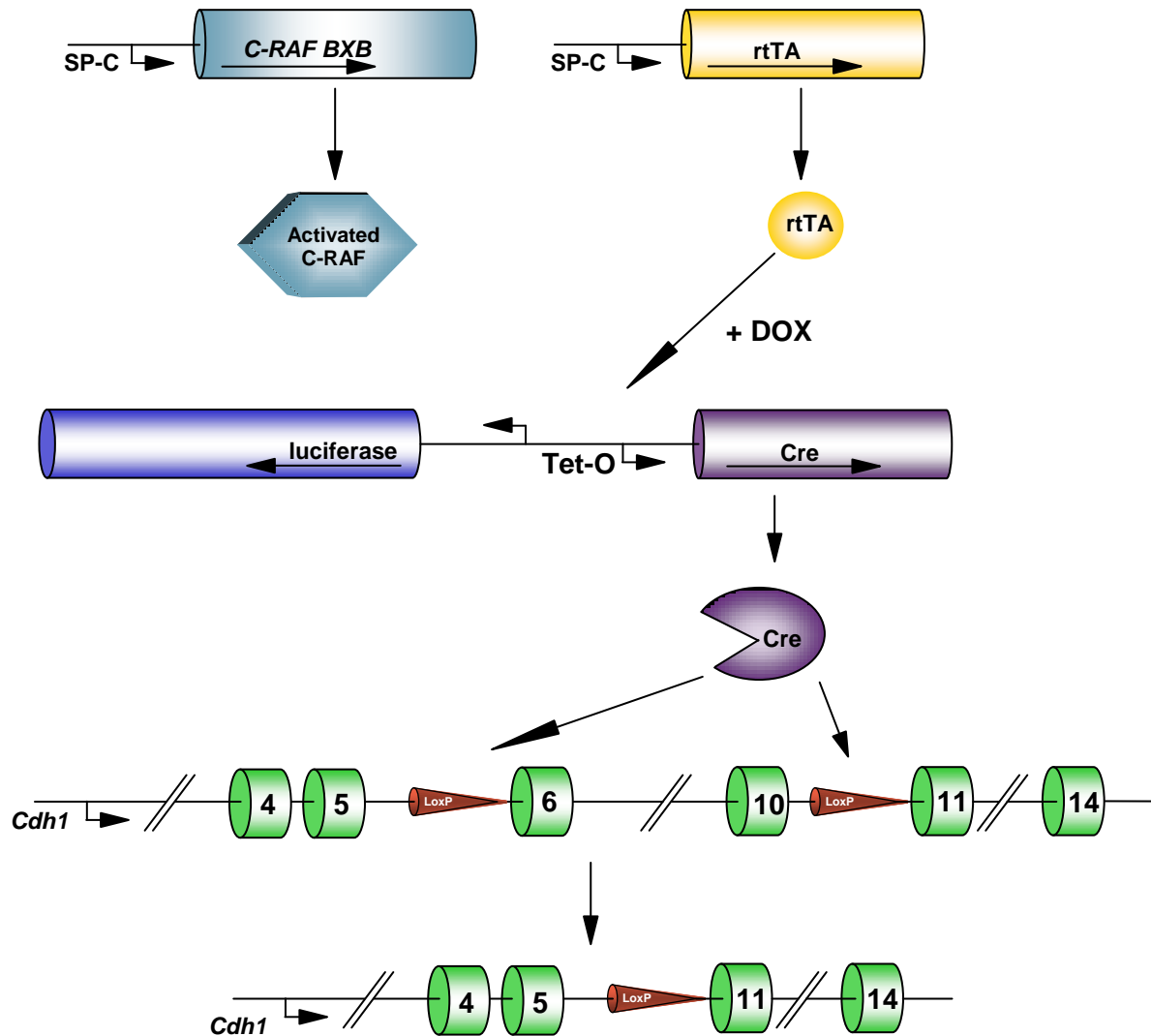


**Fig. 1.13.** Experimental strategy to investigate role of E-cadherin in normal and oncogenic lung epithelial type II pneumocytes.

## 2. RESULTS

### *Part I. Generation and characterisation of transgenic mice that express dn-E-cadherin in a switchable fashion.*

#### 2.1. Construction of PBI5 dn E-cadherin plasmid

To generate transgenic mice conditionally expressing dn E-cadherin, we used a plasmid, obtained from H. Semb, that encodes a 34 kDa myc-tagged cell surface protein where 625 amino acid residues from the extracellular domain of E-cadherin have been deleted (Dahl et al., 1996) (Fig.2.1).

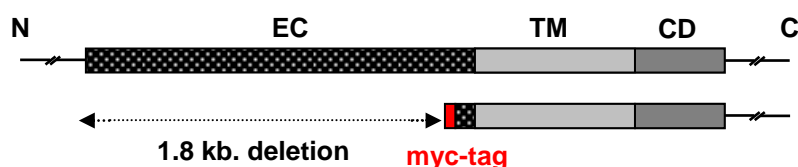


**Fig.2.1.** Structural components of E-cadherin. dn E-cadherin represents a truncated form of endogenous E-cadherin with a fused **myc-tag** epitope. EC: extracellular domain; TM, transmembrane domain; CD: cytoplasmic domain.

In order to express dn E-cadherin conditionally, it was cloned into PBI5 vector that contain a tetracycline response element (Tet-O) with a bidirectional promoter unit. PBI5 vector harbours a reporter gene, luciferase, to facilitate monitoring of gene expression. Construction and preparation of the resulting PBI5 dn E-cadherin plasmid for pronucleus injection was done by Dr. Rudolf Götz. Hilde Troll performed all the pronucleus injections. The dn E-cadherin c-DNA was isolated as a 1,3kb *XbaI* – *HindIII* fragment . The *XbaI* site was blunted with T4 DNA polymerase. The fragment was cloned into the pBI5 vector (containing a tet operator) by cutting with *NheI*/blunt – *HindIII*.

## 2.2. In vitro analysis of dn E-cadherin expression

To test resulting PBI5 dn E-cadherin construct, A-549 human lung tumor cells were co-transfected with an inducer plasmid, SP-C rtTA, in the presence and absence of DOX using lipofectamine reagent.

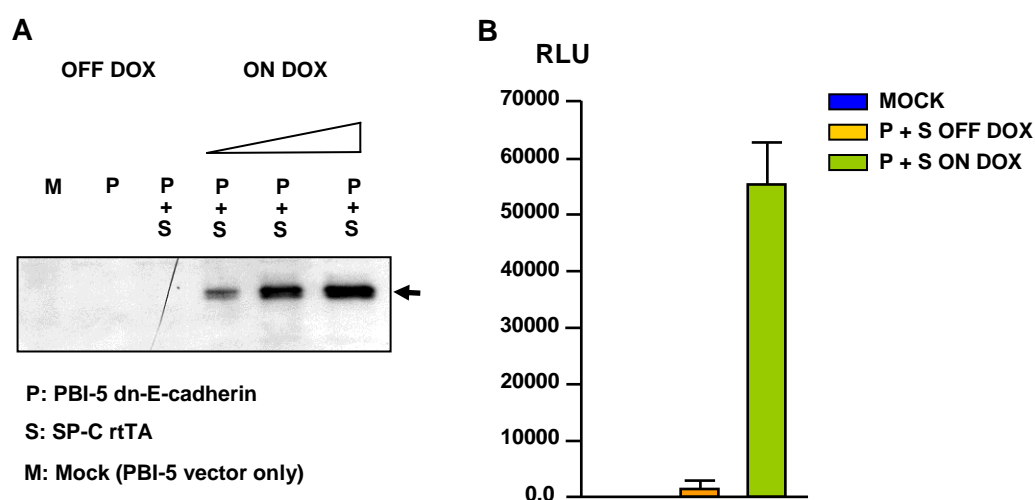


**Fig.2.2.** Conditional expression of dn E-cadherin in A-549 cells. A. Western blot analysis shows dose-dependent expression of dn E-cadherin protein (arrow) after 36 hours post transfection. Doxycycline was applied as 100, 500 and 1000  $\mu\text{g}/\text{ml}$ . dn E-cadherin was detected using an myc tag antibody. B. Post-transcriptional analysis of cells with luciferase assay shows elevated luciferase levels only in induced (ON DOX) cells. Note lack of protein and luciferase expression in the absence of induction (OFF DOX).

Addition of increasing amounts of DOX to the cell culture medium induced dn E-cadherin protein and luciferase expression 36 hours after transfection. Neither single transfection nor the co-transfection of constructs in the absence of DOX gave rise to detectable levels of dn E-cadherin and luciferase (Fig.2.2).

It was previously shown that expression of dn E-cadherin displaced endogenous E-cadherin from cell-cell contacts of  $\beta$ -cells of pancreas (Dahl et al., 1996). To examine whether expression of dn-E-cadherin affected endogenous E-cadherin localisation in a mouse lung adenocarcinoma cell line, 3041, a double immunocytochemistry were applied. As shown in Fig 2.3, endogenous E-cadherin was found to be replaced by dn E-cadherin (tracked by an



myc tag antibody) as early as 18 hours post transfection after DOX administration. Overexpression of dn E-cadherin did not seem to affect endogenous E-cadherin membrane trafficking, but rather replaced the endogenous E-cadherin localisation presumably by membrane competition. This observation is also in agreement with a previous report (Dahl et al., 1996).

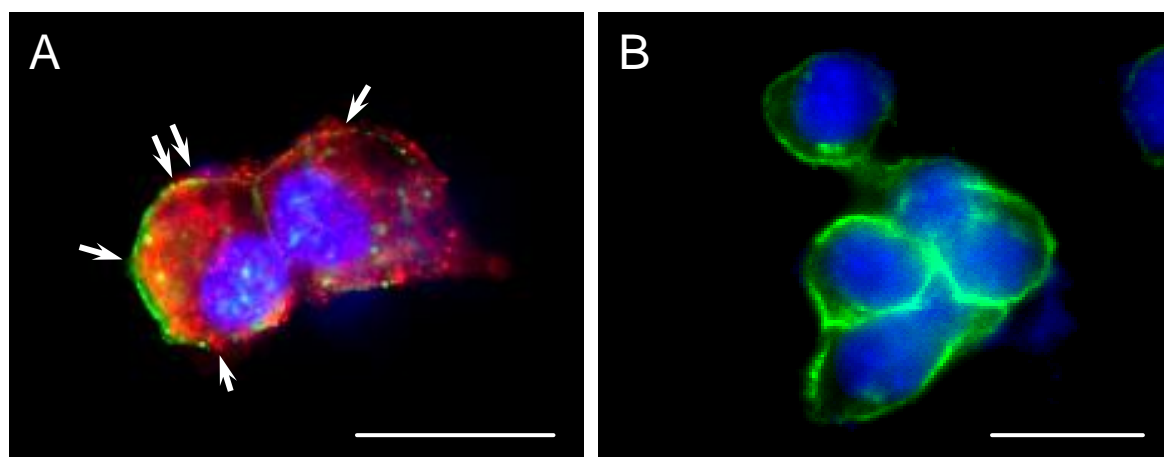


**Fig.2.3.** Immunocytochemistry of mouse 3041 cells after 18 hours post transfection. A. Left picture shows displacement of endogenous E-cadherin (green) from cell membrane after dn E-cadherin (red) overexpression. Arrows indicate cell membrane parts where competition occurred. Note relatively normal membrane transport of endogenous E-cadherin (green cytoplasmic dots) on the right cell whose membrane was completely occupied by dn E-cadherin. B. Non-transfected control cells shows typical E-cadherin membrane localisation. Dapi illustrates cell nuclei. Scale Bar: 10µm.

### 2.3. Generation and characterisation of dn E-cadherin expressing transgenic mice

To generate transgenic mice, PBI5-dn E-cadherin plasmid was cut with *AseI* to remove the vector backbone. The resulting Tet-O dn E-cadherin fragment (6.1 kb) was isolated by gel electrophoresis and injected into the pronucleus of fertilized mouse eggs. Resultant mice were first genotyped by southern blotting (Fig.2.4) and subsequently by PCR. Four germ-line transmitting founder animals (Founder number: 188, 253, 261 and 272) were generated and all of them were crossed with *SP-C-rtTA* inducer mice that express the reverse tetracycline transactivator protein (rtTA) in lung alveolar type II epithelial cells (Perl et al., 2002) to generate bitransgenic (*SP-C rtTA / Tet-O dn E-cadherin*) mice. Analysis of luciferase activity

in lung tissue extracts from DOX-induced bitransgenic mice showed 1000-fold increase luciferase levels in one line, founder number 253, after a 1-week induction period. This line was used for all further experiments presented here (Fig.2.5). As expected luciferase expression was detected only in the lung tissues of induced mice demonstrating tissue specific expression (Fig.2.6). Line 253 was backcrossed for three generations onto C57BL/6 background before crossing with *SP-C-rtTA* inducer mice.

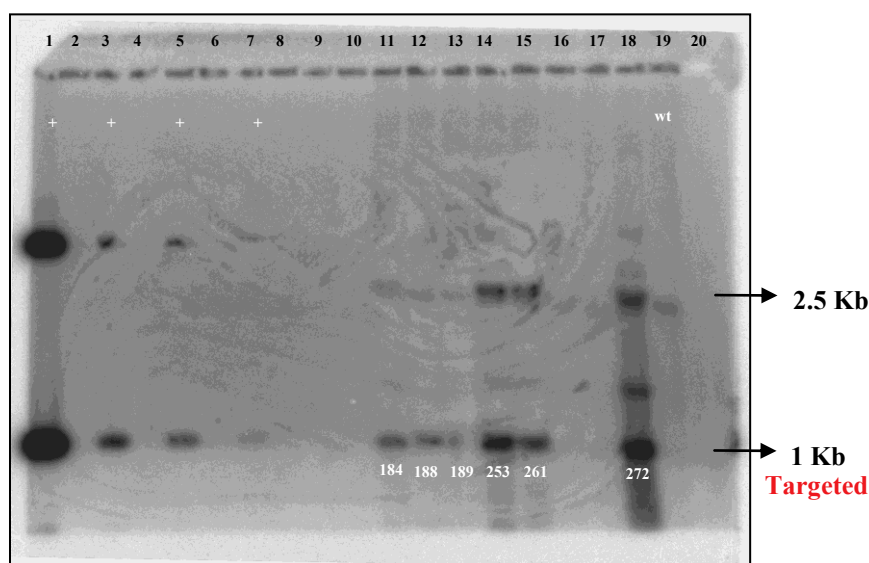


**Fig.2.4.** Southern blot analysis of potential founders for dn E-cadherin integration. Line 1, 3, 5 and 7 was used as positive control (+). Line 19 (negative control) represent genomic DNA from a wild type (wt) animal. Targeted integration was calculated as 1 Kb and showed 5 positive founders named as 184, 188, 253, 261 and 272, respectively. Wild type E-cadherin allele was detected as 2.5 Kb fragment.

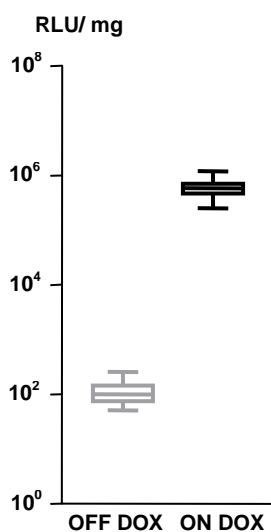


**Fig.2.5.** Relative luciferase unit (RLU) values of lung tissues from six weeks-old bitransgenic mice shows elevated luciferase levels after one week DOX administration (ON DOX). Control mice (OFF DOX) shows only background levels. 10 mice were evaluated for each group.

Since PBI5 dn E-cadherin vector contains a bi-directional promoter, simultaneous dn E-cadherin protein co-expression was also analysed in bitransgenic mice before and after DOX treatment. Immunoblot analysis of lung tissues showed tight conditional dn E-cadherin expression in vivo (Fig.2.7).

TISSUE	RLU / mg
Skin	197
Muscle	166
Blood	189
Brain	207
Heart	354
Lung	848.000
Liver	345
Spleen	198
Pancreas	286
Colon	231
Intestine	176
Testis	145
Stomach	108

**Fig.2.6.** Analysis of various tissues from bitransgenic mice showed lung specific exclusive luciferase expression after one week induction.

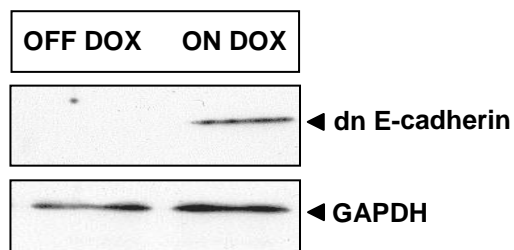


**Fig.2.7.** Western blot analysis of lung tissues from bitransgenic mice shows inducible dn E-cadherin protein expression in vivo. dn E-cadherin protein was detected using a myc tag antibody. GAPDH used as protein loading control.

To test for expression of dn E-cadherin in type II epithelial cells, paraffin embedded lung sections of bitransgenic mice were subjected to immunostaining. SP-C expressing cells stained positive for myc-tagged dn E-cadherin only after treatment with DOX, indicating that induced transgene expression was restricted to type II cells (Fig.2.8).

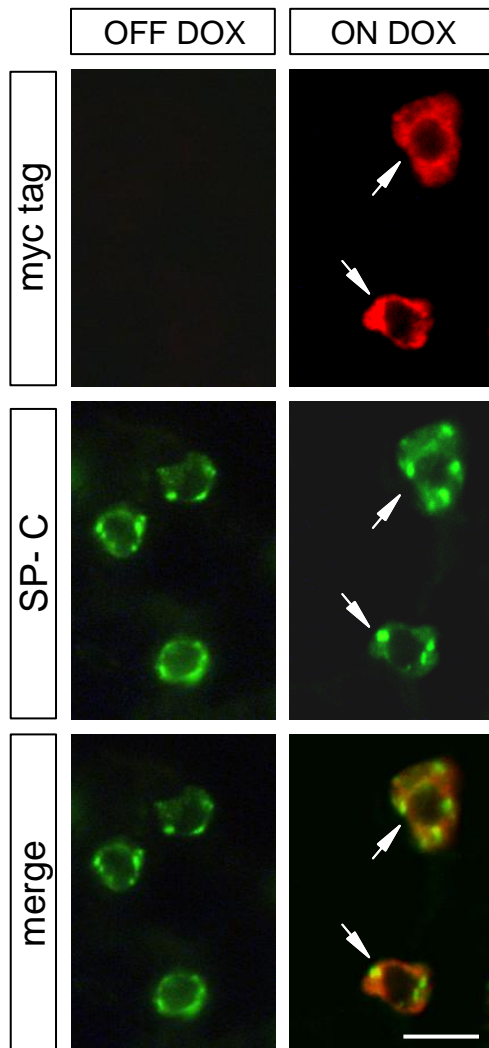


**Fig.2.8.** Double immunofluorescence staining of paraffin-embedded lung sections from bitransgenic mice before or after one week DOX pulse. Sections were stained for pro SP-C (green) and myc reactivity (red, to visualise dn E-cadherin). Merge pictures demonstrates coincident staining of dn E-cadherin and pro SP-C only after treatment (arrows). Scale bar: 10  $\mu$ m.

These experiments showed clear evidence that we have generated inducible dn E-cadherin expressing mice for the analysis of E-cadherin function of lung type II epithelial cells in the absence and presence of an oncogenic background.

**Part II. Analysis of E-cadherin function of lung alveolar type II cells by means of dn E-cadherin approach.**

**2.4. Loss of E-cadherin function in alveolar type II epithelial cells promotes hyperplasia, but is insufficient for tumorigenesis**

To investigate physiological function of E-cadherin in lung pneumocytes, bitransgenic compound mice (*SP-C rtTA/Tet-O dn E-cadherin*) were kept on continuous DOX for different periods, starting at birth. All mice were found to be viable and fertile. Induction of dn E-cadherin for two months resulted in formation of hyperplastic lesions in the lung parenchyma that contained scattered cells of unpolarized morphology (Fig.2.9). In contrast, untreated (OFF DOX) mice showed no lung pathology further confirming that transgene expression was not leaky (Fig.2.9).

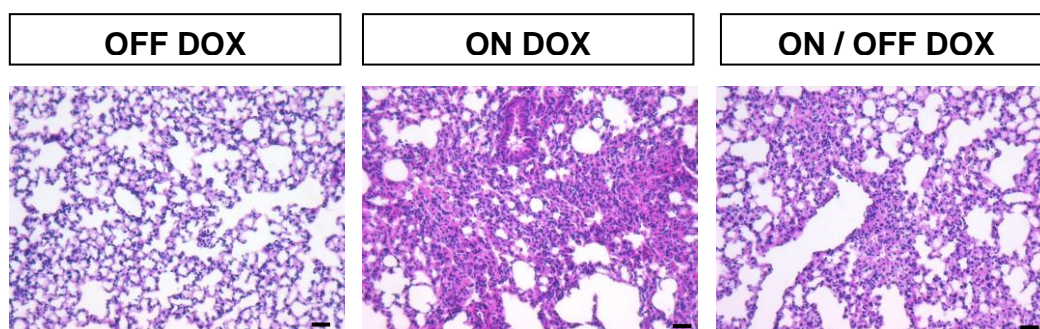


**Fig.2.9.** Haematoxylin and Eosin (H&E) staining of paraffin-embedded lung sections from bitransgenic mice before and after DOX administration. Untreated (OFF DOX) control lungs show normal histology. Induction of hyperplasia in lung parenchyma after two months of induction (ON DOX). Reversibility of hyperplastic regions into relatively normal lung tissue can be seen after two months of DOX withdrawal (ON/OFF DOX). Scale Bar: 50  $\mu$ m.

Cells in hyperplastic regions showed not only strong E-cadherin reduction but also considerably poor SP-C immune reactivity suggesting that loss (dedifferentiation) or blocking of differentiation might have occurred after E-cadherin loss in lung type II epithelial cells (Fig.2.10). These hyperplastic lesions showed a marked increase in cell proliferation as

judged by PCNA immunostaining (Fig.2.11). Prolongation of DOX treatment for additional 12 months revealed no overt tumor formation.

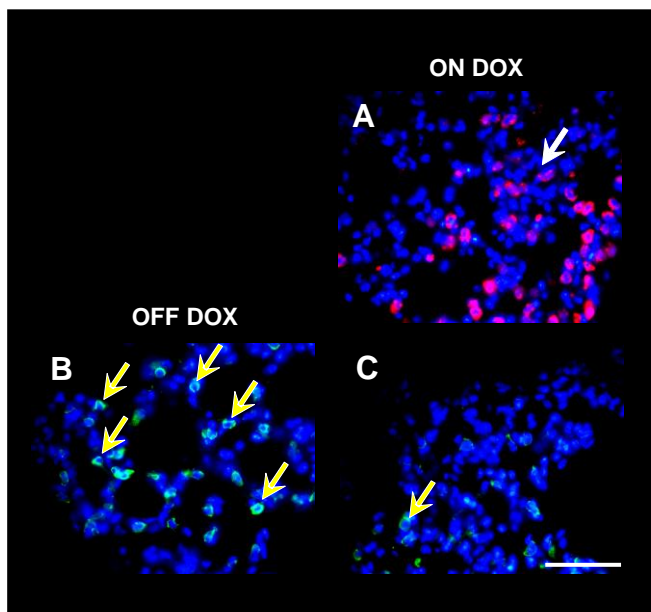


**Fig.2.10.** A. Immunofluorescence staining of frozen lung sections from two months induced bitransgenic mice shows hyperplastic region (white arrow) with weak SP-C (red) immunity. B and C. In comparison to control lung section (B) where E-cadherin (green) positive cells (yellow arrows) were abundant, two months DOX treated mice showed strong loss of E-cadherin expression in hyperplastic regions (C). Yellow arrow in picture C demonstrates a rare E-cadherin positive cell. Dapi (blue) illustrates nuclei. Scale Bar: 50  $\mu$ m.

To determine whether continued expression of dn E-cadherin is necessary for maintenance of hyperplasia, DOX was withdrawn from treated mice at different times. In mice treated for two months hyperplastic lesions disappeared and lungs reverted to almost normal histology two months after removal of DOX (Fig.2.9). To unravel underlying mechanism(s) for reversible hyperplasia we applied PCNA (Fig.2.11A) and active caspase 3 (Fig.2.12A) immunostaining. We observed dramatic increase in PCNA positive cells after two months induction that returned to baseline upon removal of DOX suggesting that E-cadherin plays a major role in cell cycle control of lung alveolar epithelial cells (Fig.2.11A). Morphometric quantification of PCNA positivity supported these findings (Fig.2.11C). As a candidate mediator of proliferation significant nuclear  $\beta$ -catenin accumulation was also noted in induced lung sections suggesting that  $\beta$ -catenin might potentially be involved in the active proliferation of

type II pneumocytes (Fig.2.11B). In contrast active caspase-3 immunostaining (Fig.2.12B) revealed no significant alteration in the number of apoptotic cells after 2 months of doxycycline withdrawal (Fig.2.13B).

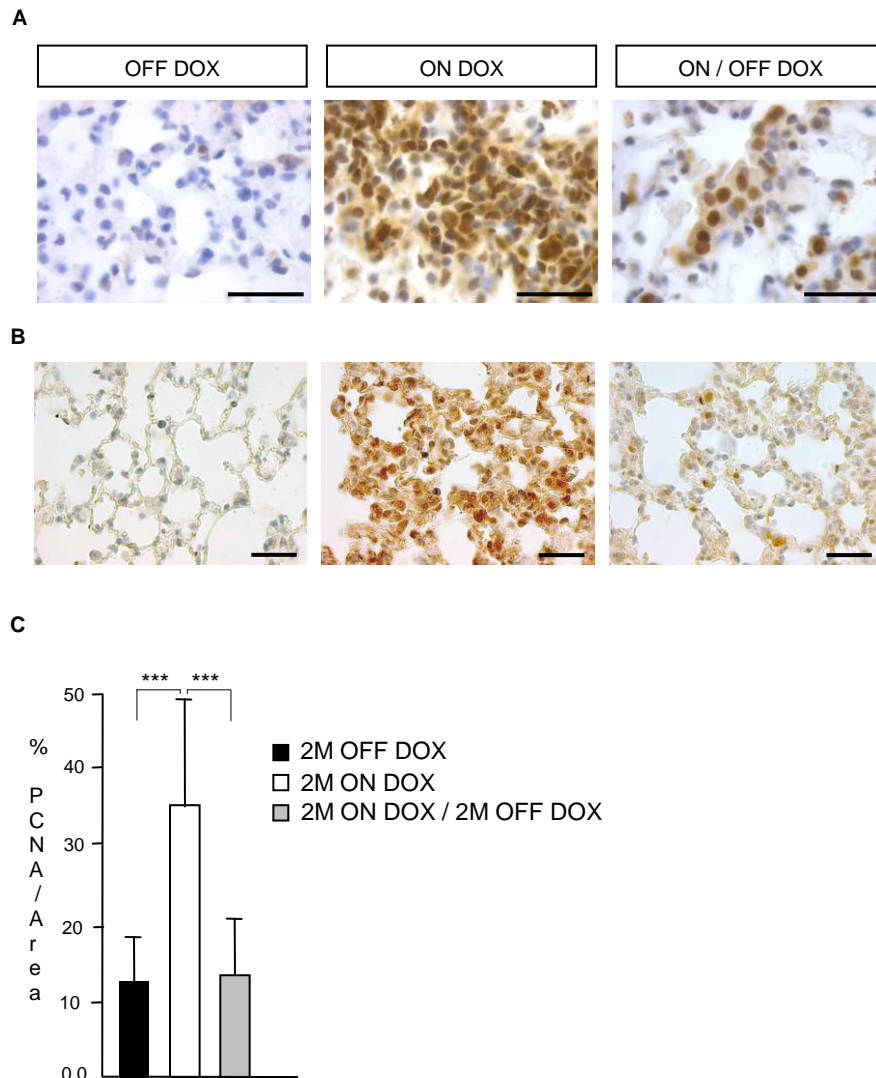


**Fig.2.11.** A. Paraffin-embedded lung sections from bitransgenic mice were stained for PCNA (brown) before and after induction. Haematoxylin staining (blue) used as counterstaining. Strong PCNA positive staining was noted in hyperplastic regions two months after induction (ON DOX) in compare to control (OFF DOX) lung section. 2 months of DOX withdrawal (ON/OFF DOX) led to relatively normal lung histology with a corresponding reduction in cell cycle. B.  $\beta$ -catenin immunostaining of consecutive lung sections reveals increased nuclear  $\beta$ -catenin localisation (brown) after induction. C. Morphometric quantitation of PCNA immunostaining between mice groups. Values represent mean  $\pm$  s.d. (\*\*\*)  $P < 0.001$ ). Scale bars: 50 $\mu$ m. M: month.

The situation was strikingly different acutely following DOX removal. 3 to 4-fold increases of caspase 3 positive cells were seen after 2 days and one week (Fig.2.12B) indicating that apoptosis plays an important role in the early clearance of hyperplastic regions.

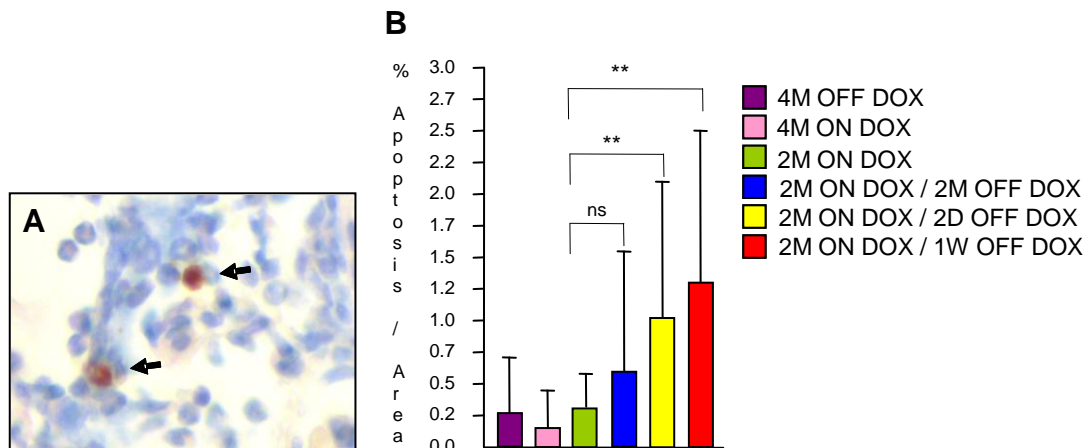


**Fig.2.12.** A. Active caspase 3 immunostaining of a lung section from 2 months induced bitransgenic mouse shows apoptotic positive (brown) cells (arrows) after 2 days of DOX withdrawal. Haematoxylin staining (blue) used as counterstaining. B. Fraction of apoptotic cells in induced lungs of bi-transgenic mice before and after DOX withdrawal. M: month; W: week; D: day. Values represent mean  $\pm$  s.d. (ns: not significant; \*\*  $P < 0.01$ ).

In conclusion, these data suggest that inhibition of E-cadherin function in type II alveolar epithelial cells is essential for initiation and maintenance of hyperplasia, pre malignant lesion, but is insufficient for tumorigenesis.



### ***Part III. Analysis of E-cadherin function in a transgenic mouse model of NSCLC using dn E-cadherin strategy***

#### **2.5. dn E-cadherin expression in C-RAF BXB adenomas**

To analyse the role of E-cadherin function in murine lung tumorigenesis, double-transgenic offspring (*SP-C rtTA / Tet-O dn E-cadherin*) were crossed with homozygous tumor mice expressing oncogenic C-RAF BXB in type II pneumocytes (Kerkhoff et al., 2000) to obtain triple transgenic progeny (*SP-C rtTA / Tet-O dn E-cadherin/ SP-C C-RAF BXB*).

It was previously shown that expression of dn E-cadherin in a mouse model for pancreatic cancer resulted in tumor progression with malignant features (Perl, AK., et al., 1999). To assess whether dn E-cadherin-mediated disruption of cell adhesion leads to malignancy in benign *SP-C C-RAF BXB* adenomas, six weeks old triple transgenic mice were treated with DOX for different periods. Already after one week of DOX administration, loss of cell-cell contact between tumor cells was observed (Fig.2.13).

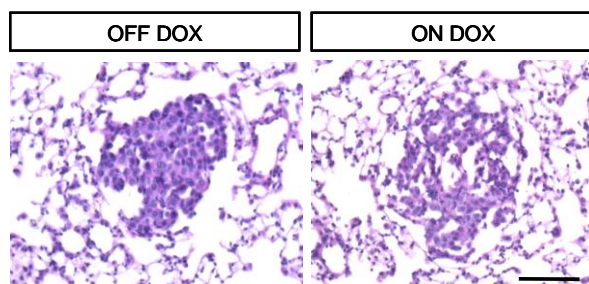


**Fig.2.13.** Expression of dn E-cadherin in C-RAF BXB adenoma leads to loss of intercellular adhesions already after one week DOX administration. H&E stained lung sections from triple transgenic mice shows an adenoma before and after treatment. Scale Bar: 50 $\mu$ m.

This disruption of tumor cell adhesion was associated with dn E-cadherin expression as strong myc tag staining (dn E-cadherin expression) was observed in the adenomas after induction (Fig.2.14).

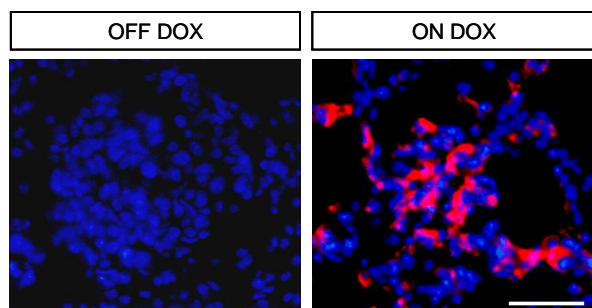


**Fig.2.14.** Immunofluorescence staining of frozen lung sections from triple transgenic mice demonstrated that the majority of the cells in the adenomas expressed dn E-cadherin only after induction. dn E-cadherin (red) was visualised using a myc tag antibody. Dapi (blue) illustrates nuclei. Scale Bar: 50 $\mu$ m.

## 2.6. Tumor progression in *SP-C C-RAF BXB* lung tumors after E-cadherin disruption

To investigate long term effects of dn E-cadherin expression, compound mice were kept under continuous DOX treatment for up to 13 months. After four months, large invasive tumors that were diffusely scattered throughout the lung parenchyma (Fig.2.15A) as well as loss of cuboidal cell morphology within tumors was observed (Fig.2.15B).

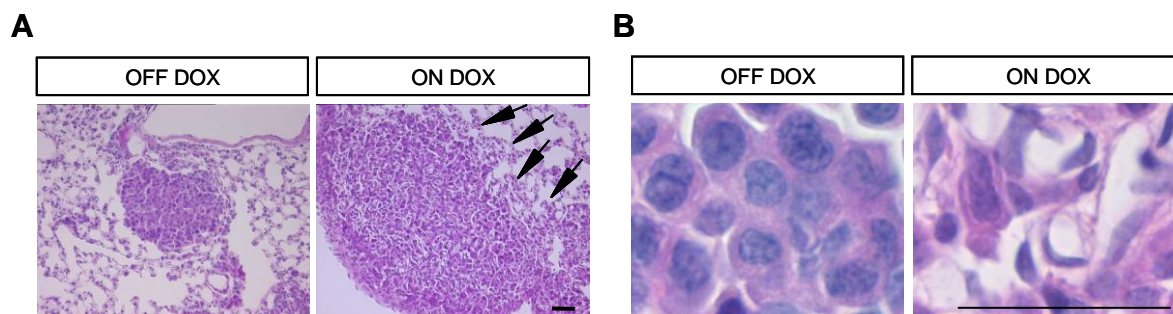


**Fig.2.15.** Paraffin embedded lung sections from triple transgenic mice stained for H&E. A. Accelerated tumor growth and formation of invasive fronts (indicated by arrows) are already apparent after four months induction of dn E-cadherin expression. B. Loss of intercellular cell adhesion with characteristics of disrupted cuboidal cell morphology. Scale Bar: 50 $\mu$ m.

Using an antibody directed against the ectodomain of E-cadherin that only detects membrane inserted E-cadherin but not dn E-cadherin, we observed almost complete removal from the membrane four months after induction (Fig.2.16A and B). Interestingly, displacement from the cell surface was not paralleled by a corresponding decrease in E-cadherin protein that was detected at only slightly decreased level (Fig.2.16C). Removal of E-cadherin from the plasma

membrane was however accompanied by nuclear relocalization of  $\beta$ -catenin in tumor cells expressing dn E-cadherin (Fig.2.17A and B). Nuclear  $\beta$ -catenin-positive cells were only a fraction (approximately 8%) of E-cadherin down-regulated cells demonstrating heterogeneity in the induced tumor cell population (Fig.2.17B).

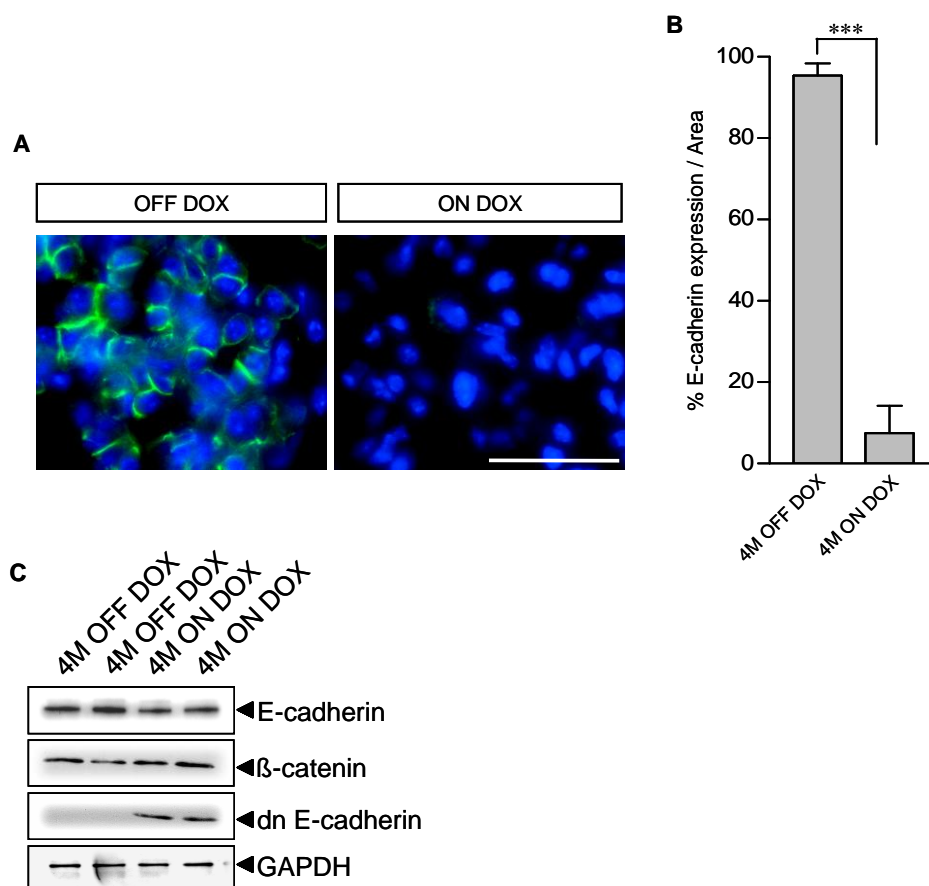


**Fig.2.16.** A. Representative frozen sections of lung tumors from triple transgenic were stained with E-cadherin. Mice were treated with DOX for four months starting at 6 weeks of age (ON DOX) and compared with untreated controls (OFF DOX). B. Quantification of E-cadherin in the membrane of intratumoral cells. C. Immunoblot of isolated tumor cells from triple transgenic mice treated as indicated were reacted with antibodies against E-cadherin,  $\beta$ -catenin, myc-epitope, (dn E-cadherin) or GAPDH as loading control. M: month. All values are mean  $\pm$  s.d. \*\*\* $P < 0.001$ . Scale bars: 50  $\mu$ m.

Histopathological analysis of tumors showed a 5-fold increase in tumor volume after E-cadherin ablation (Fig.2.18B). Prolongation of induction to eight months generated macroscopic solid tumors that were diagnosed as adenocarcinomas (Fig.2.18A). Cooperation between dn E-cadherin and C-RAF BXB in accelerating tumor growth required continued induction, as a 4M ON DOX / 4M OFF DOX schedule reduced tumor size to the level of 8M

OFF DOX C-RAF BXB only (Fig.2.18B). Macroscopic tumors mostly retained expression of SP-C suggesting that there was not prominent dedifferentiation in tumors where E-cadherin function was abrogated.

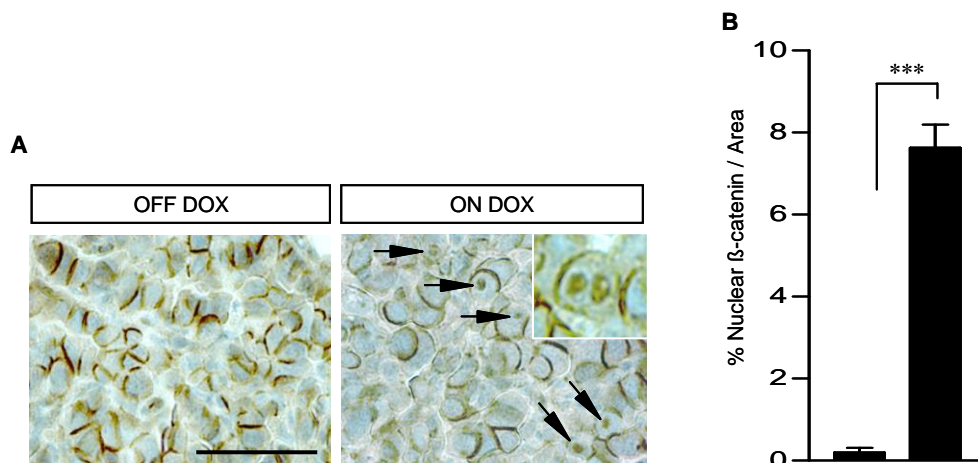


**Fig.2.17.** Representative paraffin embedded sections of lung tumors from compound mice (*SP-C C-RAF BXB/SP-C rtTA/Tet-O- dn E-cadherin*) were stained with  $\beta$ -catenin. Loss of membrane  $\beta$ -catenin and relocalization of  $\beta$ -catenin to the cytoplasm and cell nucleus (arrows and inset) was occasionally observed in induced tumors. B. Quantification of nuclear  $\beta$ -catenin of tumor cells. All values are mean  $\pm$  s.d. \*\*\* $P < 0.001$ . Scale bars: 50  $\mu$ m.

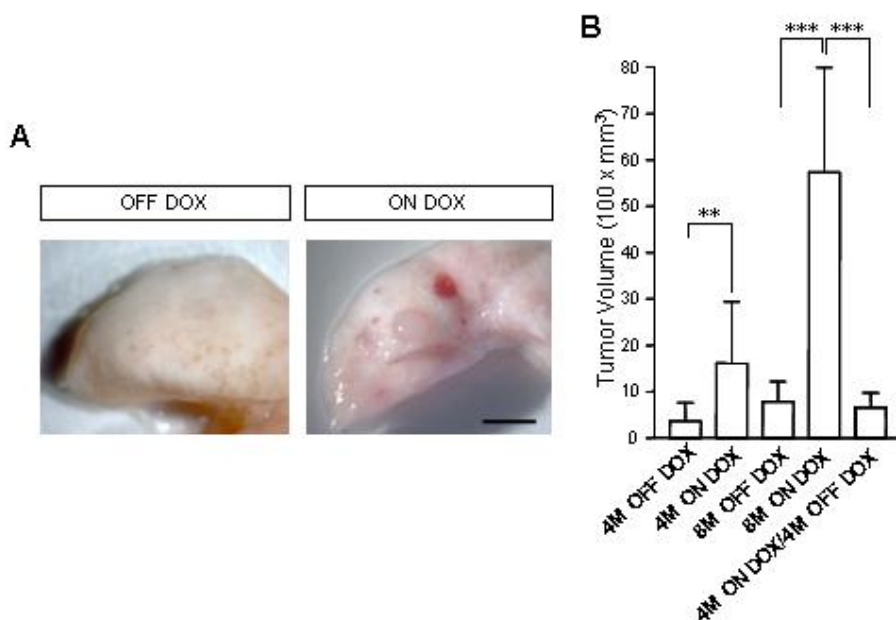


**Fig.2.18.** A. Macroscopic tumors (ON DOX) are visible after eight months DOX induction. B. Quantification of tumor volume. The difference in tumor volume between 4M ON DOX and 4M ON DOX / 4M OFF DOX is not significant ( $P = 0.126$ ). The difference between 8M OFF DOX and 4M ON DOX / 4M OFF DOX is also not significant ( $P = 0.60$ ). \*\* $P < 0.01$ , \*\*\* $P < 0.001$ .

To examine how disruption of cell-cell contacts induced tumor progression, we determined the proliferation rate of tumor cells. PCNA staining of tumor cells in *SP-C C-RAF BXB/SP-C rtTA/Tet-O dn E-cadherin* mice was highly increased, compared to animals in the absence of DOX (Fig.2.19A and B).

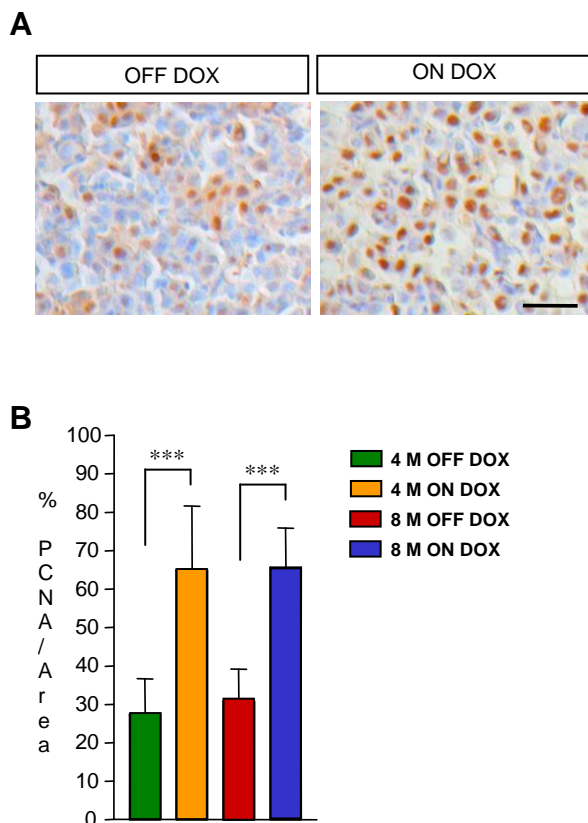
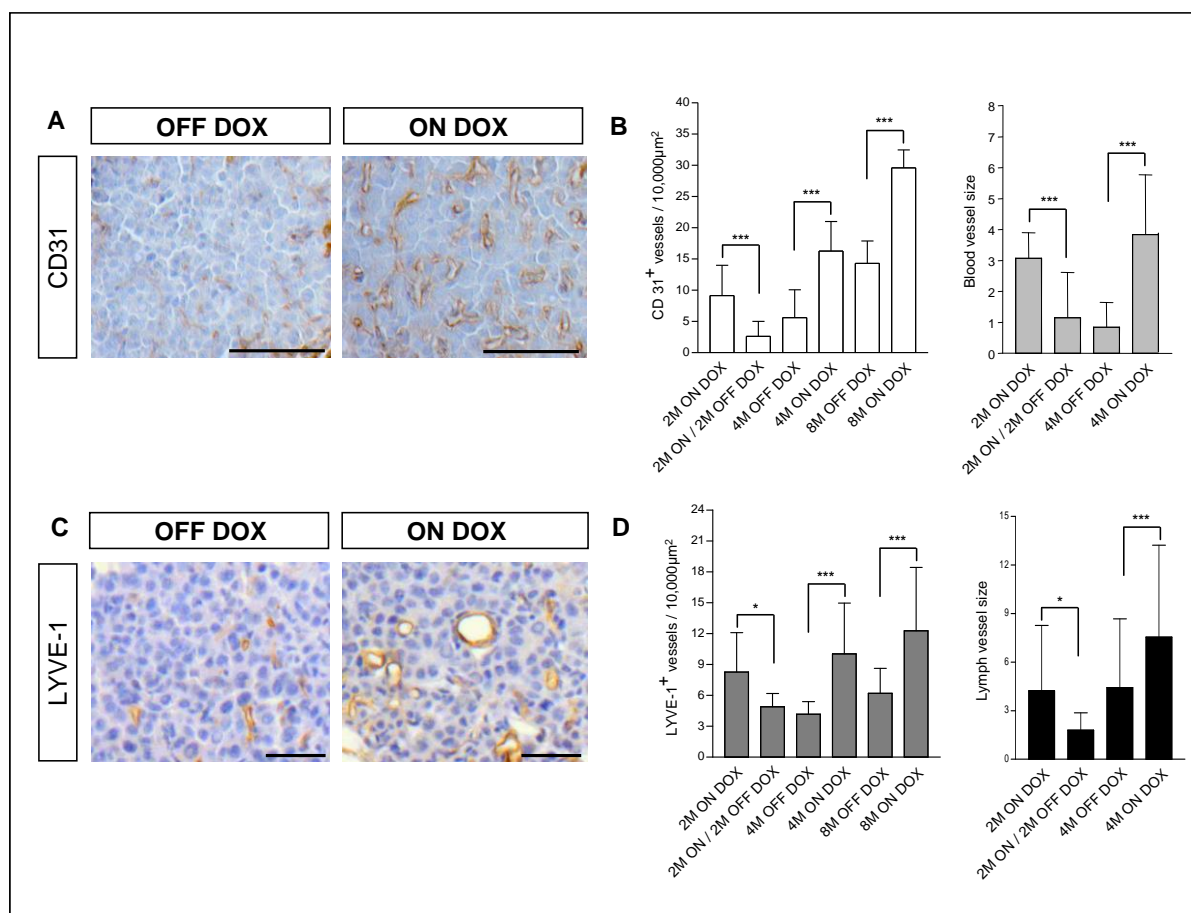


Fig.2.19. A. PCNA staining (brown) of tumors shows increased proliferation rates after four months induction of dn E-cadherin expression. B. Quantification of PCNA-positive cells in tumors before and after induction. \*\*\* $P < 0.001$ . Scale Bar: 50  $\mu\text{m}$ .

Taken together, these results demonstrate that inactivation of E-cadherin in benign *SP-C C-RAF BXB* adenomas not only promote tumor growth but also lead to progression to adenocarcinomas.

## 2.7. Expression of dn E-cadherin induces tumor vasculature.

Detailed histopathological analysis of tumors after dn E-cadherin induction not only highlighted strong loss of cell-cell contacts between tumor cells but also suggested that there might be abundant intratumoral microvessels indicating an angiogenic switch. Staining of lung sections for CD31 confirmed strong induction of intratumoral vessels (Fig.2.20A). Quantitative analysis of tumor vasculature demonstrated uniform penetration of tumors by vessels of increased size two months after dn E-cadherin expression, that was even more pronounced after four months and continued to increase in density by 8-months of induction (Fig.2.20B).



**Fig.2.20.** Triple transgenic mice (*SP-C C-RAF BXB/SP-C rtTA/Tet-O dn E-cadherin*) were treated with Dox for different periods and compared with age-matched controls. Staining for blood (CD31, A) and lymph (LYVE-1, B) endothelial cells demonstrates angiogenic switch. Scale bars: 50 μm. B and D shows quantitation of blood and lymph vessels, respectively. All values are mean ± s.d. (\* $P < 0.05$ ; \*\*\* $P < 0.001$ ). Vessel size (diameter) was presented as μm.

There was a 3-fold increase in vessel number and a 4-fold increase in vessel size (Fig.2.20B) indicating an enormous level of neo-angiogenesis. As lymphangiogenesis may be most

relevant for metastasis, we examined presence of vessels positive for the lymphangiogenesis marker LYVE-1. We observed that tumors from untreated mice revealed poor lymphatic vessels in the center of adenomas (Fig.2.20C). After four months of dn E-cadherin induction, their number and size had increased significantly and increased even further when treatment was continued for eight months (Fig.2.20D). To confirm the lymphatic nature of the vessels Prox1 staining was additionally used (Fig.2.21). Similar data also was attained with Prox-1 results.

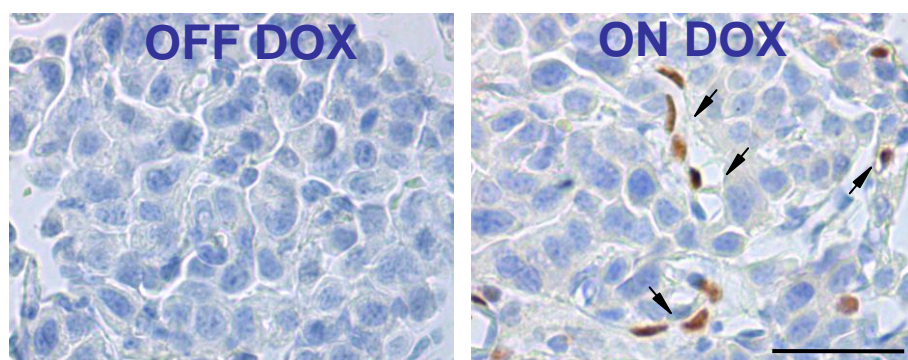


**Fig.2.21.** Increased intratumoral lymphatics were notable after lymph vessel-specific Prox-1 immunostaining. Black arrows indicate positive vessels (brown) in induced lung sections. Haematoxylin (blue) was used as counterstaining. Scale bar: 50  $\mu$ m.

We conclude that E-cadherin ablation induces the angiogenic switch that has previously been reported as a requirement for tumor progression (Folkman et al., 1989).

## 2.8. Restoration of E-cadherin expression reverses the angiogenic switch

To determine whether restoration of E-cadherin membrane expression leads to suppression of vessel growth, dn E-cadherin transgene expression was switched off by DOX withdrawal for two months. E-cadherin expression at the cell surface of tumor cells was restored demonstrating reversibility (Fig.2.22A). CD31 staining after two months of DOX removal revealed blood vessel regression in both number and size (Fig.2.22B, Fig.2.23 and Fig.2.20B). Vessels that regressed often disappeared or showed discontinuous and narrow structures around the tumor cells (Fig.2.23).

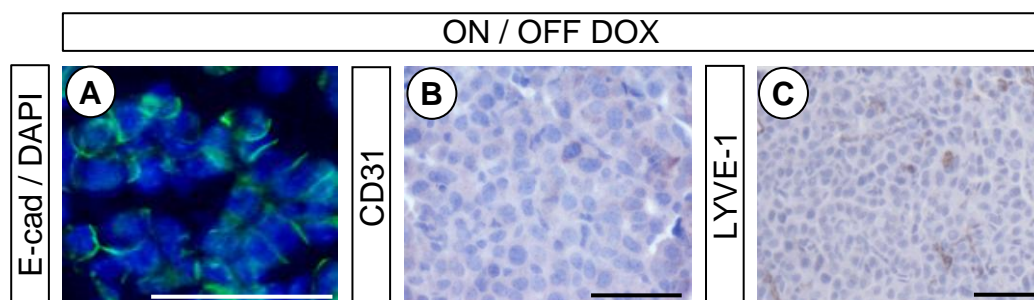


**Fig.2.22.** A. Reexpression of membrane E-cadherin (green) in tumor cells of triple transgenic mice (*SP-C C-RAF BXB/SP-C rtTA/Tet-O dn E-cadherin*) that were kept on DOX for two months followed by two months DOX withdrawal. Dapi illustrates nuclei. **B, C:** Restoration of E-cadherin expression is correlated with disappearance of blood (B, CD31) and lymph (C, LYVE-1) vessels. Scale Bar: 50  $\mu$ m.

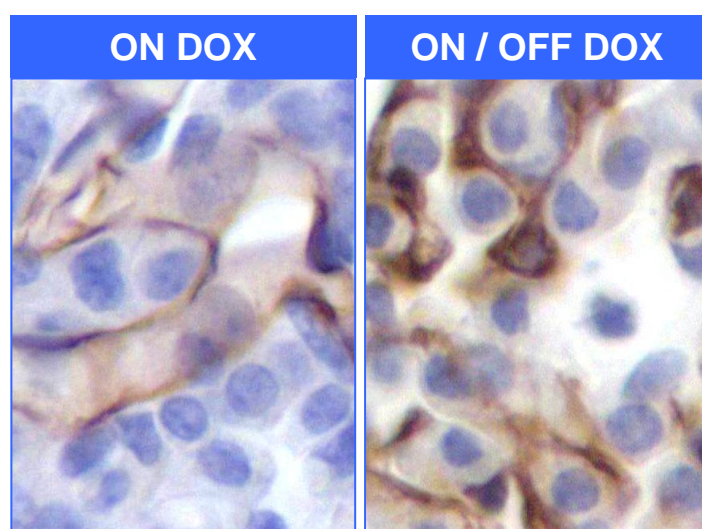


**Fig.2.23.** High magnification of CD31 immunostaining of blood vessels before and after regression shows collapse of blood vessels in the tumor. Haematoxylin (blue) was used as counterstaining.

Dn-E-cadherin mediated induction of vessels is likely to be regulated via growth factors (i.e.VEGF, FGF etc.) and shutting down of dn E-cadherin expression by withdrawal of DOX might affect endothelial cell survival. To examine whether vessel regression was caused by endothelial cell apoptosis, we performed CD31/TUNEL double staining. Sections treated without primary antibody or enzyme were used as negative control (Fig.2.24, upper panel). DNase-I treatment served as a positive control (Fig.2.24, second panel). Endothelial intratumoral apoptosis occurred in 2M ON DOX / 1-week OFF DOX mice (Fig.2.24, third



panel). Additionally there may have been tumor cell apoptosis as we also see CD31 negative apoptotic cells in the same tumor section. Interestingly, using a 4M ON DOX/1W OFF DOX schedule, almost no TUNEL positive endothelial cells were detected (Fig.2.24, bottom panel) indicating that long-term loss of membrane E-cadherin expression led to neo-vascularisation that was maintained upon re-expression of E-cadherin.

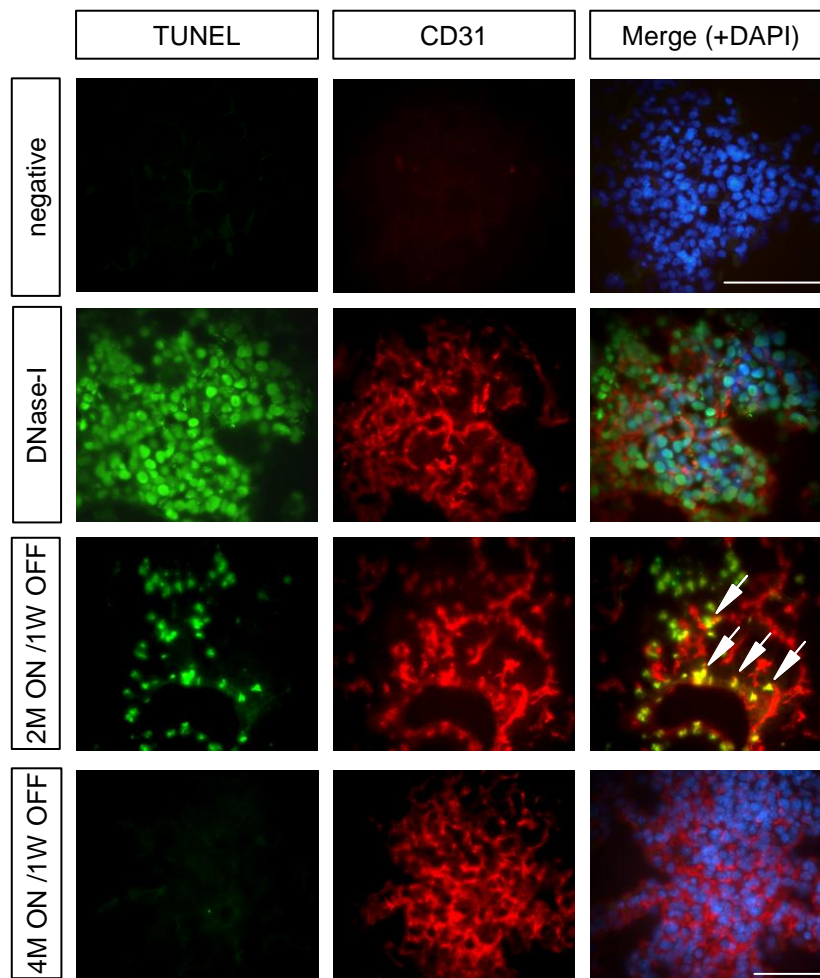


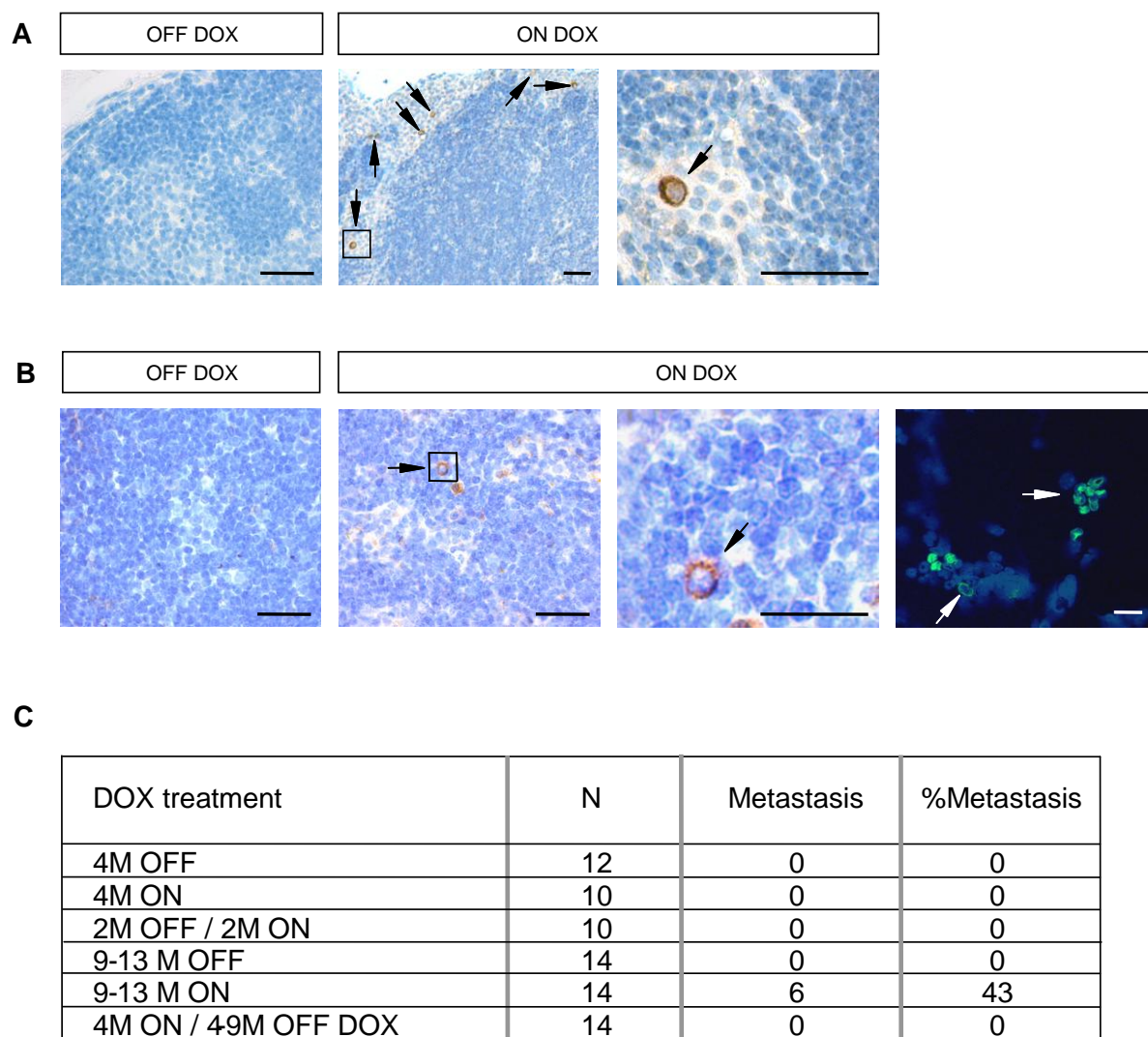
**Fig.2.24.** Detection of apoptosis of CD31 positive endothelial cells (see arrows) in frozen tumor sections after DOX withdrawal. Controls include TUNEL assay without terminal transferase (top panel left), antibody specificity (CD31, top panel middle) and apoptosis induction by DNase-I (second panel). Note that tumor vasculature in four months-induced mice is no longer DOX-dependent. For each treatment, 3 mice and at least 5 tumors per mouse were evaluated. Scale bar: 50  $\mu$ m.

Similar observations were made regarding vessel size (data not shown). As in the case of neo-angiogenesis, we tested reversibility of lymphangiogenesis using a 2M ON DOX / 2M OFF DOX schedule. The pattern of reversibility of lymphangiogenesis was similar to blood angiogenesis as complete reversibility was seen only after two months treatment (Fig.2.20D).

## **2.9. Oncogenic *C-RAF* and *E-cadherin* ablation cooperate in progression to micro-metastasis.**

To examine whether inhibition of E-cadherin function in benign *SP-C C-RAF BXB* driven lung adenomas is necessary and sufficient for the metastatic spread of tumor cells, we conducted a large scale search for ectopic cells expressing SP-C or cytokeratin before and after induction. We detected both cytokeratin (Fig.2.25A, upper panel) and SP-C (Fig.2.25B, lower panel) positive cells in the lymph nodes after dn E-cadherin expression. The metastatic cells were not growing into tumors but formed small clusters of one to five cells identifying them as micrometastasis (Schardt et al., 2005) in mediastinal and axillary lymph nodes. Neither SP-C nor cytokeratin positive cells were visible in lymph nodes from untreated age-matched control mice (Fig.2.25, left upper and lower panel). Although we were not able to detect any distant metastasis in the preferred target tissues of NSCLC such as liver and brain, we infrequently observed SP-C positive cells in the bone marrow of triple transgenic mice induced for dn E-cadherin (Fig.2.25B, lower panel on the right). Dissemination of tumor cells from primary tumors was a late event, as we never detected metastasis in transgenic mice younger than nine months (Fig.2.25C). Moreover, even in older mice, despite long term inactivation of E-cadherin, only 43% of all triple transgenic mice developed lymph node micrometastasis. Induction of dn E-cadherin alone did not result in metastasis (data not shown). As in the case of angiogenic switch induction by dn E-cadherin, we wanted to examine whether continuous induction was required for progression to metastasis. Towards

this end we performed histological analysis of tissues from mice that were kept on 4 months ON DOX / 4-9 months OFF DOX schedules (Fig.2.25C).



N = Number of animals

In case of dn E-cadherin: DOX: treatment from E 0.0 on

In case of *Cdh1<sup>fllox/fllox</sup>*: DOX: treatment after 1.5M

**Fig.2.25.** A. Paraffin-embedded lymph node sections from untreated mice or mice treated with DOX for 10 months were screened for regional and long-distance metastasis by staining for pancytokeratin (A) and pro SP-C (B). Haematoxylin staining was used as counterstaining (blue). Sections shown in higher magnifications are boxed. Arrows mark positive cells (brown colour). Pro SP-C positivity (green) in cytopspin preparations of bone marrow. Scale bars: 50µm. C. Incidence and latency of lymph node micrometastasis. M: month.

This experiment revealed that none of the transgenic mice displayed lymph node or distant metastasis after DOX removal (Fig.2.25C). We conclude that there is a direct correlation

between continuous angiogenesis induction and micrometastasis of SP-C *C-RAF BXB* driven lung tumors.

### 2.10. Lack of evidence for EMT in metastatic lung adenocarcinoma.

Tumor progression frequently involves processes such as epithelial-mesenchymal-transition (EMT), and cadherin switch (loss of E-cadherin and gain of N-cadherin) (Huber et al., 2005). For detection of EMT, lung tumor sections were stained with vimentin and N-cadherin antibodies. There were scattered vimentin or N-cadherin positive cells in the induced tumors (Fig.2.26) that most likely represent vessel associated cells as no double-positive (pro SP-C / Vimentin; pro SP-C / N-cadherin) cells were detected (Fig.2.27A).

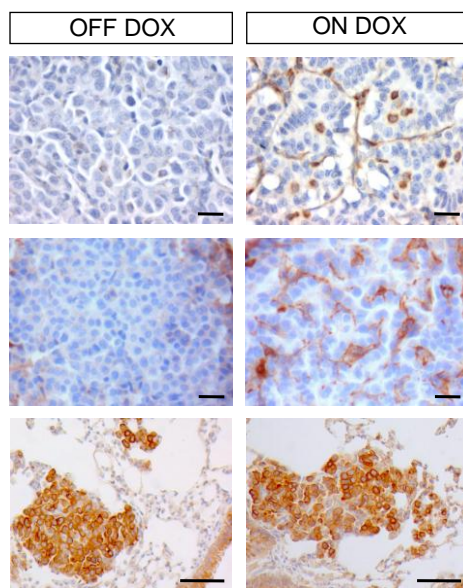


**Fig.2.26.** Triple transgenic mice were treated with DOX for nine months (ON DOX) and compared with age-matched controls (OFF DOX). Representative pictures of lung tumor sections stained as indicated for vimentin (upper panel), N-cadherin (middle panel) and cytokeratin (lower panel). Brown staining indicates positive cells. Scale bar: 50  $\mu$ m

To confirm that the increased N-cadherin staining resulted from endothelial rather than tumor cells, we have isolated tumor and endothelial cell fractions by panning from triple transgenic mice and performed western blotting. There was no N-cadherin protein detectable in tumor cells from untreated or treated mice (Fig.2.27B), whereas the endothelial fraction showed

positive staining independent of DOX treatment (Fig.2.27C). These data suggested that there was no cadherin switch in our lung tumors that has been frequently observed in EMT (Birchmeier, W., and Behrens, J., 2004).

**A**

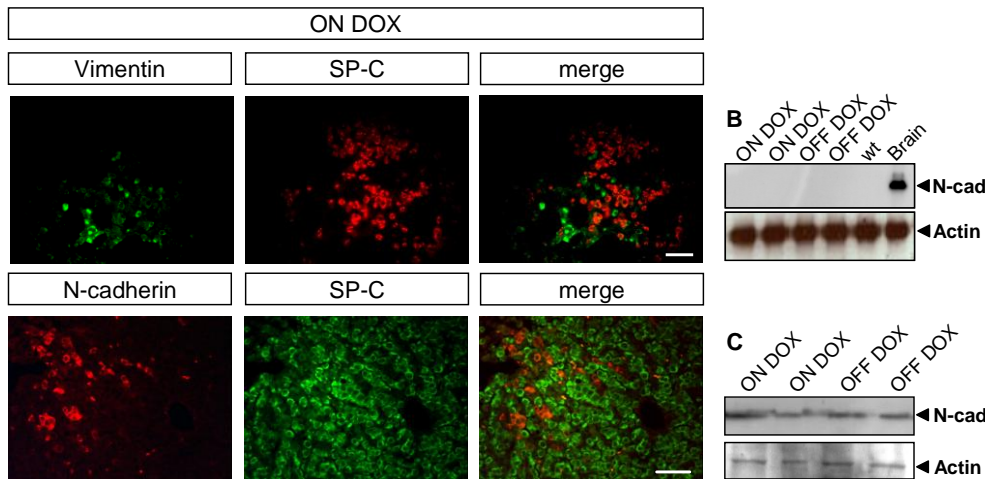


**Fig.2.27.** Representative pictures of lung tumor sections stained as indicated. A. Double-immunofluorescence for pro SP-C/vimentin and pro SP-C/N-cadherin. B. Western blot analysis of N-cadherin in isolated type-II cells from 10-months old triple transgenic mice. Lysate from total brain was used as positive control. C. Western blot analysis of N-cadherin in the endothelial fraction. Actin was used as loading control. Scale bars: 50  $\mu$ m.

Finally, tumor cells from induced mice had stable epithelial features as cytokeratin staining was retained (Fig.2.26, lower panel). We conclude that dn E-cadherin-induced tumor progression of *SP-C C-RAF BXB* driven lung adenomas may not involve classical EMT although there might be a transient EMT that would not have been detected from steady state analysis.

***Part IV. Analysis of E-cadherin function in normal and oncogenic (C-RAF BXB targeted) lung alveolar type II pneumocytes using conditional Cre-mediated Cdh1 knock-out strategy.***

**2.11. Consequences of E-cadherin ablation in normal and oncogenic type II pneumocytes of mouse lung.**

Since dn E-cadherin was previously shown to affect not only E-cadherin but also N-cadherin (Dahl. et al., 1996) membrane localisation, it was crucial to discriminate the exclusive E-cadherin function in parallel to dn E-cadherin approach. Therefore a lung alveolar type II epithelial cell specific conditional knock-out strategy was designed.

In order to determine E-cadherin function in adult type II pneumocytes, conditional *Cdh1* gene inactivation using a DOX inducible Cre/*loxP* site-specific recombination system (see Fig. 1.12) was employed together with SP-C rtTA inducer mice first in the absence of oncogenic background. For this, Cre recombinase was induced in six week-old compound mice (*SP-C rtTA/Tet-O-cre/Cdh1<sup>flox/flox</sup>*) by DOX treatment, and lungs were analysed after a two-months period. In the presence of DOX no tumors were formed though there was diffuse hyperplasia accompanied by enlargement of alveolar spaces in the absence of inflammation (Fig. 2.28).

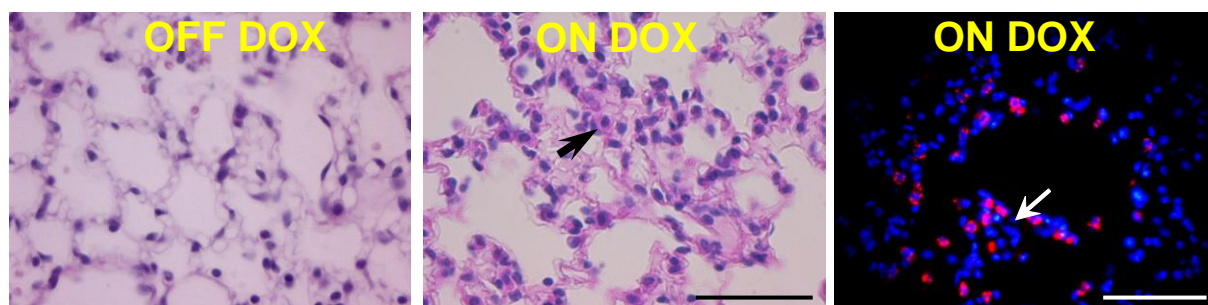


**Fig.2.28.** H&E staining of paraffin embedded lung sections from compound mice (*SP-C rtTA/Tet-O-cre/Cdh1<sup>flox/flox</sup>*) shows emergence of hyperplastic regions (see black arrow) in DOX treated mice (ON DOX) after knock-out of E-cadherin. Immunostaining for SP-C (red) demonstrates a hyperplastic region with poor immunoreactivity for SP-C (white arrow). Dapi (blue) illustrates nuclei. Scale bars: 50  $\mu$ m.

Further evaluation of these mice for periods up to one year did not reveal overt tumor formation.

To evaluate the effect of *Cdh1* loss on tumorigenesis, tumor-bearing mice (*SP-C C-RAF BXB/SP-C rtTA/Tet-O-cre/Cdh1<sup>flox/flox</sup>*) of six weeks of age were treated with DOX for four months and subsequently examined histologically. Similar to dn E-cadherin-induced tumors, tumor foci showed cell separation and partial loss of cuboidal morphology after E-cadherin loss (Fig 2.29). Notably, ablation of E-cadherin did not occur in all cells, consistent with scattered Cre staining in only 35-50 percent of cells in tumor foci (Fig.2.29 and Fig.2.30).

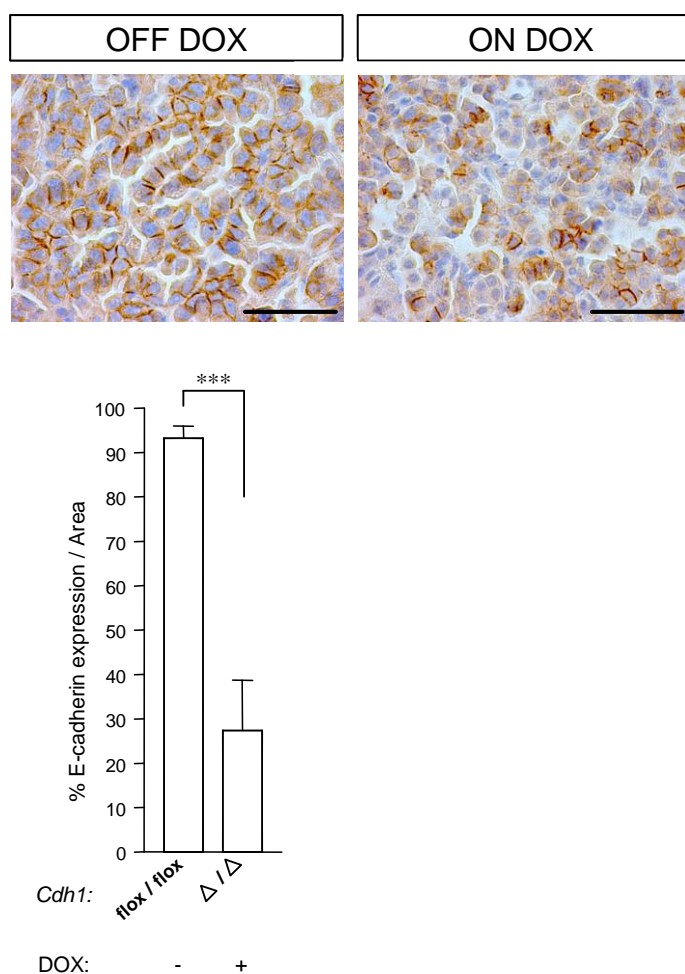


**Fig.2.29.** Representative paraffin embedded sections of lung tumors from compound mice (*SP-C C-RAF BXB/SP-C rtTA/Tet-O-cre/Cdh1<sup>flox/flox</sup>*) were stained for E-cadherin (brown). Note membrane loss of E-cadherin leads to cell-cell separation. Haematoxylin (blue) was used as counterstaining. Quantitation (bottom) of tumor cell membrane E-cadherin expression shows a significant loss of E-cadherin between two groups. All values are mean  $\pm$  s.d. (\*\*\*) $P < 0.001$ . Scale bars: 50  $\mu$ m.

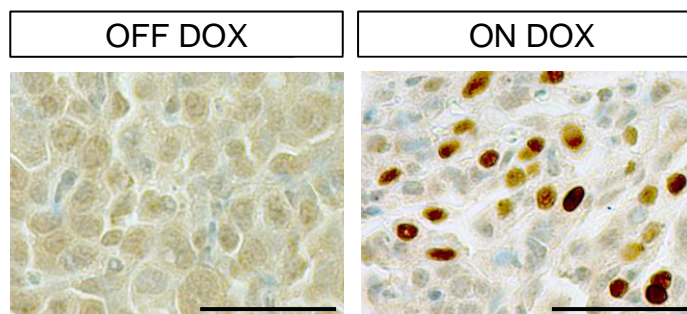


**Fig.2.30.** Representative paraffin embedded sections of lung tumors from compound mice (*SP-C C-RAF BXB/SP-C rtTA/Tet-O-cre/Cdh1<sup>flox/flox</sup>*) were stained for Cre expression (brown). Haematoxylin (blue) was used as counterstaining. Scale bars: 50  $\mu$ m.

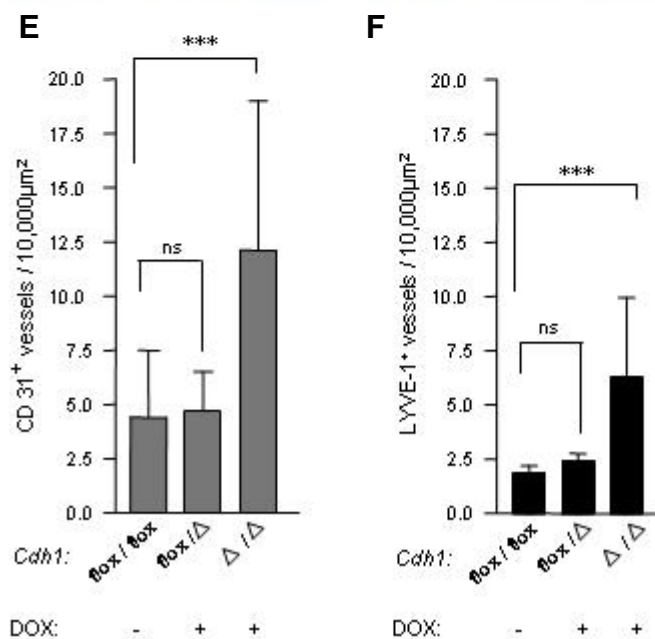
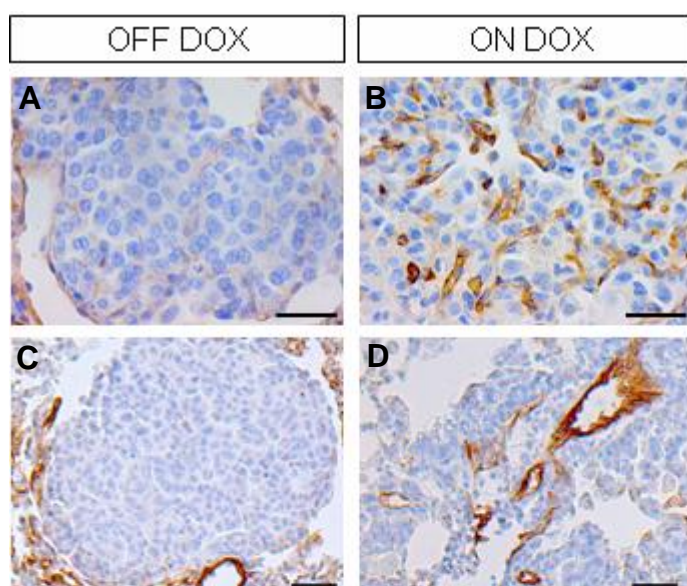


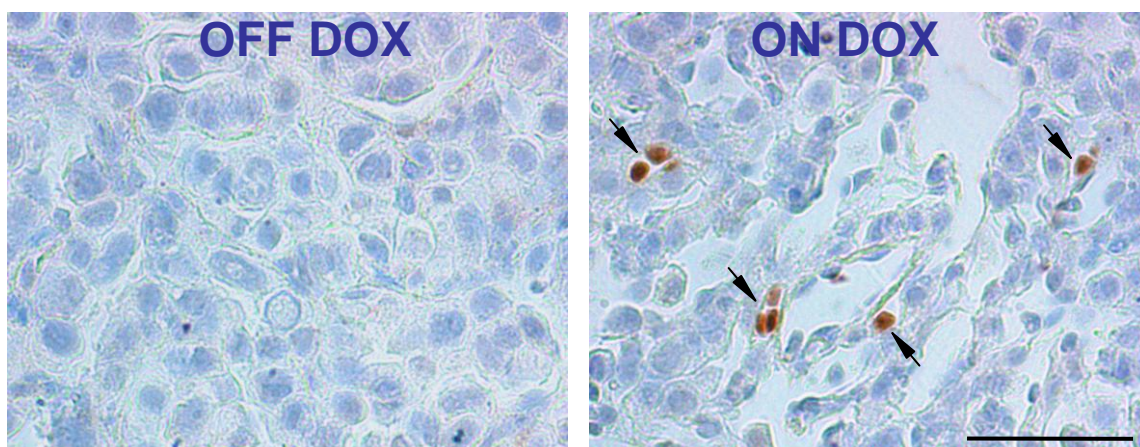


**Fig.2.31.** Representative paraffin embedded sections of lung tumors from compound mice (*SP-C C-RAF BXB/SP-C rtTA/Tet-O-cre/Cdh1<sup>flox/flox</sup>*) were stained for CD31 and LYVE which are the markers for blood and lymphatic endothelial cells, respectively. Deletion of *Cdh1* in C-RAF-driven tumors was accompanied by massive invasion of blood (A and B) and lymph vessels (C and D). Quantification of intratumoral blood (E) and lymph vessels (F). All values are mean  $\pm$  s.d. (\*\* $P < 0.001$ ; ns= not significant). Scale bars: 50  $\mu$ m.

As in the case of dn E-cadherin analysis of blood vessel density by CD31 staining revealed massive intratumoral invasion after *Cdh1* inactivation (ON DOX), whereas adenomas harboring intact *Cdh1* (OFF DOX) alleles were poorly vascularized (Fig. 2.31 A, B and E).

Vessel induction outside of tumors was difficult to evaluate because of the abundance of vessels in normal lung. To examine whether *Cdh1* loss had any effect on intratumoral lymphangiogenesis, we stained tumors with a lymphatic-specific marker, LYVE-1.

A



B

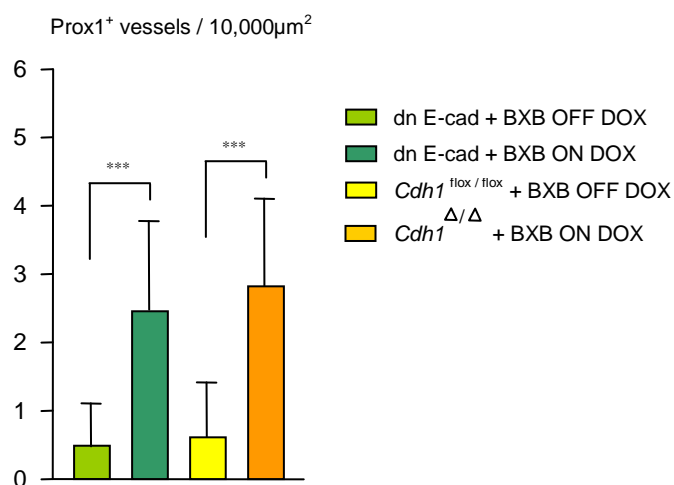


**Fig.2.32.** A. Paraffin embedded sections of lung tumors from four months induced quadruple compound mice (*SP-C C-RAF BXB/SP-C rtTA/Tet-O-cre/Cdh1<sup>flox/flox</sup>*) were stained with Prox1 antibody. Arrows indicate lymph vessels. Brown nuclear staining identifies lymph endothelial cells. Haematoxylin was used as counterstaining. Scale bar: 50  $\mu$ m. B. Quantitation of intratumoral lymphatics shows increased number of vessels in lung tumors after four months of treatment (ON DOX). All values are mean  $\pm$  s.d. \*\*\* $P < 0.001$ .

Whereas tumors from untreated mice revealed poor lymphatic vessels in the centre of adenomas, their number and size have significantly increased by four months of DOX induction (Fig. 2.31C, D and F). To further support the identification of lymphatic vessels, a second lymph vessel marker, Prox1, was used (Fig. 2.32).

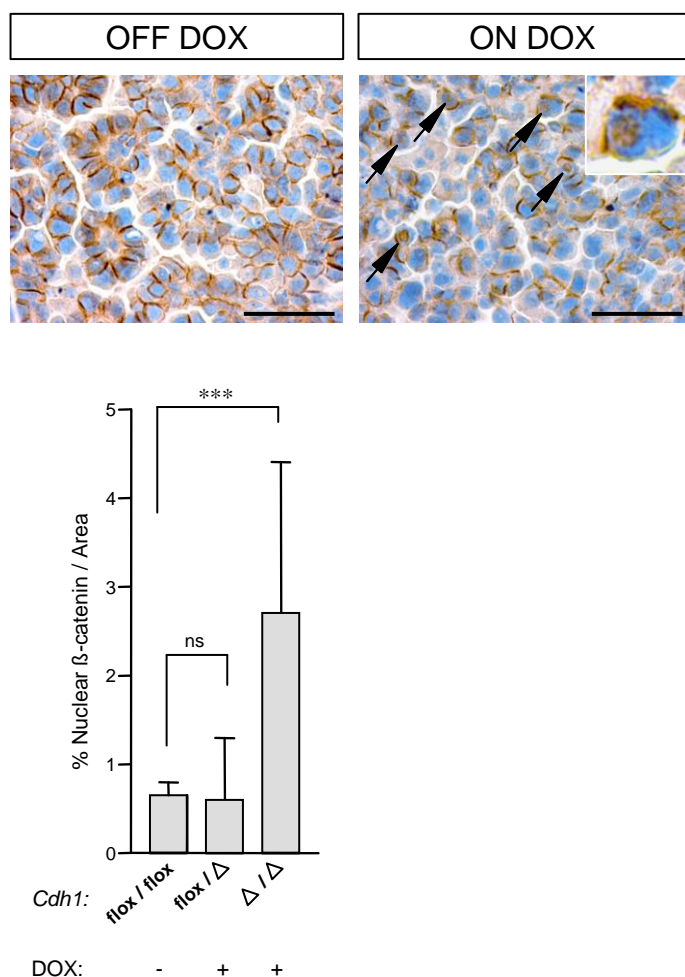


**Fig.2.33.** Representative paraffin embedded sections of lung tumors from compound mice (*SP-C C-RAF BXB/SP-C rtTA/Tet-O-cre/Cdh1<sup>flox/flox</sup>*) were stained for  $\beta$ -catenin. Relocalization of  $\beta$ -catenin to the cytoplasm and cell nucleus (arrows and inset) after induction (ON DOX). Quantitation of intratumoral nuclear  $\beta$ -catenin reveals significant increase after E-cadherin ablation. Scale bars: 50  $\mu$ m.

Prox1 staining yielded similar data to LYVE1 staining indicating that ablation of E-cadherin not only provokes intratumoral blood vessel induction but also lymphatics.

Increased nuclear  $\beta$ -catenin accumulation after dn E-cadherin expression suggested that interference of E-cadherin function might signal to nucleus by means of  $\beta$ -catenin. In order to support this finding, tumor sections after *Cdh1* ablation were stained for  $\beta$ -catenin. There was a significant loss of membrane staining (data not shown) and an increased nuclear accumulation of  $\beta$ -catenin in a small fraction of tumor cells (Fig. 2.33).

To examine how interference of cell-cell contacts induced tumor progression, the proliferation rate of tumor cells was determined. Ki67 staining of tumors from *SP-C C-RAF BXB/SP-C rtTA/Tet-O-cre/Cdh1<sup>fllox/fllox</sup>* mice showed increased cell proliferation in comparison to uninduced (OFF DOX) counterparts (Fig. 2.34).

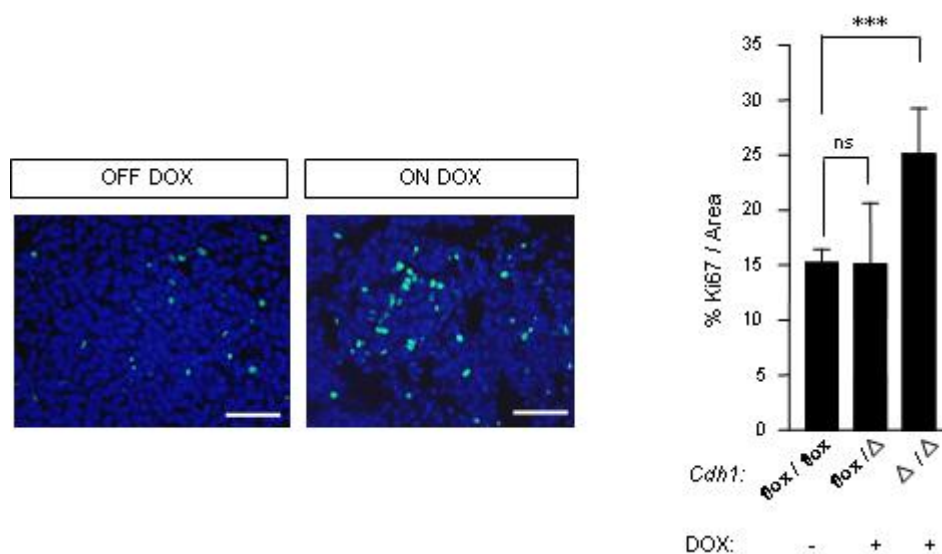


Fig.2.34. Ki67 (green) staining of tumors from compound mice show increased proliferation rates after four months induction (ON DOX) of Cre recombinase to delete the *Cdh1* gene. Dapi (blue) illustrates nuclei. Quantification of Ki67-positive cells between uninduced and induced heterozygous and homozygous *Cdh1*-ablated tumors. Values represent mean  $\pm$  s.d. (\*\*\*)  $p < 0.001$ . ns: not significant. Scale bars: 50 $\mu$ m.

To examine the rate limiting role of E-cadherin ablation in *SP-C C-RAF BXB*, transgenic mouse model for NSCLC, a large scale search for ectopic cells expressing cytokeratin was conducted. As in the dn E-cadherin case, micrometastasis consisting of single or double

cytokeratin positive cells in the lymph nodes was detected after *Cdh1* deletion. There was no distant micro/macro metastasis in any other organs. Dissemination of tumor cells from primary tumors was also late event and not frequent (25%) as in the dn E-cadherin (43%) model. Ablation of *Cdh1* alone did not result in metastasis.

Taken together, these results demonstrate that inactivation of E-cadherin either by dn E-cadherin or by gene ablation promotes tumor progression in a transgenic mouse model for NSCLC.

## Part V. Mechanism of Angiogenesis

### 2.12. Analysis of dn E-cadherin-mediated angiogenesis.

To further resolve by which mechanism dn E-cadherin provokes tumor angiogenesis (Fig.2.35) and micrometastasis during *SP-C C-RAF BXB* lung tumor progression, expression of a panel of candidate genes known to play a crucial role in angiogenesis induction was scanned by using real time RT-PCR analysis.

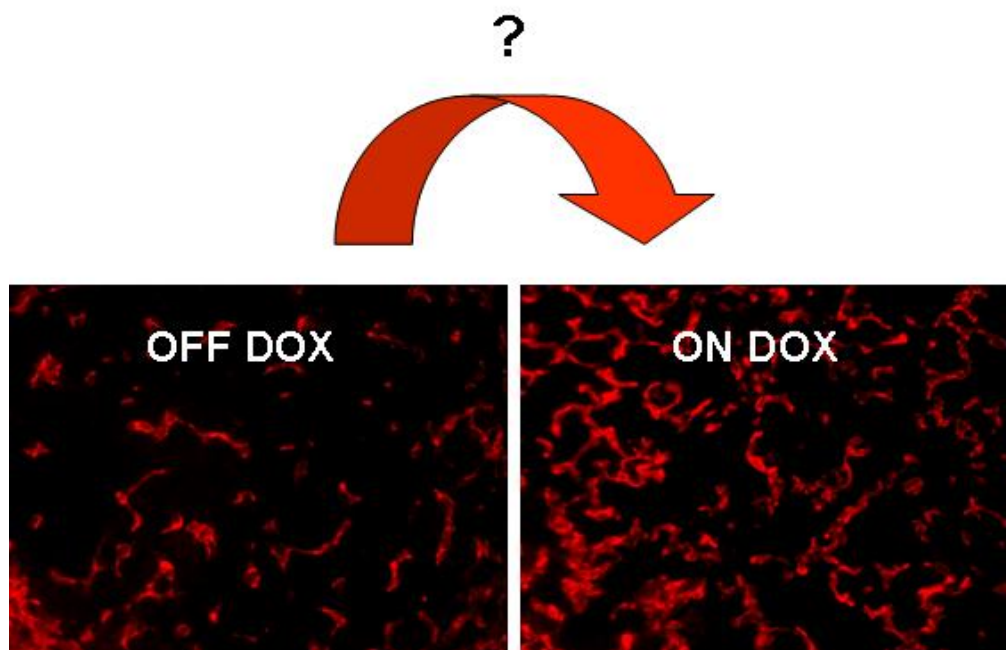
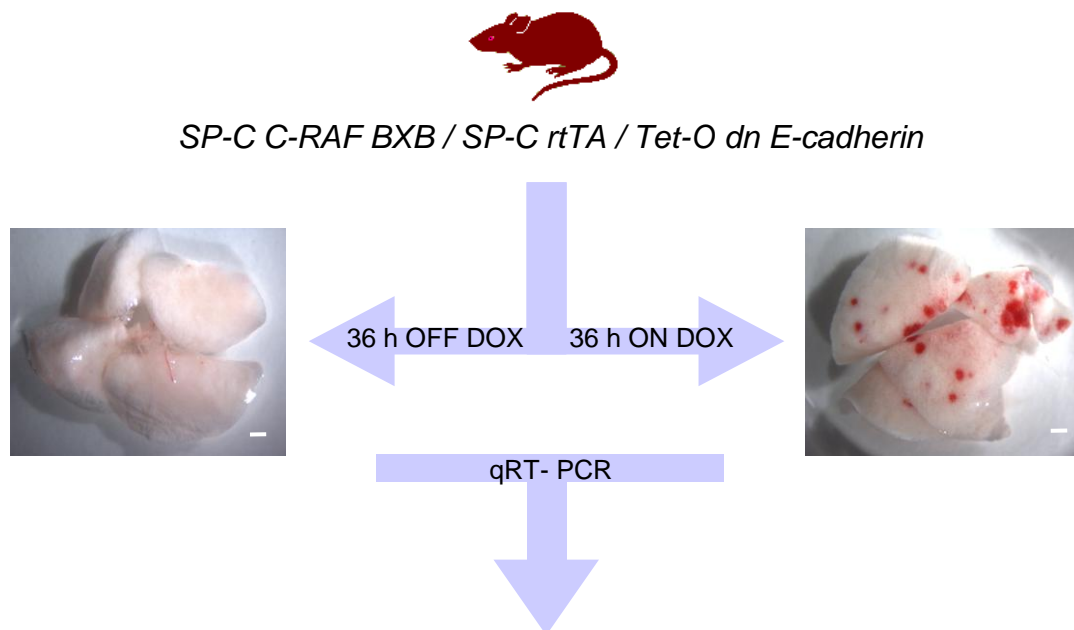


Fig.2.35. CD31 (red) staining of lung tumors from triple transgenic mice before (OFF DOX) and after (ON DOX) 8 months of DOX treatment shows increased intratumoral blood vessels.

To avoid secondary gene expression changes due to tissue disaggregation, we chose to focus on early events taking place during tumor progression. Adult triple transgenic mice were treated with DOX for 36 hours. Increased luciferase expression was observed and confirmed that transgene induction had occurred (data not shown). Short term induction typically led to haemorrhage at multiple sites, presumably as a result of vessel leakage (Fig. 2.36A). Because VEGF family members were shown to be primary regulators of angiogenesis in NSCLC (Nakashima et al., 2004), we first evaluated VEGF mRNA expression levels. Interestingly, in comparison to the untreated control mice, we consistently observed a 1.8-fold increase in the

level of VEGF-A and a 1.9-fold increase VEGF-C but not VEGF-D expression (Fig.2.36B and Table 2).

**A**



**B**

Genes	ON DOX	OFF DOX	Fold Change	P values
<i>VEGF-A</i>	1.31	0.74	1.8	0.0041
<i>VEGF-C</i>	4.41	2.36	1.9	0.0113
<i>Flt-4</i>	0.22	0.07	3.1	0.0010
<i>Cyclin D1</i>	3.52	1.70	2.1	0.0005
<i>β-catenin</i>	0.61	0.30	2.0	0.0276

Fig.2.36. Strategy for detection of transcripts during angiogenic switch induction. A. Six-week old triple transgenic mice were induced (36hr DOX pulse) or left untreated; note vessel leakage in the induced lung. Scale Bars: 2mm. B. Quantitative real time RT-PCR from total lung. Transcripts included candidate angiogenic switch genes as well as  $\beta$ -catenin target genes that have been functionally linked to angiogenesis and cell cycle control. Values represent the average of triplicates samples of six mice for each condition. hr: hour.

Additionally, we noted a 3-fold increase in the level of VEGFR-3 (*Flt-4*), a tyrosine kinase receptor for VEGF-C, suggesting that an autocrine loop may contribute to the higher proliferation observed in induced tumor cells (Fig.2.36). Transcripts for the endothelial cell

adhesion molecules VE-cadherin (*Cdh5*) and PECAM-1 (CD31) were significantly amplified, indicating a dynamic angiogenesis process in *SP-C C-RAF BXB* lung tumors in response to dn E-cadherin expression (Table 2).

Table 2. Real time RT-PCR with RNA from total lung of triple transgenic mice before and after DOX treatment.

GENE	Mean on DOX (A)	Mean off DOX (B)	Difference Between Mean (A+B)	P Values	Significance	N
<i>VEGF-A</i>	1.309 ± 0.2818	0.7400 ± 0.1070	0.5690 ± 0.3014	0,0041	**	12
<i>VEGF-C</i>	4.409 ± 2.013	2.358 ± 0.8861	2.051 ± 2.199	0,0113	*	12
<i>VEGF-D</i>	0.2252 ± 0.09746	0.4025 ± 0.1070	-0.1773 ± 0.1447	0,3929	ns	12
<i>Flt-1</i>	0.4630 ± 0.09224	0.2920 ± 0.07611	0.1710 ± 0.1196	0,2880	ns	12
<i>KDR</i>	1.267 ± 0.2110	1.078 ± 0.1818	0.1890 ± 0.2785	0,3325	ns	12
<i>Flt-4</i>	0.2145 ± 0.07534	0.0704 ± 0.02363	0.1441 ± 0.0789	0,0010	***	12
<i>Ang-1</i>	0.5084 ± 0.1490	0.4330 ± 0.09842	0.0754 ± 0.1785	0,1164	ns	12
<i>Ang-2</i>	0.2006 ± 0.02558	0.2989 ± 0.06509	-0.0982 ± 0.0672	0,0081	**	12
<i>TIE-1</i>	0.5373 ± 0.1827	0.2658 ± 0.04720	0.2715 ± 0.1982	0,0003	***	12
<i>TIE-2</i>	0.5960 ± 0.1427	0.4628 ± 0.2225	0.1332 ± 0.2589	0,1326	ns	12
<i>PECAM-1</i>	1.878 ± 0.5282	1.400 ± 0.2715	0.4783 ± 0.6106	0,0167	*	12
<i>VE-CAD</i>	2.740 ± 0.7635	0.9573 ± 0.2059	1.783 ± 0.8229	P<0.0001	***	12
<i>β-Catenin</i>	0.6094 ± 0.1975	0.2955 ± 0.1001	0.3139 ± 0.2214	0,0276	*	12
<i>c-myc</i>	0.05127 ± 0.02037	0.02914 ± 0.01324	0.0221 ± 0.0243	0,0951	ns	12
<i>Cyclin D1</i>	3.520 ± 0.8650	1.702 ± 0.2262	1.818 ± 0.8941	0,0005	***	12
<i>c-Fos</i>	1.699 ± 0.6450	1.851 ± 0.7948	-0.1518 ± 1.024	0,2718	ns	12
<i>c-Jun</i>	1.093 ± 0.3278	0.8430 ± 0.2196	0.2499 ± 0.3945	0,1391	ns	12
<i>Jun-D</i>	0.05127 ± 0.02037	0.02914 ± 0.01324	0.0221 ± 0.0243	0,0951	ns	12
<i>Thr-1</i>	0.3900 ± 0.07424	0.4560 ± 0.05246	-0.0660 ± 0.0909	0,1577	ns	12
<i>SDF-1</i>	0.5813 ± 0.1981	0.6468 ± 0.1722	-0.0654 ± 0.2624	0,3509	ns	12
<i>CxCR4</i>	0.3660 ± 0.1990	0.1933 ± 0.1035	0.1728 ± 0.2243	0,1556	ns	12
<i>MMP-9</i>	0.3133 ± 0.1345	0.3933 ± 0.09615	-0.0800 ± 0.1653	0,3383	ns	12
<i>EGR1</i>	0.2125 ± 0.09844	0.3150 ± 0.1685	-0.1025 ± 0.1952	0,6183	ns	12

Table.2. RNA was isolated from total lung of 36 hours induced (ON DOX, n=6) and control (OFF DOX, n=6) triple transgenic mice at six weeks of age, converted to cDNA and subjected to quantitative RT-PCR. The results were normalised on the basis of microglobulin. N= total number of mice. Values represent mean ±s.d. (ns=non significant; \**P*<0.05; \*\**P*<0.01; \*\*\**P*<0.001).

These data demonstrate that the onset of angiogenesis in triple transgenic lung tumors may be a direct effect of dn E-cadherin signaling via VEGF-A and VEGF-C.

Since E-cadherin competes with Apc for the binding of  $\beta$ -catenin, the potential involvement of Wnt/ $\beta$ -catenin signalling was examined in the co-operation of oncogenic C-RAF in conjunction with dn E-cadherin induction. Comparison of  $\beta$ -catenin mRNA levels in *SP-C C-RAF BXB* lung tumors revealed increased expression of  $\beta$ -catenin after 36 hours DOX treatment (Fig.2.36B and Table 2). Among various  $\beta$ -catenin target genes investigated, cyclin D1 was significantly elevated (Fig.2.36B). Thus,  $\beta$ -catenin may be an important effector of dn-E-cadherin induction. This possibility was further examined using two lung epithelial cell lines derived from NSCLC-type tumors, the mouse 3041 line (Rizzino et al., 1982) and the human A-549 cell line. Transfection of *Tet-O dn E-cadherin* and a *SP-C rtTA* expressing activator plasmid alone or in conjunction with *SP-C C-RAF BXB* showed elevated VEGF staining 24 hours after transfection (Fig.2.37). By transfection of a constitutively active  $\beta$ -catenin,  $\beta$ -catenin 4S, a similar level of VEGF induction was achieved (Fig.2.37). Notably, neither in 3041 nor in A-549 cells did *SP-C C-RAF BXB* induce VEGF expression (Fig.2.37). After dn E-cadherin,  $\beta$ -catenin was relocalised from the membrane and presumably made available to the cytoplasmic signaling pool similar to the constitutively active  $\beta$ -catenin 4S (Herzig et al., 2006) (Fig.2.37, Fig.2.38). To unravel the signaling cascade between dn E-cadherin and VEGF induction, we next investigated the role of  $\beta$ -catenin by addition of  $\beta$ -catenin siRNA. Notably,  $\beta$ -catenin siRNA suppressed VEGF expression in both 3041 and A-549 tumor cell lines (Fig.2.37). To further evaluate these observations, we determined the mRNA levels of VEGF-A and VEGF-C expression by real-time PCR analysis. Expression of dn E-cadherin increased the level of VEGF-A transcripts in a  $\beta$ -catenin dependent fashion, irrespective of C-RAF BXB co-expression in either cell line (Fig.2.39). Different results were



observed when we analyzed VEGF-C mRNA expression that was  $\beta$ -catenin independent (Fig.2.39 D), even though  $\beta$ -catenin 4S was a powerful inducer of VEGF-C in both cell lines.

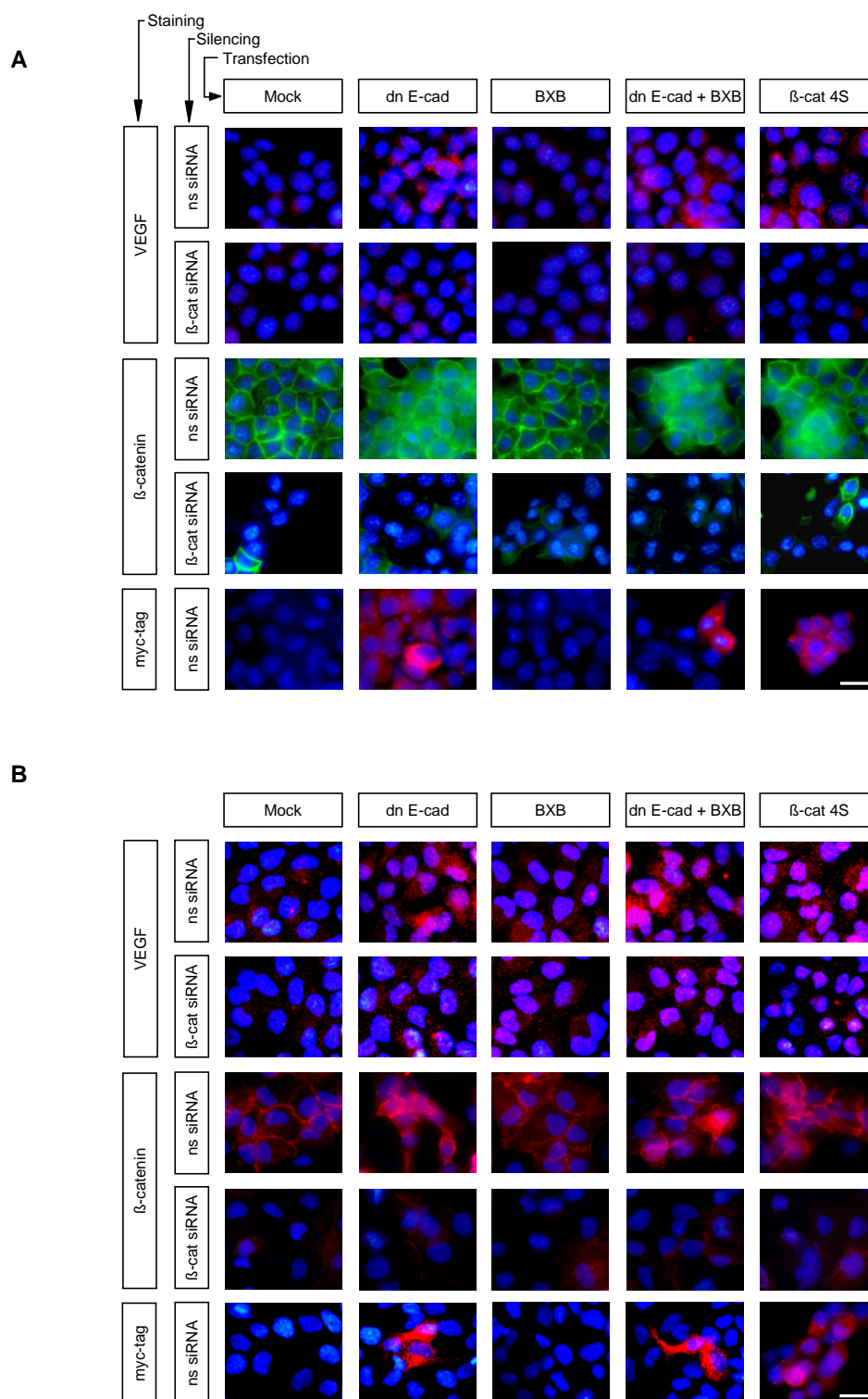


Fig.2.37. Epithelial mouse lung 3041 (A) and human NSCLC A-549 (B) cells were transfected with non specific siRNA (ns siRNA),  $\beta$ -catenin specific siRNA ( $\beta$ -cat siRNA) and DNA constructs as indicated. A constitutively active mutant of  $\beta$ -catenin,  $\beta$ -catenin 4S, was included. Representative immunocytochemistry staining identifies VEGF expression (red)

in tumor cells transfected with dn E-cadherin in the presence or absence of *C-RAF BXB*. Expression of VEGF is strongly reduced by  $\beta$ -catenin siRNA.  $\beta$ -catenin siRNA also strongly reduced endogenous  $\beta$ -catenin (green in A or red in B) in transfected tumor cells. Note the redistribution of  $\beta$ -catenin from membrane to cytosol in cells expressing dn E-cadherin or  $\beta$ -catenin 4S. Scale Bars: 10  $\mu$ m.

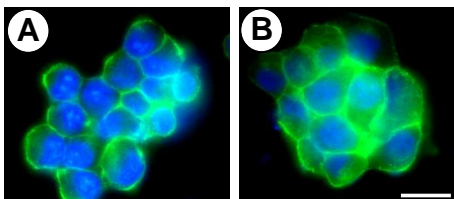


Fig.2.38. Epithelial mouse lung 3041 were transfected with empty plasmid or SP-C rtTA/tetO dn E-cadherin plasmids and stained for  $\beta$ -catenin (green). Note relocation of  $\beta$ -catenin in the cytoplasm. Scale Bar: 10  $\mu$ m.

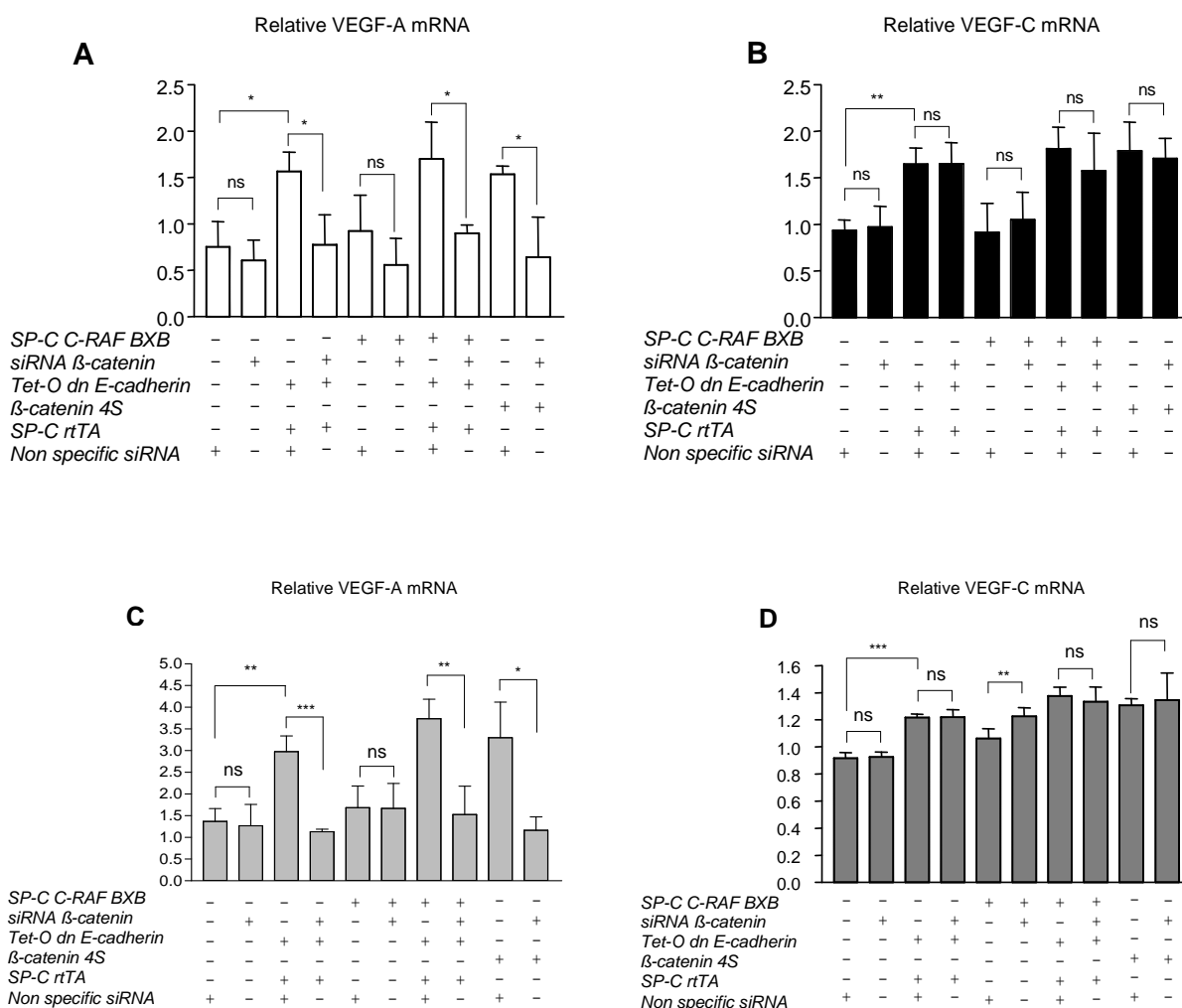


Fig.2.39. Quantitative RT-PCR from epithelial mouse lung 3041 cells that had been transfected with siRNA and DNA constructs as indicated. Non specific siRNA (ns siRNA) served as negative control. A constitutively active mutant of  $\beta$ -catenin ( $\beta$ -cat 4S), was included. Relative VEGF-A (A) and VEGF-C (B) expression in the absence or presence of  $\beta$ -

catenin siRNA in 3041 cells. (C) Relative VEGF-A and VEGF-C (D) expression in the absence or presence of  $\beta$ -catenin siRNA in A-549 cells. Histograms represent the mean of results from triplicate experiments repeated 3 times. Values represent mean  $\pm$ s.d. (ns= not significant; \* $P$ <0.05; \*\* $P$ <0.01; \*\*\*  $P$ <0.001).

These differences suggest that for VEGF-C induction by dn E-cadherin other pathways exist besides  $\beta$ -catenin-mediated signaling. There was also suggestive evidence for a suppression of VEGF-C by  $\beta$ -catenin in both cell lines although the effect was significant only in A-549 cells (Fig.2.39).

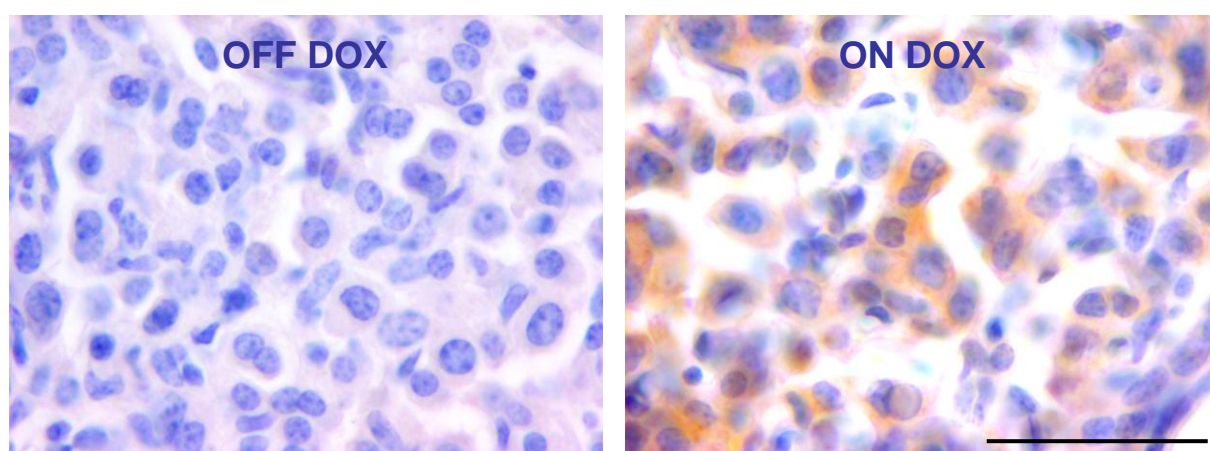


Fig.2.40. VEGF immunostaining of mouse lung tumors before and after dn E-cadherin expression demonstrates increased intratumoral VEGF proteins. Scale Bar: 50  $\mu$ m. DOX induction period for induced mice is eight months.

Similar to in vitro data, lung tumors from DOX treated triple transgenic mice stained strongly positive for VEGF arguing that angiogenic switch induction that was seen in this mouse model was mediated by a VEGF-driven mechanism (Fig.2.40).

In summary, in our transgenic NSCLC model,  $\beta$ -catenin presumably plays a key role in the induction of cell cycle progression of tumor cells and angiogenesis and that angiogenic switch mediated by a VEGF-driven process.

### 2.13. Chronic expression of dn E-cadherin in SP-C RAF BXB expressing lung epithelial cells up-regulates $\beta$ -catenin-responsive genes that include endodermal and other lineage markers.

Previous data on SP-C-driven  $\beta$ -catenin signaling in embryonic lung, using expression of a fusion protein containing the aminotermminus of LEF-1 linked to the transactivation domain of  $\beta$ -catenin, had highlighted increased expression of genes associated with other endodermal lineages (Okubo and Hogan, 2004). We therefore extended our RT-PCR analysis to lung tumors from four months induced mice.

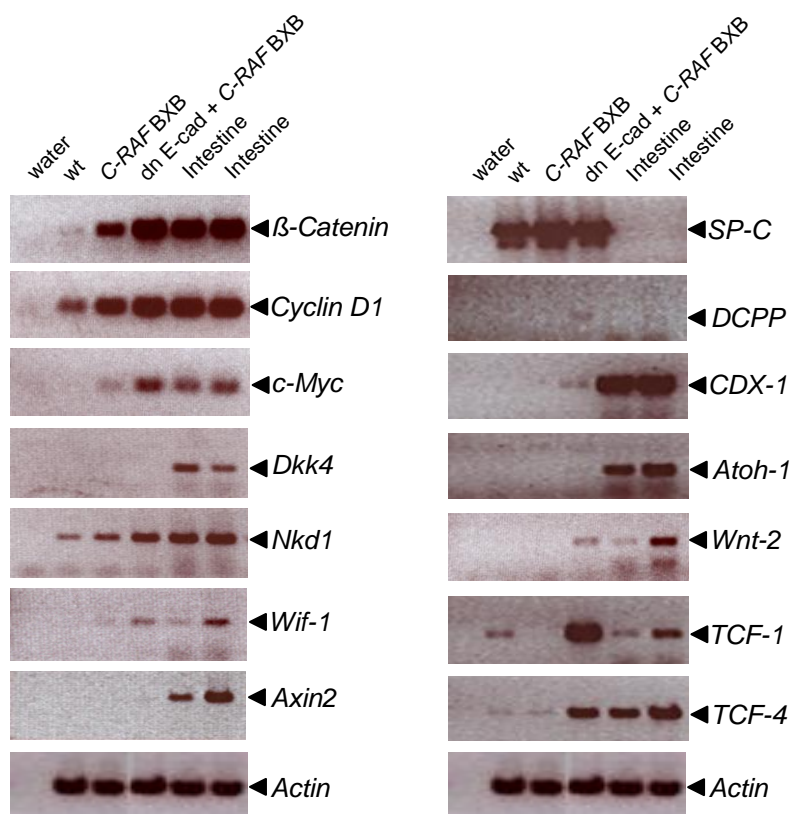


Fig.2.41. Type II pneumocytes were prepared from mice of different genotypes as indicated. Triple transgenic mice were induced for four months and used for RT-PCR. The panel of  $\beta$ -catenin responsive target genes includes components of the Wnt pathways (*Wnt-2*, *Tcf-1*, *Tcf-4*, *Dkk4*, *Nkd1*, *Wif-1*, *Axin2*), cell cycle regulators (*cyclin D1*, *c-myc*) and previously identified endodermal selector genes (*Atoh-1*, *Cdx-1*), secretory lineage of the trachea (*D CPP*). *SP-C* was used to confirm the identity of the type II epithelial cells, and  $\beta$ -actin was used as control for RNA integrity.

Importantly, six of six genes selected from the list found to be ectopically expressed during embryogenesis (Okubo and Hogan, 2004) were up-regulated in alveolar type II cells in adult mice to various extents (Fig.2.41). Most prominent was ectopic expression of the transcriptional regulators *Tcf4* and *Tcf1* and high mobility group box transcription factor *Cdx1*. Moreover, *Wnt-2* was induced which is normally expressed preferentially in mesenchymal cells and has a role in early development of lung and intestine but has also been shown to be up-regulated in NSCLC as well as other human carcinomas (Mazieres et al., 2004). As in the case of lung-targeted expression of constitutive  $\beta$ -catenin signaling during embryogenesis, ectopic expression was not confined to genes of the intestinal endoderm but included for example *DCPP* that is normally active in sublingual and salivary glands. Considering that we have constitutive  $\beta$ -catenin signaling in the DOX-treated triple transgenic mice, we also considered that negative feed-back regulators of the Wnt pathway (*Dkk4*, *Nkd1*, *Wif1*, *Axin-2*) might be up-regulated (Dequéant et al., 2006). Of these, *Wif1* and *Nkd1* were clearly up-regulated whereas *Axin-2* showed weekly increased levels. Taken together, these data support the notion that  $\beta$ -catenin is a major effector of dn E-cadherin and raise the possibility that forced simultaneous Wnt/RAF signaling generates phenotypic heterogeneity in tumors that may contribute to metastatic conversion.

### 3. DISCUSSION

Two strategies were followed to disrupt E-cadherin function in normal and *SP-C C-RAF BXB* transgenic adenomatous alveolar type II cells, DOX inducible *Cdh1* gene ablation and expression of dn E-cadherin. Use of this transgenic strain with its discrete premalignant lesion allowed us to study NSCLC progression and to evaluate the role of cell-cell adhesion in progression of NSCLC-like lung adenomas to metastatic adenocarcinoma. The striking finding was that interference with E-cadherin function not only broke cell-cell contacts but contributed to tumor progression by massive induction of angiogenesis. Attempts to delineate the mechanism of angiogenesis induction highlighted  $\beta$ -catenin as a critical effector of VEGF induction by abrogation of E-cadherin. Disruption of cell-cell contacts and induction of angiogenesis was sufficient to promote micrometastasis.

#### **Is interference with E-cadherin function oncogenic?**

Both strategies to genetically disrupt E-cadherin mediated cell-cell contacts, ablation of *Cdh 1* or dn E-cadherin induction failed to induce tumor formation in normal lung. Similar observations about lack of tumor formation upon loss of function of E-cadherin has been reported previously (Boussadia et al., 2002) by conditional knock out of *Cdh1* in alveolar epithelial cells of the mammary gland using *MMTV-Cre* mice. More recently, the effects of E-cadherin loss on mammary tumorigenesis were studied by use of *K14cre* mice leading to E-cadherin loss in ductal and alveolar epithelium (Derksen et al., 2006). No tumor formation was observed in the mammary gland or in the skin which also expresses Cre in epithelium (Jonkers et al., 2001; Derksen et al., 2006). These data on skin were similar to an earlier report by Tinkle et al. who in addition observed compensatory up-regulation of P-cadherin resulting in a hyperproliferative response (Tinkle et al., 2004). Our data in the lung are comparable to those of Tinkle et al., as we observe diffuse hyperplasia in mice with either

genetic condition to disable E-cadherin in lung alveolar type II cells. In contrast to skin, we did not observe a compensatory P-cadherin up-regulation. N-cadherin expression also remained unchanged. We conclude that *Cdh1* knock-out or dn E-cadherin induction is not sufficient for lung tumorigenesis.

#### **Induction of angiogenic switch by disruption of E-cadherin.**

Lung adenomas induced by C-RAF BXB are notoriously stable, a feature that may result from high E-cadherin expression. One way by which cadherin junctions may contribute to stability of C-RAF BXB adenomas is by suppression of angiogenesis. Evidence for suppression was obtained by our findings that disruption of cell-cell contact by *Cdh1* gene ablation or expression of dn E-cadherin in C-RAF BXB adenomas was followed by massive angiogenesis correlating with appearance of nuclear  $\beta$ -catenin in a fraction of tumor cells and their invasive behavior. These data demonstrate for the first time that the disruption of E-cadherin leads to the induction of the angiogenic switch in a preexistent adenoma and consequent progression to adenocarcinomas. Consistent data regarding blood angiogenesis were presented in a recent publication who examined effects of *Cdh1* loss in a model for invasive lobular breast cancer (Derksen et al., 2006). However, no data on lymphangiogenesis were included in this study. In the pioneering studies of Folkman et al. large T antigen was expressed under the control of rat insulin promoter (Folkman et al., 1989). Large T antigen was sufficient by itself to promote the full course of tumor progression from hyperplasia of pancreatic  $\beta$ -cells to carcinoma. Emergence of carcinoma was preceded by angiogenesis in a small fraction of hyperplastic islands that correlated with carcinoma incidence. This phenomenon was called the angiogenic switch. In subsequent studies Perl et al. used crosses between Rip1Tag2 and Rip1dn E-cadherin mice and suggested that dn E-cadherin can induce tumor progression. Double transgenic mice showed doubling of carcinoma incidence and low level of lymph node metastasis (Perl et al., 1998). In their study, no data on angiogenesis were reported.

Moreover, causal evidence for the role of dn E-cadherin at specific steps of tumor progression was not provided and would have required use of reversible expression systems. We have used such a conditional expression system and demonstrated that formation of blood and lymph vessels in tumors entirely depends on disruption of E-cadherin expression. Reversibility was maintained for up to two months after induction and involved apoptosis of endothelial cells upon restoration of E-cadherin expression. Appearance of blood and lymph vessels in the tumors correlated with increased size of individual tumor nodules some of which reached macroscopic scale. As in the case of angiogenesis, the dn E-cadherin induced increase in tumor volume required continuous presence of DOX. Long-term treatment did uncover another important aspect of tumor vasculogenesis relating to reversibility. After 4-months induction vessels self-stabilized, presumably due to acquisition of a quiescent differentiated phenotype and recruitment of pericytes (Risau et al., 1997 and Nikolopoulos et al., 2004). As a consequence, DOX withdrawal no longer leads endothelial cells to apoptosis. Although these findings support the concept of tumor therapy with angiogenesis inhibitors (Folkman, 2006), they also point to a limitation. It may be that treatment of patients with established tumors with a mature vasculature will only induce stasis but not tumor regression.

### **E-cadherin disruption promotes progression of angiogenic tumors to invasive growth and micrometastasis**

Besides induction of angiogenesis, *Cdh1* deletion or dn E-cadherin induction also co-operates with C-RAF BXB in driving proliferation and invasive growth. The increase in proliferation rates was in the order of 50% and led to appearance of macroscopic tumors on the surface of lungs by the age of 8-months. Co-operation in growth stimulation required continuous induction of dn E-cadherin as a 4M ON DOX /4M OFF DOX schedule reduced tumor volume to the level C-RAF BXB. These data may suggest a continuous need for neoangiogenesis or result from cell-autonomous effects of E-cadherin loss on cell cycle control. In addition to co-



operation in proliferation, loss of E-cadherin function changed the growth pattern of tumor cells in tumor foci. Tumors in compound mice were more dispersed and expanded into the lung parenchyma without signs of classical EMT. This finding is consistent with a previous study where expression of dn E-cadherin in Rip1Tag2 transgenic mice also led to invasive growth and lymph node metastasis without complete EMT conversion (Perl et al., 1998). Furthermore our data on E-cadherin gene ablation in *SP-C C-RAF BXB* mice are in agreement with a large body of literature that links loss of E-cadherin expression with adenoma-carcinoma progression (Birchmeier et al., 2005; Berx and Van Roy, 2001; Cavallaro and Christofori, 2004) and with a recent publication by Derksen et al. who did not observe classical EMT in invasive lobular breast cancer upon *Cdh1* loss (Derksen et al., 2006). Our data on EMT agree well with those of Perl and Derksen (Perl et al., 1998; Derksen et al., 2006). While we cannot exclude that dispersed cells in tumor foci of induced compound mice have a transient EMT in their history, we have no evidence for such an event as we did not find cells double-positive for vimentin/pro SPC or N-cadherin/pro SPC expression. On the other hand, as cells with disrupted E-cadherin appear spindle-shaped, this may be considered as a partial EMT.

Angiogenic switch followed by progression of induced tumors to invasive adenocarcinomas was not in itself sufficient to promote metastatic spread. This required additional time (at least 5 months) and led to micrometastasis into regional lymph nodes and occasionally into bone marrow. Micrometastasis was completely dependent on continuous DOX treatment. One explanation for the time requirement might be increase in tumor mass that would raise the probability for an infrequent event such as generation of metastatic cells to take place. The fact that micrometastasis occurred late whereas angiogenesis and cell dispersion were early events is consistent with the concept that additional genetic changes are required in the tumor cells before they express (mutated) metastasis gene(s) (Hanahan and

Weinberg, 2000). Tumor cells equipped with a “metastatic signature” should be able to grow into new tumors at distant sites. That is not the case in micrometastasis (Schardt et al., 2005) that may spread dormant tumor cells. Dormant tumor cells are initiated cells using the language of two-stage carcinogenesis (Rous and Kidd, 1941; Berenblum, I., 1954). These cryptic transformants require a tumor-promoting condition which may utilize regenerative signaling pathways (Maurange et al., 2006). The dependence of micrometastasis on continued dn E-cadherin expression suggests that the ability of tumor cells to induce angiogenesis may be required for seeding at distant sites but may not be sufficient for clonal expansion at that site. The combined data suggest that the step in tumor progression that is being induced by disruption of E-cadherin may be limited to acquisition of a self-seeding phenotype that include micrometastasis (Norton and Massagué, 2006). It will be interesting to determine whether strengthening the growth engine by combination of *RAF* with other oncogenes would overcome this limitation. We are currently exploring this possibility in transplantation experiments with fractionated tumor cells.

### **Disruption of E-cadherin activates $\beta$ -catenin signaling**

Quantitative RT-PCR of acutely induced compound mice identified 3 classes of angiogenic factors that showed a 2-fold increase. These were VEGF-A, VEGF-C and its receptor Flt-4, as well as Tie1, endothelial cell adhesion molecule VE-cadherin and  $\beta$ -catenin together with cyclin D1. VEGF-A and VEGF-C were also induced *in vitro* in transient transfection experiments with a dn E-cadherin expression vector in mouse and human cell lines derived from NSCLC. The simplest explanation for the combined *in vivo* and *in vitro* findings is a signaling cascade connecting dn E-cadherin or *Cdh1* inactivation via  $\beta$ -catenin with angiogenesis target genes. Such a chain is supported by *in vitro* siRNA experiments against  $\beta$ -catenin and identifies E-cadherin disruption for the first time as a signaling condition. Induction of VEGF-A, not VEGF-C was  $\beta$ -catenin dependent consistent with an earlier report

which described VEGF-A as a direct  $\beta$ -catenin target gene in human colon cancer cell lines (Easwaran et al., 2003). In human endothelial cells (HUVECs),  $\beta$ -catenin was described to mediate both VEGF-A and VEGF-C expression (Skurk et al., 2005) which parallels the pattern we found in our lungs from DOX induced triple transgenic mice. VEGF-A and VEGF-C have prognostic value for NSCLC (Nakashima et al., 2004) and the VEGF-C/Flt-4 axis has been shown to promote invasion and metastasis of lung A549 and other cancer cell lines (Su et al., 2006). On the basis of our and these literature data we conclude that the mechanism of angiogenic switch induction and subsequent tumor progression induced by disruption of E-cadherin involves signaling via  $\beta$ -catenin and VEGF-A/VEGF-C.

**Up-regulation of  $\beta$ -catenin targets by chronic disruption of E-cadherin in alveolar epithelial cells includes genes from endodermal lineages.**

Further evidence that  $\beta$ -catenin functions as a critical effector of chronic E-cadherin disruption was obtained by RT-PCR experiments using RNA from purified type II cells of lung tumors. These experiments revealed up-regulation of a set of genes that was previously reported to be induced in embryonic lungs with a SP-C promoter-driven constitutively active  $\beta$ -catenin transgene (Okubo and Hogan, 2004). Selected candidate genes included endodermal and other lineage markers, Wnt pathway- and cell cycle- regulators. Our data suggest reprogramming of C-RAF-transformed type II cells and raise the possibility that constitutive signaling by the Wnt pathway simultaneously with mitogenic cascade signaling may erode phenotypic stability. There is evidence that these two pathways normally function in an alternating fashion and thus constitute the core element of a developmental oscillator (Dequéant et al., 2006). As combined signaling is a prerequisite for micrometastasis in our model it is tempting to speculate that ontogenetically younger programs are used as a resource for acquisition of metastatic behavior.

## 4. MATERIALS AND METHODS

The methods described in this section are all based upon today's standard molecular and cellular biology techniques.

### 4.1. Materials

#### 4.1.1. Instruments

Hardware	Manufacturer
100/40/20 µm cell strainer	BD Falcon
Berthold Luminator	Bio-Rad
BioRobot EZ1	Qiagen
Cell culture hood	Heraeus Instrument
Cell culture incubator	Heraeus Instrument
Cryo microtome	Leica
Developing machine	Agfa
Electrophoresis power supply	Bio-Rad
Electrophoresis unit, small	Bio-Rad Mini-Protean II
Fine scale	Scaltec SBC 21
Fluorescence Microscope (CCD)	Leica (Hamamatsu Orca)
Glass coverslip	Leica
Heat block	Liebisch, Type 2099-DA
Homogenizer	Ultra-Turrax <sup>®</sup>
Horizontal electrophoresis gel	PEQLAB
Incubator (37 °C)	Heraeus B 6200
Inverted microscope	Olympus
Laser microdissection microscope	Leica
Mini centrifuge	Eppendorf; Biofuge 15, Heraeus
Mega centrifuge	J-6B, Beckman; Megafuge 1.0 R
Microlumat	EG&G, Berthold
Microscope Slides, Super Frost <sup>®</sup> Plus	Menzel-Gläzer
Microtome (rotating/sliding)	Leitz Wetzlar
Paraffin embedding machine	Leica
pH meter	Microprocessor, WTW
Phosphoimager	Fujix BAS-2000 III, Fuji
Roto-Gene 2000	Corbett Research
Scale	BP2100S, BP310S, Sartorius
Shaker	New Brunswick Scientific
Sonicator	Sono Plus HD 70

Spectrophotometer	Ultraspec 3000, Pharmacia Bio.
Thermocycler	PE9600, Perkin Elmer ; T3, B.M.
Ultraviolet Crosslinker	UVC500 Hoefer Scientific
Vortex	Scientific Industries Genie-2
Water bath	GFL 1083, Amersham-Buchler

#### 4.1.2. Chemical reagents and general materials

Reagent	Purchased from
[ $\alpha$ - <sup>32</sup> P]dCTP (370MBq/ml)	Amersham
1 kb DNA ladder	Invitrogen, MBI
Acetone	A. Hartenstein
Acrylamide (30%)/Bisacrylamide (0.8%)	Roth
Adenosin-5' Triphosphate (ATP)	Sigma
Agarose, ultra pure	Invitrogen
Ammonium Acetate	Sigma
Ammonium peroxydisulfate (APS)	Sigma
Ampicillin	Sigma
Aprotinin	Roth
Bacto-Agar	Roth
BCP	Molecular Research Center Inc.
Bovine serum albumin (BSA)	Sigma
Bradford-reagent	Bio-Rad
Bromodeoxyuridine (BrdU)	Sigma
Bromophenolblue	Sigma
$\beta$ -Mercaptoethanol	Roth
Calciumchloride (CaCl <sub>2</sub> )	Sigma
Chloroform	Roth
Chloralhydrate	Roth
Diaminobenzidine (DAB)	Sigma
DAPI	Sigma
Deoxycholate (DOC)	Sigma
Diethyl pyrocarbonate (DEPC)	Merck
Dimethylsulfoxide (DMSO)	Sigma
Dithiothreitol (DTT)	Sigma
DNase I (for type II cell isolation)	Sigma
dNTPs	MBI
Doxycycline	Sigma
ECL-System	Amersham
EDTA	Sigma

EGTA	Sigma
Entellan	Merck
Eosin	Merck
Ethanol	Roth
Ethidiumbromide	Invitrogen
Formaldehyde	Roth
Formamide	Roth
Glutathion-sepharose	Pharmacia
Glycerol	Sigma
Guanidine thiocyanate	Roth
Haematoxylin	Merck
Hepes	Roth
Hydrochloride (HCl)	Roth
Hybond-N membrane	Amersham
Hydrogen Peroxide (30 %)	A. Hartenstein
IGEPAL (NP-40)	Sigma
Isoropyl-1-thio- $\beta$ -D-thiogalactopyranoside	Roth
Isopropanol	Merck
Ketanest	Pfiser
Leupeptin	Sigma
Low melting agarose (LMP)	peqLab
Magnesiumchloride	Sigma
Methanol	A. Hartenstein
Mowiol	Calbiochem
3-(N-morpholino)propanesulfonic acid	Sigma
Paraffin wax (Histosec Pastillen)	Merck
Paraformaldehyde (PFA)	Sigma
Pefablock	Roth
Phenol	Roth
Phenol:Chloroform:Isoamylacohol	Roth
Phenol/Chloroform (TE saturated)	Roth
Ponceau S	Sigma
Potassium acetate (KAc)	Sigma
Potassiumchloride (KCl)	Sigma
Potassiumdihydrophosphate (KH <sub>2</sub> PO <sub>4</sub> )	Merck
Protein ladder, BenchMark™	Invitrogen, MBI
PROTRAN membrane	Schleicher & Schüll
QIAzol	Qiagen
Rnase-free water	Fermentas

Rompun	Bayer
SDS ultra pure	Roth
Serum (goat)	Chemicon
Serum (rabbit)	Chemicon
Serum (donkey)	Chemicon
Sodium citrate	Merck
Sodium Chloride	Roth
Sodiumdihydrophosphate (NaH <sub>2</sub> PO <sub>4</sub> )	Merck
Sodiumhydrophosphate (NaHPO <sub>4</sub> )	Merck
Sodiumhydroxide (NaOH)	Sigma
Sodium orthovanadate	Sigma
Sonicated fish sperm DNA	Roche
TEMED	Roth
Tissuetec (OCT)	Chemicon
Tris-(hydroxymethyl)-aminomethane (Tris)	Roth
TriZOL Reagent	Invitrogen
Triton-X100	Sigma
Whatman 3MM Paper	Schleicher & Schüll
X-gal	Sigma
X-ray film	Amersham
Xylen	J. T. Baker
Yeast extract	Invitrogen

#### **4.1.3. Cell culture materials**

Reagent	Source
DMSO	A. Hartenstein
OPTI-MEM	Invitrogen
Cover slips	A. Hartenstein
Thoma Lam	A. Hartenstein
DMEM	Invitrogen
Fetal calf serum (FCS)	Invitrogen
Lipofectamine 2000	Invitrogen
Phosphate buffered saline (PBS)	Invitrogen
Penicillin/Streptomycin	Invitrogen
Dispase	Invitrogen
Flasks	Cell Star
Plates	Sarstedt

**4.1.4. Antibodies**

Primary Antibody	Cat.or Clone Nr	Company
anti- $\beta$ -catenin (mouse)	610154	BD Transduction Lab.
anti $\beta$ -catenin (rabbit)	06-734	Upstate
anti-E-cadherin (rat)	ECCD-2	Zymed Lab.
anti-E-cadherin (mouse)	Decma-1	Sigma
anti-E-cadherin (mouse)	C20820	BD Biosciences
anti-E-cadherin (mouse)	610181	BD Biosciences
anti-E-cadherin (rabbit)	gp84	Gift from R. Kemmler
anti-myc tag (mouse)	Sc-40	Santa Cruz
anti-GAPDH (rabbit)	ab9485	Abcam
anti-N-cadherin	33-3900	Zymed Lab.
anti-Actin	A 2066	Sigma
anti-Actin	Sc-1616-R	Santa Cruz
anti-GAPDH	Ab 9485-100	Abcam
anti-P-cadherin (rat)	PCD-1	Zymed Lab.
anti-pro-SPC (rabbit)		Gift from J. Whitsett
anti-pro-SPC (rabbit)	AB 3786	Chemicon
ananti-CCSP (Goat)	Sc-9772	Santa Cruz
anti-Prox1 (rabbit)	102-PA30	ReliaTech
anti-VEGF (rabbit)	Sc-507	Santa Cruz
anti cow cytokeratin (rabbit)	Z0622	DAKO
anti-LYVE-1 (rabbit)	11-034	Angio Bio Co.
anti-PECAM-1 (rat)	553370	BD Pharmingen
anti-PCNA (mouse)	555556	BD Pharmingen
anti-Cre (rabbit)	69050-3	Novagen
anti-Vimentin	Sc-7557	Santa Cruz
anti-active caspase-3	5A1	Cell Signaling
anti-Ki67	ab15580	Abcam
anti mouse CD45 (Rat)	553076	Pharmingen
anti mouse CD16/CD32 (Rat)	553142	Pharmingen
anti-TTF-1 (Rat)	86763/1	Dako
Secondary Antibody	Catalog No	Company
anti-Mouse IgG conjugated peroxidase	NA931 V	Amersham
anti-Rabbit IgG conjugated peroxidase	NA934	Amersham
anti-Rat IgG conjugated peroxidase	NA935	Amersham
anti-Rabbit Alexa Fluor 488 (Donkey)	A 11008	Molecular Probes
anti-Rat Alexa Fluor 488 (Donkey)	A 21212	Molecular Probes



anti-Goat Alexa Fluor 555 (Donkey)	A 21432	Invitrogen
anti-Rabbit Cy5 (Donkey)	711-175-152	Jackson ImmunoResearch
anti-mouse Cy3 (Goat)	115-165-166	Jackson ImmunoResearch
anti-Rabbit Cy3 (Donkey)	711-165-152	Jackson ImmunoResearch
anti-Rabbit FITC (Donkey)	711-095-152	Jackson ImmunoResearch
anti-Rat FITC (Donkey)	712-095-153	Jackson ImmunoResearch
anti-Rabbit TRITC (Donkey)	711-025-152	Jackson ImmunoResearch
anti-mouse TRITC (Donkey)	715-025-151	Jackson ImmunoResearch
anti-Rat Texas Red (Goat)	112-075-167	Jackson ImmunoResearch
anti-cow biotinylated (Rabbit)	Z0622	Dako
anti-goat biotinylated (Rabbit)	E0466	Dako
anti-mouse biotinylated (Rabbit)	E0354	Dako
anti-mouse biotinylated (Goat)	EO433	Dako
anti-rabbit biotinylated (Goat)	EO32	Dako

#### 4.1.5. Enzymes

Items	Source
BioTherm DNA polymerase	Gene Craft
Calf Intestinal Phosphatase (CIP)	New England Biolabs (NEB)
DNase I, PCR grade	MBI
Klenow Fragment	MBI
M-MuLV-RT (reverse transcriptase)	MBI
Pfu polymerase	Stratagene
Proteinase K	Roth
Restriction Endonucleases	MBI, NEB, Amersham
RNaseA	Roche
T4 Ligase	NEB

#### 4.1.6. Kits

Items	Source
siRNA Transfection Reagent	Santa Cruz
ECL Western blotting detection reagents	Amersham
Luciferase Assay Kit	Promega
NucTrap <sup>®</sup> column purification Kit	Stratagene
QIAEX II Gel Extraction Kit	Qiagen
QIAGEN Plasmid Kit (Maxi)	Qiagen
EZ1 DNA Kit	Qiagen
EZ1 RNA Kit	Qiagen
DyNamo HS SYBR Green qPCR Kit	Finnzymes

RNeasy micro Kit	Qiagen
Ribogreen RNA Quantitation Kit	Molecular Probes
DNAeasy Tissue Kit	Qiagen
c-DNA synthesis Kit	Fermentas
DNase I treatment Kit	Fermentas
Protein concentration Kit	Millipore
Dead End Fluorometric TUNEL Kit	Promega
QIAquick PCR purification Kit	Qiagen
Quikhyb solution	Stratagene
TRIzol <sup>®</sup> LS reagent	Invitrogen
Vectastain <sup>®</sup> ABC-peroxidase kit	Vectastain

#### 4.1.7. Plasmid DNA

Plasmids	Source
PBi5	R. Götz
dn E-cadherin (myc-tagged)	H. Semb
pBi5 dn E-cadherin	R. Götz
SP-C rtTA	R. Götz
CMV-tTA	J. Troppmaier
dn E-cadherin without luciferase	F. Ceteci
TOP / FOP Flash	Upstate
pEGFP	Chaemai Xiang
$\beta$ -catenin 4S	Gerhart Christofori

#### 4.1.8. Oligonucleotides

##### Genotyping primers for mice

Genes	Oligo Sequences	Ann. Tem.
<i>PBi5 dn E-cad</i>	as : 5'- AGT AGG CGT GTA CGG TGG GAG - 3' s : 5'- TCG GAG ATC AGC TTC TGC TCG - 3'	60 °C
<i>SP-C C-RAF BxB 23</i>	as : 5'- GCT GGT GTT CAT GCA CTG CAG - 3' s : 5'- AAA GAC TCA ATG CAT GCC ACG - 3'	60 °C
<i>SP-C rtTA</i>	as : 5'- TCC TGG CTG TAG AGT CCC TG - 3' s : 5'- CTC CAG GAA CCC ACT CTC TG - 3'	60 °C
<i>Tet-O Cre</i>	as : 5'- GTG ATC AGC TCC AGG TTT GAC TT - 3' s : 5'- GAG GAG GAT GAG GGT GTC TAT AGG T - 3'	60 °C

<i>flox E-cad.</i>	as : 5'- CAA AGC ATT GCC CAT TCG AT - 3' s : 5'- GCC CTG CTG TGG TCT CAC TAC - 3'	60 °C
<i>K.O. allele of E-cad.</i>	as : 5'- CTT CTA CAG GGG ACT TGA GAT - 3' s : 5'- GTG ACA CAT GCC TTT ACT TTA - 3'	60 °C

Semi-quantitative RT-PCR primers and conditions

Genes	Oligo Sequences	Ann. Tem.
<i>E-cadherin</i>	as : 5'- TTG GAC GTC CAT GTG TGT GAC - 3' s : 5'- GTT GCC CCA CTC GTT CAG ATA - 3'	64 °C
<i>β-actin</i>	as : 5'- GTC GTA CCA CAG GCA TTG TGA TGG - 3' s : 5'- GCA ATG CCT GGG TAC ATG GTG G - 3'	56 °C
<i>β-catenin</i>	as : 5'-CTTGGATATCGCCAGGATGATC-3' s : 5'-TATCAAACCAGGCCAGCTGATT-3'	56 °C
<i>TCF-1</i>	as : 5'-AGG AGG CTA AGA AGC CAG TC-3' s : 5'-TAG AGC ACT GTC ATC GGA AG-3'	56 °C
<i>TCF-4</i>	as : 5'-GGC CCT GC AGA TGC AAA TAC-3' s : 5'-CTT GGT CAC CAG AGA CAG AG-3'	56 °C
<i>Cyclin D1</i>	as : 5'-CCT CCT CCT CAG TGG CCT TG -3' s : 5'-CAT CAA GTG TGA CCC GGA CTG-3'	56 °C
<i>c-myc</i>	as : 5'-GCC CGA CCT CTT G-3' s : 5'-CAC CAG CAG CGA CTC TGA A-3'	56 °C
<i>Atoh-1</i>	as : 5'-TTG CCG GAC TCG CTT CTC AG-3' s : 5'-CTA ACT GGC CTC ATC AGA GTC-3'	56 °C
<i>Wif-1</i>	as : 5'-ATC AAC TGA CAC AAT ATA AGA TCT GT-3' s : 5'-GCT GGC ACG GCA GAC ACT-3'	56 °C
<i>Cdx-1</i>	as : 5'-GGA CGC CCT ACG AAT GGA TG-3' s : 5'-AAC TCC TCC TTG ACG GGC AC-3'	58 °C
<i>DCPP</i>	as : 5'-AGA TGT TCC AGC TGG AGG CC-3' s : 5'-TAT GCC ACC TGC CCT CCA AG-3'	59 °C
<i>SP-C</i>	as : 5'-GGA CAT GAG TAG CAA AGA GG-3' s : 5'-GTA GAG TGG TAG CTC TCC AC-3'	58 °C
<i>Wnt2</i>	as : 5'-AGA GGA AAG GCA AGG ATG CC-3' s : 5'-TTG CAT GTG TGC ACG TCC AG-3'	59 °C

qRT-PCR primers

Genes	Oligo Sequences	Ann. Tem.
-------	-----------------	-----------

<i>VEGF-A</i>	as : 5'- GGC GAT TTA GCA GCA GAT ATA AGA A - 3' s : 5'- GGA GAT CCT TCG AGG AGC ACT T - 3'	60 °C
<i>hu. VEGF-A</i>	as : 5'- TTC TTT GGT CTG CAT TCA CAT T- 3' s : 5'- CCT CCG AAA CCA TGA ACT TT - 3'	60 °C
<i>VEGF-C</i>	as : 5'- GCT GGT GTT CAT GCA CTG CAG - 3' s : 5'- AAA GAC TCA ATG CAT GCC ACG - 3'	60 °C
<i>hu. VEGF-C</i>	as : 5'- CCC ACA TCT GTA GAC GGA CA - 3' s : 5'- GCC AAC CTC AAC TCA AGG AC - 3'	60 °C
<i>VEGF-D</i>	as : 5'- TCC TGG CTG TAG AGT CCC TG - 3' s : 5'- CTC CAG GAA CCC ACT CTC TG - 3'	60 °C
<i>Flt-1</i>	as : 5'- GTG ATC AGC TCC AGG TTT GAC TT - 3' s : 5'- GAG GAG GAT GAG GGT GTC TAT AGG T - 3'	60 °C
<i>KDR</i>	as : 5'- CAA AGC ATT GCC CAT TCG AT - 3' s : 5'- GCC CTG CTG TGG TCT CAC TAC - 3'	60 °C
<i>Flt-4</i>	as : 5'- TTC ACA CAC GTA GTC ACC CTC G - 3' s : 5'- GCC ACG CCA CCC TCA G - 3'	60 °C
<i>Ang-1</i>	as : 5'- GCA CAT TGC CCA TGT TGA ATC - 3' s : 5'- CAT TCT TCG CTG CCA TTC TG - 3'	60 °C
<i>Ang-2</i>	as : 5'- TTT TGT GGG TAG TAC TGT CCA TTC A - 3' s : 5'- TTA GCA CAA AGG ATT CGG ACA AT - 3'	60 °C
<i>TIE-1</i>	as : 5'- GCC AGT CTA GGG TAT TGA AGT AGG A - 3' s : 5'- CAA GGT CAC ACA CAC GGT GAA - 3'	60 °C
<i>TIE-2</i>	as : 5'- CGA ATA GCC ATC CAC TAT TGT CC - 3' s : 5'- ATG TGG AAG TCG AGA GGC GAT - 3'	60 °C
<i>PECAM-1</i>	as : 5'- TCC TTC CTG CTT CTT GCT AGC T - 3' s : 5'- GAG CCC AAT CAC GTT TCA GTT T - 3'	60 °C
<i>VE-CAD</i>	as : 5'- GTA AGT GAC CAA CTG CTC GTG AAT - 3' s : 5'- TCC TCT GCA TCC TCA CTA TCA CA - 3'	60 °C
<i>β-catenin</i>	as : 5'- CAA CCC TGA GGA AGA AGA - 3' s : 5'- TGC CCG CAA TAT CAG CTA - 3'	55 °C
<i>c-myc</i>	as : 5'- CAC CAG CAG CGA CTC TGA A - 3' s : 5'- GCC CGA CCT CTT G - 3'	55 °C
<i>Cyclin D1</i>	as : 5'- CAT CAA GTG TGA CCC GGA CTG - 3' s : 5'- CCT CCT CCT CAG TGG CCT TG - 3'	55 °C
<i>c-Fos</i>	as : 5'- TTC AGA CCA CCT CGA CAA TG - 3' s : 5'- TTC CTG GCA ATA GCG TGT TC - 3'	60 °C
<i>c-JUN</i>	as : 5'- TGA AAG CTG TGT CCC CTG TC - 3' s : 5'- ATC ACA GCA CAT GCC ACT TC - 3'	60 °C
	as : 5'- AAA AGA GAG GGG ATG GTG TC - 3'	

<i>Jun-D</i>	s : 5'- TGG AAG AGA GAA CGG GAG TG - 3'	60 °C
<i>Thr-1</i>	as : 5'- TTT GTG GCC GAT GTA GTT GGT - 3' s : 5'- TGC TGC AGA ATG TGA GGT TTG - 3'	60 °C
<i>MMP-9</i>	as : 5'- GGA AAC TCA CAC GCC AGA AG - 3' s : 5'- CCC TGG AAC TCA CAC GAC A - 3'	54 °C
<i>EGR1</i>	as : 5'- TGG GCA CCC CAG ACC AGA AG - 3' s : 5'- GTG TCT TGC TGG GCC GGT TG - 3'	55 °C
<i>CxCR4</i>	as : 5'- TCA GTC AGG GGG ATG ACA GG- 3' s : 5'- TGG CCC TTG GAG TGT GAC AGC- 3'	54 °C
<i>SDF-1</i>	as : 5'- ACC AGT CAG CCT GAG CTA CC - 3' s : 5'- CAC TTT AAT TTC GGG TCA ATG C- 3'	54 °C
dn <i>E-cad.</i>	as : 5'- AGA ATC AGC AGG GCG AGG AT - 3' s : 5'- GAG AGG CAC CTG GAG AGA GG - 3'	55 °C
BxB	as : 5'- CAA GGA TGG CTC GGA AGC GC- 3' s : 5'- TGG GCC GAG GAT ATG CCT CC - 3'	60 °C
<i>Microglob.</i>	as : 5'- CAG TCT CAG TGG GGG TGA AT - 3' s : 5'- ATG GGA AGC CGA ACA TAC TG - 3'	60 °C

#### 4.1.9. Cell lines, mouse lines and bacterial strains

Cell lines	Source
3041	Mouse lung adenocarcinoma cell line (MSZ)
A-549	Human lung adenocarcinoma cell line (MSZ)
N-CMV tTA	NIH3T3 constitutively expressing tTA transactivators (MSZ)
<i>Mouse lines</i>	Source
B6D2F1	All were obtained from Harlan Winkelmann GmbH
C57Bl6	All were obtained from Harlan Winkelmann GmbH
NMRI	All were obtained from Harlan Winkelmann GmbH
FVB	All were obtained from Harlan Winkelmann GmbH
Bacterial str.	Source
DH5 $\alpha$	Bethesda Research Laboratories

#### 4.2. Solutions and buffers

##### 4.2.1. Bacterial medium and plasmid isolation buffers

LB (Luria-Bertani) medium

10g/L Bacto-tryptone

10g/L NaCl

5g/L yeast extract

Adjust pH to 7.5 with NaOH

For plates, add 15 g Bacto-agar per liter

SOB medium (1 L)

20g Bacto-tryptone

0.5g NaCl, 5g yeast extract

10ml 250mM KCl

Adjust pH to 7.5 with NaOH

(Before use add 5ml 2M MgCl<sub>2</sub>)

Buffer P1 (resuspension buffer)

50mM Tris-HCl

10mM EDTA

10µg/ml RNaseA; pH 8.0

Buffer P2 (Lysis buffer)

10% SDS

200 mM NaOH

Buffer P3 (Neutralization buffer)

3 M potassium acetate, pH5.5

Buffer QBT

15% ethanol

0.15% Triton X-100

Buffer QC (Wash buffer)

2.0 M NaCl

50 mM MOPS, pH7.0

15% ethanol

Buffer QF (Elution buffer)

1.25 mM NaCl

50 mM Tris-HCl, pH 8.5

15% ethanol

**4.2.2. DNA buffers**

Tail Lysis Buffer

50 mM EDTA

50 mM Tris-HCl

0.5% SDS; pH8.0

10x TE

0.1 M Tris-HCl

10 mM EDTA; pH 7.5

10x DNA Gel Loading Buffer  
40% (w/v) saccharose  
0.25% bromphenolblue  
0.25% xylencyanol; use as 1x solution  
1x Tris-Acetate-EDTA (TAE)  
40 mM Tris-HCl  
40 mM acetic acid  
2 mM EDTA; pH7.8  
20x SSC  
175.3g/L NaCl  
88.2g/L sodium citrate; pH 7.0  
Washing buffer 1  
2x SSC  
0.1% SDS  
Washing buffer 2  
0.1x SSC  
0.1% SDS

#### **4.2.3. Protein analysis buffers**

##### NP40 lysis buffer

10 mM Hepes, pH 7.4  
145 mM KCl  
5 mM MgCl<sub>2</sub>  
1 mM EGTA  
0.2% IGEPAL  
1 mM pefablock  
1 mM sodium vanadate  
5 mM benzamidine  
5 µg/ml aprotinin  
5 µg/ml leupeptin

##### RIPA Buffer

50 mM Tris-HCl pH: 7.4  
150 mM NaCl  
1% NP 40  
0.25% Na-deoxycholate  
1 mM PMSF  
1X Roche complete mini protease inhibitor cocktail  
5x SDS-loading Buffer (for SDS-PAGE)  
31 mM Tris-HCl, pH6.8

1% SDS

5 % Glycerin

2.5 %  $\beta$ -Mercaptoethanol

0.05 % Bromphenolblue; use as 1x solution

Running buffer (for SDS-PAGE)

25 mM Tris

250 mM Glycine

0.1 % SDS

Blotting buffer

25 mM Tris

192 mM Glycine

10% Methanol

10x Tris-Buffered Saline (TBS)

500 mM Tris-HCl, pH7.4

1.5 M NaCl

TBST

1x TBS + 0.05% Tween 20

Blocking Buffer

5% (w/v) of non-fat dry milk in TBST

**4.2.4. Histological buffers**

Eosin solution

1% Eosin in H<sub>2</sub>O

Hematoxylin solution (per 100 ml)

1 g Hematoxylin

0.2 g NaIO<sub>3</sub>

50 g KAl(SO<sub>4</sub>)<sub>2</sub>·12H<sub>2</sub>O

1 g sodium citrate

25 g chloral hydrate

**4.3. Methods**

**4.3.1. Bacterial manipulation**

**4.3.1.1. Transformation of competent bacteria**

Thaw the competent bacteria on ice. Add a maximum of 20 ng ligated DNA or purified plasmid-DNA to 100  $\mu$ l competent cells in a cold 1.5 ml microfuge tube. Mix carefully and keep on ice for 30 min or longer. Heat-shock the bacteria then at 42°C for 90 sec, add 1 ml antibiotic-free LB medium, and incubate at 37°C for 45 min. Selection of transformed bacteria is done by plating 100  $\mu$ l of the bacterial suspension on antibiotic containing agar plates. Only bacteria that have taken up the desired plasmids, which contain



ampicillin or kanamycin resistance cassette, can grow on the agar plates. A single colony can then be expanded in LB medium and used for DNA preparation.

#### **4.3.2. DNA methods**

##### **4.3.2.1. Electrophoresis of DNA on agarose gel**

Double stranded DNA fragments with lengths between 0.5 kb and 10 kb can be separated according to their lengths on agarose gels. Agarose is added to 1X TAE to obtain a final concentration between 0.7-2 percent. Boil the suspension in the microwave until the agarose is completely solubilised. Allow the agarose to cool down to around 50°C before adding ethidium bromide up to 0.5 µg/ml and pour into the gel apparatus. Add DNA gel loading buffer to the DNA sample and apply on the gel. Electrophorese in 1X TAE buffer at 100 volts. The DNA can be visualised under UV-light.

##### **4.3.2.2. Isolation of plasmid DNA from agarose (QIAEX II agarose gel extraction protocol)**

Excise the desired DNA band from the agarose gel under the UV light. Weigh the gel slice and add 3 volumes of Buffer QG to 1 volume of gel for DNA fragments 100-bp to 4 kbp; for DNA fragments more than 4 kbp, add 2 volume of QG plus 2 volumes of H<sub>2</sub>O. Resuspend QIAEA II by vortexing for 30 sec; add 10 µl (or 30 µl) of QIAEX II to the sample containing not more than 10 µg of DNA (between 2-10 µg). Incubate at 50°C for 10 min to solubilise the agarose and bind the DNA. Mix by vortexing every 2 min to keep QIAEX II in suspension. Centrifuge the sample for 30 sec and carefully remove supernatant with a pipette. Wash the pellet with 500 µl of Buffer QG and then twice with Buffer PE. Air-dry the pellet and elute the DNA in 10 mM Tris-HCl (pH 7.8) or H<sub>2</sub>O and resuspend the pellet by vortexing. Incubate at RT for 5 min (or at 50°C for 5 min) for DNA fragments not more than 4 kbp (for DNA fragments between 4-10 kbp).

##### **4.3.2.3. Purification of plasmid DNA (QIAquick PCR purification kit)**

This protocol is designed to purify single- or double-stranded PCR products or DNA plasmids ranging from 100 bp to 10 kb. DNA adsorbs to the silica-membrane in the presence of high salt while contaminants pass through the column. The impurities are washed away and pure DNA is eluted with Tris buffer or H<sub>2</sub>O.

Add 5 volume of buffer PB to 1 volume of the contaminants and mix. Place a QIAquick spin column in a 2 ml collection tube. Apply the mixed sample to the QIAquick column and centrifuge 30-60 sec. Discard flow-through and place QIAquick column back into the same collection tube. Add 0.75 ml Washing Buffer PE to column and centrifuge 30-60 sec. Discard flow-through and place QIAquick column back into the same collection tube. Centrifuge column for an additional 1 min at maximum speed. Place QIAquick column in a clean 1.5 ml microfuge tube. Add 50 µl Elution Buffer EB or H<sub>2</sub>O to the centre of the QIAquick column and centrifuge for 1 min. Store the purified DNA at - 20°C.

##### **4.3.2.4. Ligation of DNA fragments**

Alkaline phosphatase catalyses the removal of 5' phosphate groups from DNA, RNA and ribo- and deoxyribonucleoside triphosphates. For blunt end ligation, the 5' phosphate group of the vector must be

removed by Calf-intestinal-phosphatase (CIP) reaction. This reaction is also used to prevent the re-ligation of the vectors. 2.5 µg of DNA fragments is phosphorylated at 37°C for 30 min in 100 µl of reaction volumes consisting of 1x CIP buffer and 1 µl of phosphatase. 5 mM EDTA is then added to the reaction and incubated with the reaction at 65°C for 15 min to inactivate the enzyme. The DNA fragments are purified by phenol and ethanol precipitation before ligation reaction.

#### **4.3.2.5. Cohesive-end ligation**

Prepare the plasmid DNA or DNA fragment by cutting it with suitable restriction enzymes, which is followed by purification. 1:3 molar ratio of vector: insert DNA fragments together with 1 µl of T4 ligase are incubated in 1x Ligation Buffer in a total volume of 20 µl for 4 hr at RT or overnight at 16°C. Heat the mixture at 65°C for 10 min to inactivate the enzyme.

#### **4.3.2.6. Mini-preparation of plasmid DNA**

Grow 3 ml overnight culture in LB with 100 µg/ml ampicillin at 37°C overnight. Pellet the cells at 14,000 rpm for 1 min. Remove the supernatant and resuspend the pellets in 100 µl Buffer. Add 200 µl Buffer P2 (Lysis Buffer) and incubate at RT for 5 min. Add 150 µl ice-cold 3 M acidic KAc (Neutralisation Buffer), mix by inverting the tubes for 6-7 times and incubate on ice for 5 min. Centrifuge at 15,000 rpm for 3 min. Transfer the supernatant to a fresh Eppendorf tube and add 900 µl of pre-cooled 100% ethanol, precipitate at -70°C for 10 min. Centrifuge the pellet at 15,000 rpm for 10 min. Wash the pellet with 200 µl 70% ethanol. Air-dry the pellet and resuspend it in 30-50µl 10 mM Tris-HCl, pH 7.8.

#### **4.3.2.7. Maxi-preparation of plasmid DNA**

Grow culture in 50 ml LB media containing plasmids or recombinant plasmids overnight in a 37°C incubator with shaking at 200 rpm. Collect the bacteria and isolate DNA plasmids by using a Qiagen Plasmid Maxi Kit. This extraction method is based on Birnboim's alkali lysis principle. Resuspend the bacterial pellet in 10 ml of Buffer P1. Add 10 ml of Buffer P2, mix gently, and incubate at RT for 5 min. Add 10 ml of chilled Buffer P3, mix immediately, and incubate on ice for 20 min. Centrifuge at 4,000 rpm for 30 min at 4°C. Filter the supernatant over a prewetted, folded filter. Apply the supernatant to an equilibrated QIAGEN-tip 500 and allow it to enter the resin by gravity flow. Wash the QIAGEN-tip twice with Buffer QC. Elute DNA with 15 ml Buffer QF. These processes result in the isolation of a DNA-salt pellet, which is precipitated by 0.7 volumes (10.5 ml) of isopropanol and centrifuged further at 4000 rpm for 30 min. Washed the resulting pellet twice with 70% ethanol and air-dry at RT. The pellet is then carefully resuspended in TE buffer and used for transfection of cultured mammalian cells.

#### **4.3.2.8. Measurement of DNA concentration**

The DNA concentration is determined by using a UV spectrophotometer at wavelength of 260 nm. The absorption of 1 at 260 nm corresponds to a concentration of 50 µg/ml double stranded DNA. Identity, integrity and possible purity of the DNA can be subsequently analysed on an agarose gel.

#### **4.3.2.9. Isolation of genomic DNA from cells and tissues**

Digest a small piece of mouse tail (0.5-1 cm), 50-100 mg of other tissues or  $5 \times 10^6$  cells in 500  $\mu$ l of the Tail Lysis Buffer with 0.4 mg/ml Proteinase K overnight at 55°C. Vortex and spin down the lysate, then transfer the supernatant to the new tube. Add 160  $\mu$ l ~6M NaCl and vortex, followed by incubation for 5 min at RT. Therefore, centrifuge at 10,000 rpm for 15 min and transfer the supernatant (~600  $\mu$ l) to the new tube. After adding 400  $\mu$ l Isopropanol, mix carefully and pellet the DNA by the same centrifuge. Wash the pellet with 75% Ethanol, air dry and then dissolve in 150-200  $\mu$ l TE. Measure DNA concentration, and store at 4°C for PCR genotyping or Southern blot analysis.

#### **4.3.2.10. Southern blot**

After sufficient digestion of genomic DNA by specific restriction enzymes, separate the fragments on 0.7-0.9% agarose gel with ethidium bromide in TAE at 3V/cm overnight. Photograph the gel and then capillary transfer DNA onto Hybond-N membrane in 20x SSC Buffer according to manufacturer instruction (Hybond-N, Amersham). Cross-link DNA to membrane using UV-light, 120 mJ/cm<sup>2</sup>. The membrane is first incubated in QuikHyb solution with 100 $\mu$ g/ml single-stranded fish sperm DNA, for 30 min at 68°C. During the prehybridization, 5' and 3' probes are <sup>32</sup>P-labelled according to the Rediprime™ kit protocol as a standard Klenow based technique, and purified through a column purification kit. The solution is mixed with one radiolabelled probe before hybridisation is done for 1-2 hour at 68°C. Following hybridisation, the membrane is then subjected to washing at 68°C. The membrane is washed once with washing buffer 1, followed by three times with washing buffer 2, each for 15 min. The membrane is then rinsed to remove excess SDS and exposed with X-ray film overnight or longer at -80°C.

### **4.3.3. RNA methods**

#### **4.3.3.1. Isolation of RNA from cells and tissues using TRIzol Reagent**

For isolation of RNA from cells, wash the cells at least 2X with cold PBS before supplementing TRIzol on them. In case of frozen or fresh organ pieces (50-100 mg), mechanical homogenization is necessary and this procedure mostly applied by means of ultrathorax homogenizer. After homogenization (or 10 minutes post lyses of cells) store the homogenate for 5 minutes at room temperature (RT). Supplement the homogenate with 100  $\mu$ l BCP. Cover the samples tightly and vortex vigorously for 20 seconds. Store the resulting mixture for 2-3 minutes at RT. Centrifuge at 10,500 rpm for 15 minutes at 4°C. After centrifugation isolate the aqueous upper RNA phase into a separate epi. Add 500  $\mu$ l isopropanol and vortex it strongly. Store the sample at RT for 5 minutes and centrifuge it at 10,500 rpm for 8 minutes. Remove the supernatant and wash the pellet with 1 ml 75% ethanol. Centrifuge it again with 8,500 rpm for 5 minutes. Remove ethanol after centrifugation and air-dry the pellet for 2-5 minutes. Dissolve the RNA with RNase-free water and incubate at 55°C for 5-10 minutes. Store the RNA at -20°C.

#### **4.3.3.2. Isolation of RNA from cells and tissues using BioRobot EZ1 Technology**

This protocol can be used with a maximum of 50 mg animal or human tissues. Fresh, frozen, or RNAlater stabilized tissue can be used. Excise the tissue sample from the animal. Stabilize the tissue in RNAlater

solution. Disrupt tissue and homogenize lysate in 750-1000  $\mu$ l QIAzol Lysis Reagent. Place the microcentrifuge tubes containing the homogenates on the benchtop at room temperature for 5 minutes. Add 150  $\mu$ l chloroform to each microcentrifuge tube containing the homogenized sample. Vortex it shortly but vigorously. Place the microcentrifuge tubes on the benchtop at room temperature for 2-3 minutes. Centrifuge at 12,000 x g for 15 minutes at 4°C. Transfer the upper, aqueous phases (300-400  $\mu$ l each) to the 2 mL sample tubes. Insert the EZ1 RNA Card completely into the EZ1 Card slot of the BioRobot EZ1 and follow the commands.

#### **4.3.3.3. Quantification and determination of Quality of RNA**

The concentration of RNA should be determined by measuring the absorbance at 260 nm ( $A_{260}$ ) in a spectrophotometer. To ensure significance,  $A_{260}$  readings should be greater than 0.15. An absorbance of 1 unit at 260 nm corresponds to 44  $\mu$ g of RNA per mL ( $A_{260} = 1 \rightarrow 44 \mu\text{g/mL}$ ). Concentration of RNA sample = 44  $\mu\text{g/mL} \times (A_{260} - A_{320}) \times \text{dilution factor}$ . This relation is valid only for measurements at a neutral pH. Therefore, if it is necessary to dilute the RNA sample, this should be done in a buffer with neutral pH. The ratio between the absorbance values at 260 and 280 nm gives an estimate of RNA purity.

#### **4.3.3.4. RT-PCR**

Total RNA prepared from cells or tissues are treated with RNAase-free DNase I. For RT-PCR, cDNA is prepared by reverse transcription (RT) of 1 $\mu$ g of each RNA sample using Moloney-murine leukaemia virus reverse transcriptase (M-MuLV-RT) and oligo d (T) primers. Steps of RT-PCR was given bellow.

##### DNase I treatment:

1 $\mu$ g RNA  
1 $\mu$ l DNase I Buffer  
RNase-free water until 10  $\mu$ l  
Incubate for 20 minutes at 37 °C  
Stop reaction by adding 1  $\mu$ l EDTA (25mM)  
Incubate at 65°C for 10 minutes  
Chill on ice

##### c-DNA Synthesis:

Take 10  $\mu$ l DNase I-treated RNA  
Add 1  $\mu$ l Oligo d (T)  
Incubate the mix at 70 °C for 5 minutes  
Chill on ice  
Add reaction buffer (9 $\mu$ l) as indicated;

1. 5X Reaction Buffer : 4  $\mu$ l
2. RNase inhibitor: 1 $\mu$ l
3. 10mM dNTP: 2  $\mu$ l
4. Reverse Transcriptase Ezyme : 2 $\mu$ l

Incubate the total reaction (20µl) at 37 °C for one hour

Terminate the reaction by incubating at 70 °C for 10 minutes

Chill on ice or freeze at -20°C

#### **4.3.3.5. Isolation and RT-PCR analysis of RNAs that were obtained from microdissected tissues**

After surgery, lung samples were frozen over dry ice in O.C.T. compound and stored at -80°C. 10 µm frozen tissue sections were prepared using a cryostat. Sections were then mounted on membrane coated glass slides (Leica) and stained with Gill's haematoxylin (Sigma Chemical) for 30 seconds and rinsed with water. Slides were air-dried and stored at -80°C. Tumor areas were micro-dissected with a laser beam on a Leica DMLA microscope. Total RNA was extracted using an RNeasy Micro Kit (Qiagen). Briefly, 35 µl of lysis buffer was used for lysis of micro-dissected tissues. The RNA was eluted in 14 µl of RNase-free water and then quantified by using the ribo green quantitation kit (Molecular Probes) according to the manufacturer's protocol. One-step RT-PCR was performed according to the manufacturer's specifications (Qiagen) with 250 ng of RNA. DNA fragments were visualized and photographed under UV light after ethidium bromide staining.

#### **4.3.3.6. Real –Time PCR analysis**

General protocol for quantitative RT PCR indicated below;

1. Template (c-DNA) : 2-4 µl
2. Master Mix : 10 µl
3. Sense Primer: 0.5 µl from 20 pmol
4. Antisense Primer: 0.5 µl from 20 pmol
5. H<sub>2</sub>O until 20µl

RNA from total lung was extracted with Bio Robot EZ1 technology (Qiagen) according to the manufacturer's description. 1 µg RNA was reverse transcribed using first strand cDNA synthesis kit by following the manufacturer's protocol (K 1612, Fermentas). 2 µl (50 ng) from the resulting cDNA and 0.5 µM of each gene-specific forward or reverse primer was used for amplification with SYBR green PCR master mix (F-410S/L, DyNAmo HS SYBR Green qPCR Kit). As an internal control, the mRNA for the microglobulin gene (Micro) and GAPDH (in case of human material) was used. To calculate the relative amounts of various genes, the amplification efficiency was raised to the power of the threshold cycle ( $amp^{Ct}$ ). This gives the number of amplification necessary for the product to be detectable. The resulting number was normalised to the level of microglobulin / gapdh mRNA for all probes in the same experiment ( $amp^{Ct} / amp_{micro}^{Ct_{micro}}$ ). These normalised numbers were used to compare the relative expression between different samples. Assays were performed in triplicate following the manufacturer's instructions. Real-time PCR analysis was performed in a Roto- Gene 2000 detection system (Corbett Research).

#### **4.3.4. Protein methodologies**

##### **4.3.4.1. Measurement of Protein concentration (Bio-Rad protein assay)**

The Bio-Rad Protein Assay is based on the observation that when Coomassie Brilliant Blue G-250 binds to the protein, the absorbency maximum shifts from 450 nm to 595 nm. Equal volume of precleared cell or

tissue lysate, in either NP40 lysis buffer or CCLR buffer, containing 1-20 µg of protein is added to diluted Dye Reagent and mixed well (1:5 dilution of Dye Reagent Concentrate in ddH<sub>2</sub>O). After a period of 5-10 min, the absorption at wavelength 595 is measured versus reagent blank (which contains only the lysis buffer). By the way, BSA is used as a standard.

#### **4.3.4.2. Sodium dodecyl sulfate polyacrylamide gel electrophoresis (SDS PAGE)**

Proteins can be easily separated on the basis of mass by electrophoresis in a polyacrylamide gel under denaturing conditions. 5x SDS-loading Buffer is used to denature 20-50 µg protein in precleared lysates, and then heated at 95°C for 5 min. SDS is an anionic detergent that disrupts nearly all noncovalent interactions in native proteins. β-Mercaptoethanol is also included in the sample buffer to reduce disulfide bonds. The SDS complexes with the denatured proteins are then electrophoresed on a polyacrylamide gel in the form of a thin vertical slab. Vertical gels are set in between 2 glass plates with an internal thickness of 1.5 mm between the two plates. In this chamber, the acrylamide mix is poured and left to polymerise for at least 30 min at RT. The gels are composed of two layers: a 6-15% separating gel (pH 8.8) that separates the proteins according to size; and a lower percentage (5%) stacking gel (pH 6.8) that insures the proteins simultaneous entry into the separating gel at the same height.

	<b>Separating gel</b>	<b>Stacking gel</b>
Tris pH 8.8	2.5 ml.	1.25 ml
Acrylamide/bisacrylamide 29:1 (30%)	2.0-5.0 ml	1.7 ml
10% SDS	0.1 ml	0.1 ml
ddH <sub>2</sub> O	5.4-2.4 ml	6.8 ml
10% APS	0.1 ml	0.1 ml

The separating gel is poured in between two glass plates, leaving a space of about 1cm plus the length of the teeth of the comb. Isopropanol is added to the surface of the gel to exclude air. After the separating gel is polymerised, the isopropanol is removed. The stacking gel poured on top of the separating gel, the comb inserted, and allowed to polymerise. The samples are loaded into the wells of the gel and running buffer is added to the chamber. A cover is then placed over the gel chamber and 45 mA are applied. The negatively charged SDS-protein complexes migrate in the direction of the anode at the bottom of the gel. Small proteins move rapidly through the gel, whereas large ones migrate slower. Proteins that differ in mass by about 2% can be distinguished with this method. The electrophoretic mobility of many proteins in SDS-polyacrylamide gels is proportional to the logarithm of their mass.

#### **4.3.4.3. Immunoblotting**

After the lysates are subjected to SDS-PAGE, the proteins are transferred by electroblotting to Transpran™ membrane. SDS-PAGE gels are electroblotted at 400 mA in blotting buffer for 60 min. Ponceau S fixative dye solution (containing Ponceau S, trichloroacetic acid, and sulfosalicylic acid) is used to check if the transfer has occurred. Stain for 5 min and wash with deionised water. For Western blot analysis, incubate

the membranes in blocking buffer for 1 hr at RT or overnight at 4°C on a shaker. Dilute the first antibody in TBST/2% milk (unless otherwise indicated), add to the membrane, and incubate for 2 hr at RT or overnight at 4°C. Wash the membrane three times with TBST, each time for 10 min. Dilute the appropriate peroxidase-conjugated secondary antibody in TBST/2% milk (or according to manufacturer's instructions), add to the membrane, incubate at RT for 45 min, and wash. This step is followed by the standard enhanced chemiluminescence reaction (ECL-system): incubate the membrane in a 1:1 mixture of ECL solutions 1 and 2. This reaction is based on a peroxidase catalysed oxidation of Luminol, which leads to the emission of light photons that can be detected on X-ray film. Thus the peroxidase conjugated secondary antibodies bound to the primary antibody detect the protein of interest.

#### **4.3.4.4. Immunoblot stripping**

The removal of primary and secondary antibodies from a membrane is possible, so that it may be reprobed with alternative antibodies. To make 50 ml stripping buffer, mix 3.125 ml of 1M Tris-HCl solution (pH 6.7), 5 ml of 20% SDS solution and 0.35 ml of 4.3 M  $\beta$ -Mercaptoethanol with 42ml distilled H<sub>2</sub>O. Incubate the membrane in stripping buffer for 30 min at 50°C. The membrane should be washed at least 5 times with TBST. The membrane can then be reprobed as described above.

#### **4.3.4.5. Immunoblotting of proteins isolated from type II pneumocytes**

To detect tumour specific endogenous E-cadherin and  $\beta$ -catenin proteins, we used isolated pure type II cells from four months old induced and control triple transgenic mice as described (Rice et al., 2002). Cells were lysed in ice cold lyses buffer (10 mM Tris-HCl, pH 7.4, 1 % Triton X-100, 0.4 % deoxycholate, 66 mM EDTA with protease inhibitor cocktail) by careful sonication. The homogenates were centrifuged at 11,000 rpm for 10 minutes. Supernatants from samples in lysis buffer were analysed for protein concentration (based on Bradford protein assay). Samples were solubilized with an equal volume of loading buffer (125 mM Tris-HCl, pH 6.8, 4 % sodium dodecyl sulfate, 20 % glycerol, 0.05 % bromophenol blue, 5 %  $\beta$ -mercaptoethanol) and were boiled for 3 min. The samples were then separated by SDS- PAGE, transferred to nitrocellulose membranes and detected by immunoblotting with primary antibodies against  $\beta$ -catenin (clone 14, BD Transduction Lab), and rat anti E-cadherin antibodies (clone ECCD-2, Zymed Lab) respectively. After three washes with TBST buffer, the membrane was incubated with anti-mouse IgG and anti Rat IgG horseradish peroxidase conjugates (Amersham Pharmacia Biotech) for 60 min and visualized with ECL detection kit.

For the analysis of dn E-cadherin expression, anti-c-Myc mouse monoclonal antibody (Santa Cruz sc-40, clone 9E10) was used as previously described (Dahl et al., 1996). As an internal control, a rabbit antibody to GAPDH (ab9485, Abcam Ltd) was used. For N-cadherin expression, tumour cells and CD31 positive endothelial fraction were isolated (Rice et al., 2002), homogenized in RIPA buffer containing protease inhibitor cocktail and subjected to Western blot by using mouse anti N-cadherin (clone 3B9, Zymed Lab.) antibody. Attached CD31 positive endothelial fraction served as positive control for N-cadherin expression. Alpha actin was the internal control (A 2066, Sigma). Antibodies were used according to the conditions recommended by the manufacturer. Detection of P-cadherin expression from total lung of four months

DOX treated mice was performed using rat anti-P-cadherin (Clone PCD-1, Zymed, Invitrogen). Alpha actin was the internal control (A 2066, Sigma). Antibodies were used according to the conditions recommended by the manufacturer.

#### **4.3.4.6. Luciferase reporter gene assay**

Mice were sacrificed by lethal injection of ketanest (Parke-Davis) together with rompun (Bayer). After lung dissection, the tissue (or cells) was homogenized in lysis buffer containing 0.25M Tris, pH 7.6, 1% Triton X-100. After centrifugation at 11,000 rpm for 10 minutes, the luciferase activity in the supernatant (20  $\mu$ l) was measured in a luciferase assay using Berthold luminometer. Protein concentrations were determined with the Bradford protein assay. Luciferase activity was normalized to protein concentration to calculate relative light units (RLU) per mg protein.

#### **4.3.5. Cell culture techniques**

##### **4.3.5.1. Transient transfection of cells using lipofectamine reagent**

One day before transfection,  $0.5 - 1.5 \times 10^5$  cells were plated on 24-well plate and maintained in normal medium overnight. On the day of transfection, dilute 0.8  $\mu$ g DNA and 2 $\mu$ l Lipofectamine 2000 (LF2000), respectively, into 50 $\mu$ l OPTI-MEM per well. 5 minutes later, combine the diluted DNA with the diluted LF2000 and incubate for 20 min at RT. Meanwhile, remove the medium from cells, wash with 1X PBS and replace with only DMEM. After 20 minutes incubation, add the DNA-LF2000 complexes (100  $\mu$ l) directly on cells. After gently rocking the plate back and forth, incubate the cells for 4-5 h., and then change the medium with normal growth medium. Cells were then harvested after 24-48 hours later.

##### **4.3.5.2. siRNA transfection of cells**

Mouse 3041 alveologenic lung adenocarcinoma (Rizzino et al., 1982) and human lung carcinoma A-549 epithelial cells were maintained in DMEM supplemented with 10 % calf serum. Cells were seeded into 12-well plates 24 hours before transfection. For DNA transfection, Lipofectamine 2000 reagent (Invitrogen) was used. siRNA against mouse  $\beta$ -catenin (sc-29210, Santa Cruz) and human  $\beta$ -catenin (CTNNB1, M-003482, Upstate) were transfected using transfection reagent (sc-29528, Santa Cruz) according to the manufacturer's descriptions. Validated nonsilencing control siRNA (Alexa Fluor 488 Labeled, Qiagen) was always included for control cells (mock) and for siRNA transfection efficiency. Transfected cells were starved for 5 hours in the absence of serum and antibiotics followed by recovery in complete medium for 20 hours. Cells were subsequently transfected with plasmids *Tet-O dn E-cadherin*, *SP-C rtTA*, *SP-C C-RAF BXB* alone or combination,  *$\beta$ -catenin 4S* plasmid (Herzig et al., 2006) using lipofectamine reagent. Cells were harvested 24 hours later and RNA extracted using TRIzol reagent (Invitrogen). Knock-down efficiency of  $\beta$ -catenin was determined by  $\beta$ -catenin immunostaining and by qRT-PCR. Transfection efficiency of DNA constructs was monitored by qRT-PCR, staining and luciferase assay (Promega).

##### **4.3.5.3. Isolation of type II pneumocytes from mouse lung**

Lung Isolation:



Anesthetize mice intraperitoneally

Tape animal to chuck

Draw up solutions (3 ml dispase, 0,5 ml agarose-keep warm, 10 ml saline)

Remove skin from chest and neck

Open abdominal cavity

Remove intestine

Cut vena cava inferior to exsanguinate animal

Cover abdomen

Prepare trachea

Open trachea, insert needle, put all the way in, tie in securely

Open chest, remove diaphragm, anterior chest wall

Take saline syringe, lift heart, puncture right heart (2-3 mm), flush 10 ml saline in pulmonary artery, repeat until lungs are white (removing remaining blood is essential!)

Rapidly instil 3 ml dispase in trachea-without air!

Follow with 0,5 ml warm agarose-without air!

Cover animal immediately with ice to harden agarose, keep on ice for 2 minutes

Remove needle and syringe, take thorax organs out

Remove heart, lungs, thymus, prepare lungs by removing other organs

Incubate lungs in culture tube filled with 2 ml dispase at room temperature

Set timer for 45 minutes dispase exposure and begin next animal

#### Type II Cell Isolation:

Fill 3 tubes with 50 ml DMEM/HEPES each, put one on ice for centrifugation

Add 7 ml DMEM/HEPES and 100 U / ml DNase I to 60 mm culture dish

When 45 minutes dispase incubation is over, remove excess dispase, place in lungs in 60 mm dish

Tricky STEP: Do not injure the lung- Treat like a tea bag, that you want to squeeze out but not rupture !

Take lung by a trachea, use forceps to gently squeeze from trachea to peripheral lung

Continue until only connective tissue is visible (maximum 5 minutes), mince larger parts

Swirl gently for 5 minutes at room temperature (DNase I total 10 minutes)

Put on ice

Repeat for all mice

Put 100 µm cell strainer over 50 ml tube, transfer contents from 60 mm culture dish in 50 ml tube

Rinse dish with 15-20 ml DMEM/HEPES and this to strainer

Filter tube contents through a 100 µm strainer in another 50 ml tube, rinse with DMEM/HEPES

Filter tube contents through a 40 µm strainer in another 50 ml tube, rinse with DMEM/HEPES

Filter tube contents through a 20 µm strainer in another 50 ml tube, rinse with DMEM/HEPES

Place tube on ice, tube must be cold before centrifugation

Centrifuge at 130 X g for 8 minutes at 4°C

Cave: You get a soft pellet, remove carefully media, resuspend in 10 ml DMEM/HEPES + 10% FBS, avoid bubbles!

Discard antibody solution, gently wash antibody plates 2X with DMEM/HEPES (never touch bottom of plates)

Put cell suspension on plate (immune cells will stick to the plate, type II will be in suspension!)

Incubate for 2 hours at 37°C

Gently remove media from antibody plates and place in 50 ml centrifuge tubes

Centrifuge at 130 X g for 8 minutes at 4°C

#### **4.3.6. Histological methods**

##### **4.3.6.1. Embedding in paraffin**

Lungs of postnatal mice were dissected into cold phosphate-buffered saline (PBS), fixed overnight in fresh 4% paraformaldehyde at RT. Paraffinization step involves 40 min in 50% Ethanol, 40 min in 70% Ethanol, 40 min in 80% Ethanol, 40 min in 90% Ethanol, 40 min in 95% Ethanol, 3x 40 min in 100% Ethanol, 2x 30 min in 1:1 (Chloroform:Ethanol), 30 min in Chloroform:Ethanol. All procedures perform at RT. Transfer embryos or organs into melted paraffin, and incubate for 1h at 65°C. Change Paraffin and incubate for 2h or overnight at 65°C. Prepare the paraffin blocks. Embryos and organs are sectioned into 6-10 µm microsections and can be used for the further histological analysis.

##### **4.3.6.2. Hematoxylin/eosin staining for paraffin embedded sections**

Solution	Time
Xylol-I	10 minutes
Xylol -II	10 minutes
100% alcohol-I	5 seconds
100% alcohol-II	5 seconds
70 % alcohol	5 minutes
Water	5 minutes
Haematoxylin	5 minutes
Tape water	5 minutes
Eosin	45 seconds
Water	5 seconds
70 % alcohol	5 minutes
100% alcohol-I	5 seconds
100% alcohol-II	10 minutes
100% alcohol-III	10 minutes
Xylol-I	10 minutes
Xylol-II	10 minutes

##### **4.3.6.3. Hematoxylin/eosin staining for LCM**

In order to proceed with histologic staining and laser microdissection following sectioning, the paraffin must be removed from the tissue sections and the tissue must be rehydrated. Allow the slide containing the tissue section to remain in the following solutions for the specified times in the specified order:

Solution	Time
Xylene	5 minutes
100% Ethanol	30 seconds
95% Ethanol	30 seconds
70% Ethanol	30 seconds

For frozen sections, rapidly remove the slide from -80°C storage and immerse in or flood with 70% alcohol without allowing the slide to thaw and dry prior to contact with the alcohol. Allow the alcohol to remain in contact with the tissue for 30 seconds. Deparaffinized, fixed sections will already be in 70% alcohol after deparaffinization and are ready to proceed through the following steps. Allow the slide containing the tissue section to remain in the following solutions for the specified times in the specified sequence.

Solution	Time
Sterile, distilled or Rnase free water	10 seconds
Mayer's Hematoxylin	10 seconds
Bluing reagent	15 seconds
70% alcohol	15 seconds
Eosin Y	15 seconds
95% alcohol	15 seconds
100% alcohol	15 seconds - 1 minute
Xylene	5 minutes

Allow the section to air dry completely and proceed to laser microdissection.

#### 4.3.6.4. Histopathology and Immunofluorescence Microscopy

Animals were sacrificed and lungs were fixed under 25 cm water pressure with 4 % PBS buffered formalin. Histology was done on formalin-fixed, paraffin-embedded lung specimen. 6 µm-cut sections were deparaffinized, rehydrated in graded alcohols and haematoxylin-eosin stained. To quantitate membrane E-cadherin and nuclear β-catenin expression in tumors, ten random intratumoral areas (± 200 cells / area) for each of 5 mice were evaluated using specific immunohistochemistry.

Tumour volume (in mm<sup>3</sup>) was calculated from whole lung sections with a diameter of > 0.4 mm assuming a spherical tumour. 248 controls and 206 tumours were analyzed from 10 untreated control and 10 induced mice, respectively. For the quantification of proliferation, PCNA (brown nucleus) and Ki67 (red nucleus) positive cells in lung sections of *SP-C rtTA / Tet-O dn E-cadherin* double transgenic and *SP-C rtTA / Tet-O-Cre / Cdh1<sup>fllox/fllox</sup>* triple transgenic mice were counted. 25 randomly selected lung sections from 5 animals of each group were assessed, respectively. A total of 1000 cells were counted in five microscopic fields (± 200 cells / field). PCNA (brown nucleus) and Ki67 (green nucleus) index of tumors from *SP-C C-RAF BXB / SP-C rtTA / Tet-O dn E-cadherin* triple transgenic and quadruple mice were calculated screening 10 tumors per animal from 5 mice, respectively. A total of 5000 cells were counted in ten tumors (500 cells / area). The percentage of S phase cells was obtained by dividing the number of stained cells by the total number of cells counted. Fraction of apoptotic cells before and after treatment were determined using activated caspase 3 immunostaining and quantitated as PCNA staining of double transgenic mice.

Intratumoral vessel density was evaluated as previously described (Gasparini et al., 1994) with some minor modifications. For CD31 staining, at least, 10 tumours were analysed per mouse. Five randomly selected intratumoural fields (100 x 100 µm) were counted per tumor. Quantification of intratumoral lymphatic vessel density was assessed using two different markers (LYVE-1 and Prox1) in the same way. For determination of vessel diameter of the counted vessels, we used a microscope software based scaling technique (Leica DMLA).

For determination of the localisation of myc-tagged dn E-cadherin, bitransgenic mice were sacrificed, the lungs were isolated and paraffin embedded. In order to mark alveolar type II cells and dn-E-cadherin

expression, a double immunofluorescence staining was performed using a rabbit antibody against pro-SPC (1:5000, a gift from J. Whitsett) and an anti-c-myc mouse monoclonal antibody (1:200, clone 9E10, Santa Cruz, USA), respectively. Donkey anti-rabbit Alexa Fluor<sup>488</sup> (1:200, Molecular Probes) and donkey anti mouse Cy3 (1:200, Chemicon Int., USA) secondary antibodies were applied for detection. Antibody (gp84) used for E-cadherin detection in paraffin sections was a gift from R. Kemler. Immunofluorescence staining to detect endogenous E-cadherin employed frozen sections and an anti-mouse E-cadherin mouse monoclonal antibody (Zymed Laboratories, clone ECCD2) as described (Perl et al., 1999). Prox1 (1:200, ReliaTech GmbH, Mascheroder, Germany) staining was applied according to the manufacturer's instructions using paraffin embedded lung sections. Double staining for pro SP-C and N-cadherin/Vimentin was done with paraffin embedded sections employing donkey anti-rabbit streptavidin Alexa Fluor<sup>488</sup> (Molecular Probes, Eugene, Oregon, USA) and donkey anti-mouse conjugated Cy-3 (Chemicon Int., USA) / donkey anti-goat Alexa Fluor<sup>555</sup> (Invitrogen) secondary antibodies, respectively. Primary antibodies against mouse  $\beta$ -catenin (polyclonal rabbit  $\beta$ -catenin, 06-734, Upstate, 1:200), N-cadherin (clone 3B9, Zymed, 1:150), rat anti-P-cadherin (Clone PCD-1, Zymed, Invitrogen), polyclonal rabbit VEGF antibody (1:200, sc-507, Santa Cruz), Ki67 (ab15580, 1:250, Cambridge, UK), Vimentin (C-20, Santa Cruz, 1:200), Cytokeratin (DAKO, 1:400), LYVE-1 (CDS LI732C01, Hamburg, Germany, 1:200), PCNA (PC10, BD Pharmingen, 1:3000), anti-Cre antibody (Novagen, 1:500), polyclonal anti Caspase-3 (Cell Signaling, 1:100) were applied to paraffin embedded 6  $\mu$ m tissue sections according to the manufacturer's instructions. Briefly, sections were deparaffinized and rehydrated. After 15 min incubation with 1-3 % H<sub>2</sub>O<sub>2</sub> to quench endogenous peroxidase, sections were incubated in 10 mM citrate buffer (pH: 6.0) for 6-20 min for antigen retrieval. Slides were blocked and incubated with primary antibodies overnight at 4°C. Biotinylated secondary antibodies (DakoCytomation) were applied to sections at 1:200-600 and incubated for 30-90 min at room temperature. ABC reagent (Vectastain Elite ABC Kit, Vector Labs) was applied to sections and developed in diaminobenzidine (DAB). Slides were then counterstained with haematoxylin. Immunohistochemical staining with monoclonal rat anti- mouse CD31 antibody (clone MEC 13.3, BD Pharmingen) was performed as previously described (Zeng et al., 1998). For immunocytochemistry of cultured cells, primary antibodies against  $\beta$ -catenin (mouse anti- $\beta$ -catenin, 1:400, BD Transduction Lab), VEGF (polyclonal rabbit VEGF antibody, 1:200, sc-507, Santa Cruz) and myc tag (anti-c-myc mouse monoclonal antibody, 1:200, clone 9E10, Santa Cruz, USA) were used. Briefly, 3041 and A-549 lung tumor cells were fixed in 4% PFA for 15 minutes and permeabilized with 0,2% Triton X-100 for 5 minutes. After blocking with serum, primary antibodies were applied overnight at 4°C. After intensive washing with PBS, donkey anti-rabbit conjugated Cy-5 (1:300, Chemicon Int., USA) and goat anti-mouse conjugated Cy3 (1:300, Jackson ImmunoResearch) secondary antibodies were employed for detection.

#### **4.3.6.5 Terminal deoxynucleotidyltransferase-mediated dUTP-biotin nick end labeling (TUNEL) assay.**

Frozen lung sections of triple transgenic mice were stained according to the Dead End Fluorometric TUNEL System instructions (Promega). Immunofluorescence Double Staining for CD31/PECAM-1 and TUNEL was given below as described previously (Solorzano et al., 2001).

TUNEL / CD 31 Double Staining:

1. Air-dried frozen sections for 30 Minutes.
2. Fix in a pre-cold acetone for 5 Minutes.
3. Fix in a pre-cold acetone / chloroform (1:1) for 5 Minutes
4. Fix in a pre-cold acetone for 5 Minutes
5. Wash with 3X PBS (5 Minutes)
6. Incubate the slides with blocking solution for 20 minutes at R.T.  
Blocking Solution (in PBS): 5 % Normal Horse Serum, 1% Normal Goat Serum
7. Primary antibody (Rat anti mouse CD31) incubation (1:400) in blocking solution, O.N. at 4°C.
8. Thaw-up equilibration buffer at R.T.
9. Wash with 3X PBS (5 Minutes)
10. Secondary antibody (Goat anti Rat Texas-Red) incubation (1:200) in blocking solution for 1 hour at R.T in a dark chamber.
11. Wash 2X with 1XPBS containing 0.1 % Brij for 5 minutes.
12. Thaw-up nucleotide mix on ice in the dark !!!
13. Wash 1X PBS for 5 minutes.
14. Fix the slides in 4% PFA in R.T. for 10 minutes.
15. Wash 2X with 1XPBS for 5 minutes.
16. Incubate the slides with Equilibration Buffer (E.B.) for 10 minutes at R.T.
17. Drain E.B. buffer from the slides and add reaction buffer on slides. Incubate the slides in dark humid chamber for 1 hour at 37 °C.  
Reaction Buffer (pro one slide): 90 µl E.B. Buffer  
10 µl Nucleotide Mix  
1 µl rTdT Enzyme
18. Terminate the reaction by immersing the slides in 2X SSC for 15 minutes.
19. Wash with 3X PBS (5 Minutes)
20. Dapi and Mowiol.

**4.3.7. Generation of dn E-cadherin transgenic mice**

Animals were housed under barrier condition with a 12 hour light/dark cycle and access to food and water *ad libitum*. To generate transgenic mice conditionally expressing dominant negative (dn) E-cadherin, we used a plasmid, obtained from H. Semb, that encodes a 34kDa myc-tagged cell surface protein where 625 amino acid residues from the extracellular domain of E-cadherin have been deleted (Dahl et al., 1996). The

dn E-cadherin c-DNA was isolated as a 1,3kb *XbaI* – *HindIII* fragment. The *XbaI* site was blunted with T4 DNA polymerase. The fragment was cloned into the pBI5 vector (containing a tet operator) by cutting with *NheI*/blunt – *HindIII*. The resultant plasmid pBI5-dn E-cad was cut with *AseI* to remove the vector backbone and the tet-O dn E-cadherin fragment (6.1kb) was isolated by gel electrophoresis and injected into the pronucleus of fertilized mouse eggs. Resultant mice were genotyped by Southern blotting and subsequently by PCR with primers (5'- AGTAGGCGTGTACGGTGGGAG) and (5'- TCGGAGATCAGCTTCTGCTCG) to yield a 473bp DNA product. We generated four germ-line transmitting founder animals and all of them were crossed with *SP-C-rtTA* inducer mice that express the reverse tetracycline transactivator protein (rtTA) in type II pneumocytes (Perl et al., 2002). Progeny from one line (founder number 253) was used in the experiments reported here. This line was backcrossed for three generations onto C57BL/6 background before crossing with *SP-C-rtTA* inducer mice. Line 253 which can be induced up to 1000-fold within 1 week was used for all further experiments (Fig.2.5). Immunoblotting of lung lysates from bitransgenic mice after 1 week of DOX administration revealed protein expression of dn E-cadherin in vivo (Fig.2.7). To test for expression of dn E-cadherin in type II epithelial cells, paraffin embedded lung sections of bitransgenic (*SP-C rtTA / Tet-O dn E-cadherin*) mice were subjected to immunostaining. SP-C expressing cells stained positive for myc-tagged dn E-cadherin only after treatment with DOX, indicating that induced transgene expression was restricted to type II cells (Fig.2.8). Double-transgenic offspring were crossed with homozygous tumor mice expressing oncogenic C-RAF BXB in type II pneumocytes (Kerkhoff et al., 2000) to obtain triple transgenic progeny. Genotyping of *SP-C rtTA* and *SP-C C-RAF BXB* mice was as described (Kerkhoff et al., 2000; Perl et al., 2002). For induction of mice, doxycycline HCl (DOX, Sigma Chemical) was diluted in the drinking water to 500 µg/mL. Due to its light sensitivity, the DOX solution was replaced every week and was given in black, light protected bottles (Harlan). Homozygous *Cdh 1<sup>flox/flox</sup>* mice (Boussadia et al., 2002) were first crossed with *Tet-O Cre* (Schönig et al., 2002). Double transgenic mice were crossed with a *SP-C rtTA* line. The resulting triple transgenics were put on the background of homozygous *SP-C C-RAF BXB* mice thus generating quadruple transgenic strains (*SP-C C-RAF BXB / SP-C rtTA / Tet-O-cre / Cdh 1<sup>flox/flox</sup>*). Detection of *Cdh 1* flox allele was as previously described (Boussadia et al., 2002). The knock-out allele used the primers as follows: sense primer (S2): 5'-CTT CTA CAG GGG ACT TGA GAT -3'; antisense primer (S4): 5'-GTG ACA CAT GCC TTT ACT TTA -3'.

#### 4.3.8. Statistical analysis

For both sectioned material and cell culture experiments, data sets from independent experiments were pooled, and the results were expressed as mean and standard deviation (SD). Statistical significance between data sets was assessed by The Graphpad Prism version 4.00 (Graphpad Software, Inc, San Diego, CA) software program. For all tests, statistical significance was considered to be at the  $P < 0.05$  level.

## **REFERENCES**

- Aberle, H., Bauer, A., Stappert, J., Kispert, A., and Kemler, R. (1997). Beta-catenin is a target for the ubiquitin-proteasome pathway. *EMBO J.* 16, 3797-3784.
- Akimoto, T., Kawabe, S., Grothey, A., and Milas, L. (1999). Low E-cadherin and  $\beta$ -catenin expression correlates with increased spontaneous and artificial lung metastasis of murine carcinomas. *Clinical & Experimental Metastasis.* 17, 171-176.
- American Cancer Society. (2006). *Cancer Facts & Figures 2006.* Atlanta, American Cancer Society.
- Anastasiadis, P.Z., Moon, S.Y., Thoreson, M.A., Mariner, D.J., Crawford, H.C., Zheng, Y., and Reynolds, A.B. (2000). Inhibition of RhoA by p120 catenin. *Nat Cell Biol.* 2, 637-644.
- Angst, B.D., Marcozzi, C., and Magee, A.I. (2001). The cadherin superfamily: diversity in form and function. *J. Cell Sci.* 114, 629-641.
- Barth, A.I., Nathke, I.S., and Nelson, W.J. (1997). Cadherins and catenins and APC protein: Interplay between cytoskeletal complexes and signaling pathways. *Curr Opin Cell Biol.* 9, 683-690.
- Battle, E., Sancho, E., Franci, C., Dominguez, D., Monfar, M., Baulida, J., and De Garcia Herreros, A. (2000). The transcription factor snail is a repressor of E-cadherin gene expression in epithelial tumour cells. *Nat. Cell Biol.* 2, 84-89.
- Becker, K.F., Atkinson, M.J., Reich, U., Becker, I., Nekarda, H., Siewert, J.R., and Hofler, H. (1994). E-cadherin gene mutations provides clues to diffuse type gastric carcinomas. *Cancer Res.* 54, 3845-3852.
- Berenblum, I. (1954). A speculative review: The probable nature of promoting action and its significance in the understanding of the mechanism of carcinogenesis. *Cancer Res.* 14, 471-477.
- Berx, G., Cleton-Jansen, A.M., Nollet, F., de Leeuw, J.F.W., van de Vijver, M.J., Cornelisse, C., and van Roy, F. (1995). E-cadherin is a tumor/invasion suppressor gene mutated in human lobular breast cancers. *The EMBO Journal.* 14, 24, 6107-6115.
- Berx, G., Becker, K.F., Hofler, H., and van Roy, F. (1998). Mutations of the human E-cadherin (*Cdh1*) gene. *Hum Mutat.* 12, 226-237.
- Berx, G. and Van Roy, F. (2001). The E-cadherin/catenin complex: an important gatekeeper in breast cancer tumorigenesis and malignant progression. *Breast Cancer Res.* 3, 289-293.
- Birchmeier, W., and Behrens, J. (1994). Cadherin expression in carcinomas: Role in the formation of cell junctions and the prevention of invasiveness. *Biochim Biophys Acta.* 1198, 11-26.

- Birchmeier, W. (2005). Cell adhesion and signal transduction in cancer. Conference on cadherins, catenins and cancer. *EMBO Rep.* 6, 413-417.
- Boussadia, O., Kutsch, S., Hierholzer, A., Delmas, V., and Kemler, R. (2002). E-cadherin is a survival factor for the lactating mouse mammary gland. *Mech. Dev.* 115, 53-62.
- Bracke, M.E., van Roy, F.M., and Mareel, M.M. (1996). The E-cadherin/catenin complex in invasion and metastasis. In Günthert U, Birchmeier W (eds): Attempts to understand metastasis formation. Vol I. Berlin: Springer-Verlag, 123-161.
- Braga, V.M., Machesky, L.M., Hall, A., and Hotchin, N.A. (1997). The small GTPases Rho and Rac are required for the establishment of cadherin-dependent cell-cell contacts. *J Cell Biol.* 137, 1421-1431.
- Bremnes, R.M., Veve, R., Hirsch, F.R., and Franklin, W.A. (2002). The E-cadherin cell-cell adhesion complex and lung cancer invasion, metastasis, and prognosis. *Lung Cancer* 36, 115-124.
- Calvisi, D.F., Ladu, S., Conner, E.A., Factor, V.M., and Thorgeirsson, S.S. (2004). Disregulation of E-cadherin in transgenic mouse models of liver cancer. *Laboratory Investigation.* 84, 1137-1147.
- Cano, A., Gamallo, C., Kemp, C.J., Benito, N., Palacios, J., Quintanilla, M., and Balmain, A. (1996). Expression pattern of the cell adhesion molecules. E-cadherin, P-cadherin and  $\alpha 6 \beta 4$  integrin is altered in pre-malignant skin tumors of p53-deficient mice. *Int. J. Cancer* 65, 254-262.
- Carney, D.N. (2002). Lung cancer-time to move from chemotherapy. *N. Engl. J. Med.* 346, 126-128.
- Cavallaro, U. and Christofori, G. (2004). Cell adhesion and signalling by cadherins and Ig-CAMs in cancer. *Nat. Rev. Cancer* 4, 118-132.
- Chen, W.C., and Obrink, B. (1991). Cell-cell contacts mediated by E-cadherin (uvomorulin) restrict invasive behavior of L-cells. *J Cell Biol.* 114, 319-327.
- Ciruna, B. and Rossant, J. (2001). FGF signaling regulates mesoderm cell fate specification and morphogenetic movement at the primitive streak. *Dev. Cell.* 1, 37-49.
- Comijn, J., Berx, G., Vermassen, P., Verschueren, K., van Grunsven, L., Bruyneel, E., Mareel, M., Huylebroeck, D., and van Roy, F. (2001). The two-handed E box binding zinc finger protein SIP1 downregulates E-cadherin and induces invasion. *Mol. Cell.* 7, 1267-1278.
- Conacci-Sorrell, M., Simcha, I., Ben-Yedidia, T., Blechman, J., Savagner, P., and Ben-Ze'ev, A. (2003). Autoregulation of E-cadherin expression by cadherin-cadherin interactions: The roles of  $\beta$ -catenin signaling, Slug, and MAPK. *J. Cell Biol.* 163, 847-857.
- Dahl, U., Sjödin, A., and Semb, H. (1996). Cadherins regulate aggregation of pancreatic  $\beta$ -cells in vivo. *Development* 122, 2895-2902.



- Dequéant, M.-L., Glynn, E., Gaudenz, K., Wahl, M., Chen, J., Mushegian, A. and Pourquie, O. (2006). A complex oscillating network of signaling genes underlies the mouse segmentation clock. *Science* 314, 1595-1598.
- Derksen, P.W.B, Liu, X., Saridin, F., van der Gulden, H., Zevenhoven, J., Evers, B., van Beijnum, J.R., Griffioen, A.W., Vink, J., Krimpenfort, P., et al. (2006). Somatic inactivation of E-cadherin and p53 in mice leads to metastatic lobular mammary carcinoma through induction of anoikis resistance and angiogenesis. *Cancer Cell* 10, 437-449.
- Easwaran, V., Lee, S.H., Inge, L., Guo, L., Goldbeck, C., Garrett, E., Wiesmann, M., Garcia, P.D., Fuller, J.H., Chan, V., et al. (2003). beta-Catenin regulates vascular endothelial growth factor expression in colon cancer. *Cancer Res.* 63, 3145-3153.
- Fedorov, L.M., Papadopoulos, T., Tyrsin, O.Y., Twardzik, T., Götz, R., and Rapp, U.R. (2002). Bcl-2 determines susceptibility to induction of lung cancer by oncogenic C-Raf. *Cancer Res.* 62, 6297-6303.
- Fedorov, L.M., Papadopoulos, T., Tyrsin, O.Y., Twardzik, T., Götz, R., and Rapp, U.R. (2003). Loss of p53 in *craf* induced transgenic lung adenoma leads to tumor acceleration and phenotypic switch. *Cancer Res.* 63, 2268-2277.
- Florin, L., Alter, H., Szabowski, A., Schutz, G., and Angel, P. (2004). Cre recombinase-mediated gene targeting of mesenchymal cells. *38(3)*, 139-144.
- Frixen, U.H. et al. (1991). E-cadherin-mediated cell-cell adhesion prevents invasiveness of human carcinoma cells. *J Cell Biol.* 113(1), 173-185.
- Folkman, J., Watson, K., Ingber, D., and Hanahan, D. (1989). Induction of angiogenesis during the transition from hyperplasia to neoplasia. *Nature* 339, 58-61.
- Folkman, J. (2002). Role of angiogenesis in tumor growth and metastasis. *Semin Oncol.* 6(16), 15-8.
- Folkman, J. (2006). Angiogenesis. *Annu. Rev. Med.* 57, 1-18.
- Fujimori, T., and Takeichi, M. (1993). Disruption of epithelial cell-cell adhesion by exogenous expression of a mutated nonfunctional N-cadherin. *Mol. Biol. Cell.* 4, 37-47.
- Fukata, M., Kuroda, S., Nakagawa, M., Kawajiri, A., and Kaibuchi, K. (1999). Cdc42 and Rac1 regulate the interaction of IQGAP1 with  $\beta$ -catenin. *J Biol Chem.* 271, 16712-16719.
- Gasparini, G., Weidner, N., Bevilacqua, P., Maluta, S., Dalla, P.P., Caffo, O., Barbareschi, M., Boracchi, P., Marubini, E., and Pozza, F. (1994). Tumor microvessel density, p53 expression, tumor size, and peritumoral lymphatic vessel invasion are relevant prognostic markers in node-negative breast carcinoma. *J Clin Oncol.* 12, 454-466.
- Girard, L., Zochbauer-Muller, S., Virmani, A.K., Gazdar, A.F., and Minna, J.D. (2000). Genome-wide allelotyping of lung cancer identifies new regions of allelic loss, differences between small cell lung cancer and non-small cell lung cancer, and loci clustering. *Cancer Res.* 60, 4894-4906.

- Götz, R., Kramer, B.W., Camarero, G., and Rapp, U.R. (2004). BAG-1 haplo-insufficiency impairs lung tumorigenesis. *BMC. Cancer* 24, 85-?.
- Guilford, P., Hopkins, J., Harraway, J., McLeod, M., McLeod, N., Harawira, P., Taite, H., Scoular, R., Miller, A., and Reeve, A.E. (1998). E-cadherin germline mutations in familial gastric cancer. *Nature*. 392, 402-405.
- Gumbiner, B.M. (1996). Cell adhesion: the molecular basis of tissue architecture and morphogenesis. *Cell*. 84, 345-357.
- Gupta, G.P., and Massague, J. (2006). Cancer metastasis: Building a framework. *Cell*, 127, 679-695.
- Hanahan, D. and Weinberg, R.A. (2000). The hallmarks of cancer. *Cell* 100, 57-70.
- Herbst, R.S., Onn, A., and Sandler, A. (2005). Angiogenesis and lung cancer: prognostic and therapeutic implications. *J Clin Oncol*. 10, 23, 2544-2555.
- Herzig, M., Savarese, F., Novatchkova, M., Semb, H., and Christofori, G. (2006). Tumor progression induced by the loss of E-cadherin independent of beta-catenin/Tcf-mediated Wnt signaling. *Oncogene*.1-9.
- Hirohashi, S. (1998). Inactivation of the E-cadherin-mediated cell adhesion system in human cancers. *Am J Pathol*. 153, 333-339.
- Huang, C., Liu, D., Masuya, D., Nakashima, T., Kameyama, K., Ishikawa, S., Ueno, M., Haba, R., and Yokomise, H. (2005). Clinical application of biological markers for treatments of resectable non-small-cell lung cancers. *Br. J. Cancer* 92, 1231-1239.
- Huber, O., Korn, R., McLaughlin, J., Ohsugi, M., Herrmann, B.G., and Kemler, R. (1996). Nuclear localisation of  $\beta$ -catenin by interaction with transcription factor LEF-1. *Mech Dev*. 59, 3-10.
- Huber, M.A., Kraut, N., and Beug, H. (2005). Molecular requirements for epithelial-mesenchymal transition during tumor progression. *Curr. Opin. Cell Biol*. 17, 548-558.
- Huelsken, J., and Behrens, J. (2000). The Wnt signaling pathway. *J Cell Sci*. 113, 35-45.
- Ivanov, D.B., Philippova, M.P., and Tkachuk. (2001). Structure and Functions of Classical Cadherins. *Biochemistry*. 66, 1174-1186.
- Jamora, C., DasGupta, R., Kocieniewski, P., and Fuchs, E. (2003). Links between signal transduction, transcription and adhesion in epithelial bud development. *Nature*. 422, 317-322.
- Jonkers, J., Meuwissen, R., van der Gulden, H., Peterse, H., van der Valk, M., and Berns, A. (2001): Synergistic tumor suppressor activity of BRCA2 and p53 in a conditional mouse model for breast cancer *Nat. Genetics* 29, 418-425.
- Kartenbeck, J., Haselmann, U., and Gassler, N. (2005). Synthesis of junctional proteins in metastasizing colon cancer cells. *European Journal of Cell Biology*. 84, 417-430.

- Kaibuchi, K., Kuroda, S., Fukata, M., and Nakagawa, M. (1999). Regulation of cadherin-mediated cell-cell adhesion by the Rho family GTPases. *Curr Opin Cell Biol.* 11, 591-596.
- Kerkhoff, E., Fedorov, L.M., Siefken, R., Walter, A.O., Papadopoulos, T., and Rapp, U.R. (2000). Lung-targeted expression of the c-Raf-1 kinase in transgenic mice exposes a novel oncogenic character of the wild-type protein. *Cell Growth Diff.* 11, 185-190.
- Kim, J.S., Han, J., Shim, Y.M., Park, J., and Kim, D.H. (2005). Aberrant methylation of H-cadherin (CDH13) promoter is associated with tumor progression in primary nonsmall cell lung carcinoma. *Cancer* 104, 1825-1833.
- Kuroda, S., Fukata, M., Nakagawa, M., Fujii, K., Nakamura, T., Ookubo, T., Izawa, I., Nagase, T., Nomura, N., Tani, H., Shoji, I., Matsuura, Y., Yonehara, S., and Kaibuchi, K. (1998). Role of IQGAP1, a target of the small GTPases Cdc42 and Rac1, in regulation of E-cadherin-mediated cell-cell adhesions. *Science.* 281, 832-835.
- Larue, L., Ohsugi, M., Hirchenhain, J., and Kemler, R. (1994). E-cadherin null mutant embryos fail to form a trophectoderm epithelium. *Proc. Natl. Acad. Sci. USA.* 91, 8263-8267.
- Liu, D., Huang, C., Kameyama, K., Hayashi, E., Yamauchi, A., Kobayashi, S., and Yokomise, H. (2001). E-cadherin expression associated with differentiation and prognosis in non-small-cell lung cancer patients. *Ann Thorac Surg.* 71, 949-955.
- Matsumura, T., Makino, R., and Mitamura, K. (2001). Frequent down-regulation of E-cadherin by genetic and epigenetic changes in the malignant progression of hepatocellular carcinomas. *Clin Cancer Res.* 7(3), 594-599.
- Maurange, C., Lee, N. and Paro, R. (2006). Signaling meets chromatin during tissue regeneration in *Drosophila*. *Curr. Opin. Gen. Dev.* 16, 485-489.
- Mazieres, J., He, B., You, L., Xu, Z., Lee, A.Y., Mikami, I., Reguart, N., Rosell, R., McCormick, F., and Jablons, D.M. (2004). Wnt inhibitory factor-1 is silenced by promoter hypermethylation in human lung cancer. *Cancer Res.* 15, 4717-4720.
- Meuwissen, R., and Berns, A. (2005). Mouse models for human lung cancer. *Genes and Development.* 19, 643-664.
- Miller, J.R., and Moon, R.T. (1996). Signal transduction through  $\beta$ -catenin and specification of cell fate during embryogenesis. *Genes Dev.* 10, 2527-2539.
- Muta, H., Noguchi, M., Kanai, Y., Ochiai, A., Nawata, H., and Hirohashi, S. (1996). E-cadherin gene mutations in signet ring cell carcinoma of the stomach. *Jpn. J Cancer Res.* 87, 843-848.
- Nakashima, T., Huang, C., Liu, D., Kameyama, K., Masuya, D., Kobayashi, S., Kinoshita, M., and Yokomise, H. (2003). Neural-cadherin expression associated with angiogenesis in non-small-cell lung cancer patients. *Br. J. Cancer* 88, 1727-1733.
- Nakashima, T., Huang, C.L., Liu, D., Kameyama, K., Masuya, D., Ueno, M., Haba, R., and Yokomise, H. (2004). Expression of vascular endothelial growth factor-A and vascular

- endothelial growth factor-C as prognostic factors for non-small cell lung cancer. *Med. Sci. Monit.* 10, BR157-BR165.
- Nikolopoulos, S.N., Blaikie, P., Yoshioka, T., Guo, W., and Giancotti, F.G. (2004). Integrin  $\beta 4$  signaling promotes tumor angiogenesis. *Cancer Cell* 6, 471-483.
- Norton, L. and Massagué, J. (2006). Is cancer a disease of self-seeding?. *Nat. Med.* 12, 875-878.
- O'Byrne, K.J., Koukourakis, M.I., Giatromanolaki, A., Cox, G., Turley, H., Steward, W.P., Gatter, K., and Harris, A.L. (2000). Vascular endothelial growth factor, platelet-derived endothelial cell growth factor and angiogenesis in non-small-cell lung cancer. *Br. J. Cancer.* 82, 1427-1432.
- Ohsugi, M., Larue, L., Schwarz, H., and Kemler, R. (1997). Cell-junctional cytoskeletal organisation in mouse blastocysts lacking E-cadherin. *Dev. Biol.* 185, 261-271.
- Okubo, T. and Hogan, B. LM. (2004). Hyperactive Wnt signaling changes the developmental potential of embryonic lung endoderm. *J. Biol.* 3, 11.1-11.17.
- Peinado, H., Portillo, F., and Cano, A. (2004). Transcriptional regulation of cadherins during development and carcinogenesis. *Int. J. Dev. Biol.* 48, 365-375.
- Perl, A.K., Wilgenbus, P., Dahl, U., Semb, H., and Christofori, G. (1998). A causal role for E-cadherin in the transition from adenoma to carcinoma. *Nature* 392, 190-193.
- Perl, A.K., Dahl, U., Wilgenbus, P., Cremer, H., Semb, H., and Christofori, G. (1999). Reduced expression of neural cell adhesion molecule induces metastatic dissemination of pancreatic beta tumor cells. *Nat. Med.* 5, 286-291.
- Perl, A.K., Tichelaar, J.W., and Whitsett, J.A. (2002). Conditional gene expression in the respiratory epithelium of the mouse. *Transgenic Res.* 11, 21-29.
- Persad, S., Troussard, A.A., McPhee, T.R., Mulholland, D.J., and Dedhar, S. (2001). Tumor Suppressor PTEN inhibits Nuclear Accumulation of  $\beta$ -catenin and T Cell/Lymphoid Enhancer Factor-1-mediated Transcriptional Activation. *The Journal of Cell Biology.* 153, 6, 1161-1173.
- Pignatelli, M., and Vessey, C.J. (1994). Adhesion molecules: novel molecular tools in tumor pathology. *Hum Pathol.* 25, 849-856.
- Rapp, U.R., Fensterle, J., Albert, S., and Götz, R. (2003). Raf kinases in lung tumor development. *Adv. Enzyme Regul.* 43, 183-195.
- Renyi-Vamos, F., Tovari, J., Fillinger, J., Timar, J., Paku, S., Kenessey, I., Ostoros, G., Agocs, L., Soltesz, I., and Dome, B. (2005). Lymphangiogenesis correlates with lymph node metastasis, prognosis, and angiogenic phenotype in human non-small cell lung cancer. *Clin. Cancer Res.* 11, 7344-7353.
- Reynolds, A.B., Daniel, J., McCrea, P.D., Wheelock, M.J., Wu, J., and Zhang, Z. (1994). Identification of a new catenin: The tyrosine kinase substrate p120(cas) associates with E-cadherin complexes. *Mol Cell Biol.* 14, 8333-8342.

- Rice, W.R., Conkright, J.J., Na, C.L., Ikegami, M., Shannon, J.M., and Weaver, T.E. (2002). Maintenance of the mouse type II cell phenotype in vitro. *Am. J Physiol Lung Cell Mol. Physiol* 283, L256-L264.
- Risau, W. (1997) Mechanisms of angiogenesis *Nature*, 386, 671-674.
- Risinger, J.I., Berchuck, A., Kohler, M.F., and Boyd, J. (1994). Mutations of the E-cadherin gene in human gynecologic cancers. *Nat Genet.* 7, 98-102.
- Rizzino, A., Gonda, M.A. and Rapp, U.R. (1982). Dome formation by a retrovirus-induced lung adenocarcinoma cell line. *Cancer Res.* 42, 1881-1887.
- Rous, P. and Kidd, J.G. (1941). Conditional neoplasms and subthreshold neoplastic states. *J.Exper.Med.* 73, 365-90.
- Schardt, J.A., Meyer, M., Hartmann, C.H., Schubert, F., Schmidt-Kittler, O., Fuhrmann, C., Polzer, B., Petronio, M., Eils, R., and Klein, C.A. (2005). Genomic analysis of single cytokeratin-positive cells from bone marrow reveals early mutational events in breast cancer. *Cancer Cell* 8, 227-239.
- Schönig, K., Schwenk, F., Rajewsky, K., and Bujard H. (2002). Stringent doxycycline dependent control of Cre recombinase in vivo. *Nucleic Acids Research.* 30, 23-34.
- Shapiro, L. (1995). Structural basis of cell-cell adhesion by cadherins. *Nature.* 374, 327-337.
- Sharma, S.V., Bell, D.W., Settleman, J., and Haber, D.A. (2007). Epidermal growth factor receptor mutations in lung cancer. *Nature Reviews Cancer.* 7, 169-181.
- Shibamoto, S., Hayakawa, M., Takeuchi, K., Hori, T., Oku, N., Miyazawa, K., Kitamura, N., Takeichi, M., and Ito, F. (1994). Tyrosine phosphorylation of  $\beta$ -catenin and plakoglobin enhanced by hepatocyte growth factor and epidermal growth factor in human carcinoma cells. *Cell Adhes Commun.* 1, 295-305.
- Shibanuma, H., Hirano, T., Tsuji, K., Wu, Q., Shrestha, B., Konaka, C., Ebihara, Y., and Kato, H. (1998). Influence of E-cadherin dysfunction upon local invasion and metastasis in non-small cell lung cancer. *Lung Cancer* 22, 85-95.
- Skurk, C., Maatz, H., Rocnik, E., Bialik, A., Force, T., and Walsh, K. (2005). Glycogen-Synthase Kinase3 $\beta$ /beta-catenin axis promotes angiogenesis through activation of vascular endothelial growth factor signaling in endothelial cells. *Circ. Res.* 96, 308-318.
- Smith, W., and Khuri, F.R. (2004). The care of the lung cancer patient in the 21st century: a new age. *Semin Oncol.* 31, 11-15.
- Solorzano, C.C., Baker, C.H., Tsan, R., Traxler, P., Cohen, P., Buchdunger, E., Killion, J.J., and Fidler, I.J. (2001). Optimization for the blockade of epidermal growth factor receptor signaling for therapy of human pancreatic carcinoma. *Clin. Cancer Res.* 7, 2563-2572.
- Stappert, J., and Kemler, R. (1994). A short core region of E-cadherin is essential for catenin binding and is highly phosphorylated. *Cell Adhes. Commun.* 2, 319-327.

- Stemmler, M.P., Hecht, A., and Kemler, R. (2005). E-cadherin intron 2 contains *cis*-regulatory elements essential for gene expression. *Development*. 132, 965–976.
- Strathdee, G. (2002). Epigenetic versus genetic alterations in the inactivation of E-cadherin. *Semin. Cancer Biol.* **12**, 373–379.
- Su, J.L., Yang, P.C., Shih, J.Y., Yang, C.Y., Wei, L.H., Hsieh, C.Y., Chou, C.H., Jeng, Y.M., Wang, M.Y., Chang, K.J., et al. (2006). The VEGF-C/Flt-4 axis promotes invasion and metastasis of cancer cells. *Cancer Cell* 9, 209-223.
- Suzuki, K., Nagai, K., Yoshida, J., Moriyama, E., Nishimura, M., Takahashi, K., and Nishiwaki, Y. (1999). Prognostic factors in clinical stage I non-small cell lung cancer. *Ann. Thorac. Surg.* 67, 927-932.
- Takeichi, M. (1991). Cadherin cell adhesion receptors as a morphogenetic regulator. *Science*. 251, 1451-1455.
- Takeichi, M. (1995). Morphogenetic roles of classic cadherins. *Curr. Opin. Cell Biol.* 7, 619-627.
- Takaichi, M., Sasaki, T., Kotani, H., Nishioka, H., and Takai, Y. (1997). Regulation of cell-cell adhesion by rac and rho small G proteins in MDCK cells. *J Cell Biol.* 139, 1047-1059.
- Takeichi, M. (2007). The cadherin superfamily in neuronal connections and interactions. *Nature Reviews Neuroscience*. 8, 11-20.
- Thiery, J.P. (2002). Epithelial–mesenchymal transitions in tumour progression. *Nat. Rev. Cancer*. 2, 442–454.
- Tinkle, C.L., Lechler, T., Pasolli, H.A., and Fuchs, E. (2004). Conditional targeting of E-cadherin in skin: insights into hyperproliferative and degenerative responses. *Proc. Natl. Acad. Sci. U. S. A.* 101, 552-557.
- Vleminckx, K., et al. (1991). Genetic manipulation of E-cadherin expression by epithelial tumor cells reveals an invasion suppressor role. *Cell*. 66(1), 107-119.
- Zeng, X., Wert, S., Federici, R., Peters, K.G., and Whitsett, J.A. (1998). VEGF enhances pulmonary vasculogenesis and disrupts lung morphogenesis in vivo. *Dev. Dyn.* 211, 215-227.

## APPENDIX

### Abbreviations

AJ	Adherence junctions
Ann.	Annealing
Ang-1	Angiopoietin 1
Ang-2	Angiopoietin 2
Atoh-1	Atonal homolog 1
Axin2	Axin 2
APC	Adenomatosis polyposis coli
APS	Ammoniumpersulphate
bFGF	Basic fibroblast growth factor
bp	Basepair
Ca <sup>2+</sup>	Calcium
CAMs	Cell adhesion molecules
CCLR	Luciferase cell culture lysis reagent
CCSP	Clara cell secretory protein
c-DNA	Complementary DNA
CD	Cytoplasmic domain
Cdh1	Cadherin 1
Cdx-1	Caudal type homeobox 1
CELSRs	Cadherin EGF LAG seven-pass G-type receptors
c-Fos	v-fos FBJ murine osteosarcoma viral oncogene homolog C
CIP	Calf Intestinal Phosphatase
CMV	Cytomegalievirus
Ctn	catenin
CXCR4	C-X-C chemokine receptor type 4
DCPP	Demilune cell and parotid protein 1
Dkk4	Dickkopf homolog 4
DMBT1	Deleted in malignant brain tumors 1
DMEM	Dulbecco's Modified Eagle Medium
DMF	Dimethylformamide
DMSO	Dimethylsulphoxide
dn	Dominant negative
dNTP	(Di)Desoxynucleotide triphosphate
DOX	Doxycycline
DTT	Dithiothreitol
EC	Extracellular domain
E-cadherin	Epithelial cadherin
ECL	Enhanced Chemoluminescence
E. coli	Escherichia coli
EDTA	Ethylendiamintetra acetic acid
e.g.	exempli gratia
EGF	Epidermal growth factor
EGFR	Epidermal growth factor receptor
EGR-1	Early growth response 1
EMT	Epithelial-mesenchymal transition
FAT	Mouse Fat cadherin

FCS	Fetal calf serum
FGF	Fibroblast growth factor
FGFR	Fibroblast growth factor receptor
FHIT	Fragile histidine triad gene
Floxed	flanked by loxP
Flt-4	FMS-like tyrosine kinase 4
g	Gram
GAPDH	Glyceraldehyde-3-phosphate dehydrogenase
GSK-3 $\beta$	Glycogen synthase kinase 3 beta
H&E	Hematoxylin/eosin staining
hm	Hyper methylation
hu	Human
IC	Immunocytochemistry
kb	Kilo basepair
kDa	Kilo dalton
KDR	Kinase insert domain receptor
K14	Keratin 14
KO	Knockout
L	Liter
LCM	Laser Capture Microdissection
Lef	Lymphoid enhancer factor
LOH	Loss of heterozygosity
Luc	Luciferase reporter gene
LYVE-1	Lymphatic vessel endothelial hyaluronan receptor 1
M	Month
MMP-9	Matrix metalloproteinase-9
MMTV	Mouse mammary tumor virus
MSZ	Institut für Medizinische Strahlenkunde und Zellforschung
Myc	v-myc myelocytomatosis viral oncogene homolog
N	Neural
N-cadherin	Neural cadherin
Nkd-1	Naked cuticle homolog 1
NP40	Nonidet 40
NSCLC	Non-small-cell lung cancer
OCT	Optimal cutting temperature
OD	Optical density
PAGE	Polyacrylamide-Gel electrophoresis
PBS	Phosphate buffered saline
P-cadherin	Placental cadherin
PCNA	Proliferating cell nuclear antigen
PCR	polymerase chain reaction
PFA	Para form aldehyde
pfu	Plaque forming unit
PROX1	Prospero-related homeobox 1
RAR- $\beta$	Retinoic acid receptor
RB	Retina blastoma
RIP1Tag2	Rat insulin promoter 1 T-antigen 2
RLU	relative luciferase unit
rpm	revolutions per minute
RTK	Receptor protein tyrosine kinase
RT-PCR	Reverse transcriptase polymerase chain reaction



---

RT	Room temperature
rtTA	Reverse tetracycline transactivator
SCLC	Small-cell lung cancer
SDF-1	Stromal cell-derived factor-1
siRNA	Small interfering RNA
SP-C	Surfactant protein C
TCF	T-cell factor
Tem.	Temperature
tet	tetracycline-regulated
Tet-O	tetracycline operator
Thr-1	Thrombospondin-1
TIE-1	Tyrosine kinase with immunoglobulin homology domain 1
TIE-2	Tyrosine kinase with immunoglobulin homology domain 2
TIMP-3	Tissue inhibitor of metalloproteinase 3
TJ	Tight junctions
TP53	Tumor protein 53
TTF-1	Thyroid transcription factor 1
TUNEL	Terminal deoxynucleotidyltr.-mediated dUTP-biotin nick end labeling
v	Volume
V	Volt
VE-cadherin	Vascular endothelial cadherin
VEGF	Vascular endothelial growth factor
w	Weight
WB	Western blot
Wif-1	Wnt inhibitory factor 1
Wnt	Wingless-type MMTV integration site family
WT	Wild type

## C.V.

### Personal data

**Name:** Fatih Ceteci

**Sex:** Male

**Date of Birth:** 24.05.1975

**Place of Birth:** Solingen, Germany

**Marital Status:** Married

**Nationality:** Turkish

**Languages:** English, German, Turkish (mother language)

**Email:** [Fatih-Ceteci@mail.uni-wuerzburg.de](mailto:Fatih-Ceteci@mail.uni-wuerzburg.de)

**Telephone (Mobil):** 0179 473 44 77

**Address :** Werner von Siemens Str. 51-G, 97076, Würzburg

### Graduations

General University Entrance Qualification; Turkey, 1992.

B.Sc. Degree; Uludag University, Faculty of Science, Department of Biology, Turkey, 1993-1997.

Honour student prize by the Dean of Faculty, 1997.

M.Sc. Degree; Uludag University, Institute for Nature Science, Department of Molecular Biology, Turkey, 1997-2000.

Practice in Molecular Biology Techniques, University of Heinrich Heine, Düsseldorf, Germany, 2001/2002.

Ph.D Degree; University of Würzburg, Institute for Medical Radiation and Cell Research, Würzburg, Germany, 2002-2008.

### Publications

1. **Ceteci F**, Ceteci S, Karreman C, Kramer BW, Asan E, Götz R, Rapp UR. Disruption of tumor cell adhesion promotes angiogenic switch and progression to micrometastasis in RAF-driven murine lung cancer. *Cancer Cell*. 2007 Aug;12(2):145-59.
2. Rapp UR, **Ceteci F**, Schreck R. Oncogene-induced plasticity and cancer stem cells. *Cell Cycle*. 2008 Jan;7(1):45-51.

## **Talks**

**Ceteci F.** O-64 Raf/Myc cooperation in lung tumor induction in mice. AEK Cancer Congress, Würzburg, Mar 2005.

**Ceteci F.** Angiogenic switch induction by abrogation of E-cadherin function in C-Raf driven murine lung cancer. 6th EMBL Mouse Molecular Genetics Meeting, Heidelberg, 2005.

## **Posters**

**Ceteci F.** Analysis of the role of E-cadherin in lung tumorigenesis. Graduate's Day "Advances in Cancer Therapeutics", Ulm, Oct 2004.

**Ceteci F.** Analysis of the role of E-cadherin in lung tumorigenesis. AEK Cancer Congress, Würzburg, Mar 2005.

**Ceteci F.** Analysis of the role of E-cadherin in lung tumorigenesis. 6th EMBL International Predoc Symposia "Animal Models", Rome, Italy, May 2005.

**Ceteci F.** Dysregulation of E-cadherin/Wnt signaling in epithelial cells of distal lung induces reprogramming and metastasis of C-RAF driven adenomas. Myc and the Transcriptional Control of Proliferation and Oncogenesis. Spain, Madrid, June 2007.

## **Declaration:**

I hereby declare that the submitted dissertation was completed by myself and no other. I have not used any sources or materials other than those enclosed.

Moreover I declare that the following dissertation has not been submitted further in this form or any other form, and has not been used for obtaining any other equivalent qualifications at any other organization/institution.

Additionally, I have not applied for, nor will I attempt to apply for any other degree of qualification in relation to this work.

Würzburg, den

Fatih Ceteci